ACS SASSI Application to Seismic Soil-Structure Interaction (SSI) Analysis of Highway Bridge Structures

ACS SASSI による高速道路橋梁の地盤-構造物連成耐震解析

Dr. Dan M. Ghiocel

Email: dan.ghiocel@ghiocel-tech.com

Phone: 585-641-0379

Ghiocel Predictive Technologies Inc.

http://www.ghiocel-tech.com

Ghiocel Predictive Technologies Inc.

ACS SASSI 2-Days SSI Workshop
Sola City Conference Center, Ochanomizu
May 12-13, 2016

Purpose of this Presentation

Discuss the state-of-the-art seismic SSI analysis of the concrete bridges on pile-foundations using the specialized ACS SASSI FEA software. ACS SASSI による杭基礎コンクリート橋の最先端技術によるSSI耐震解析を解説します.

ACS SASSI is a specialized software applied largely in nuclear industry where seismic SSI analysis is required to be done in detail. Used in North America, Europe, Asia, South America and Africa. In Japan used for nuclear projects by MHI, Toshiba, Hitachi-GE, Obayashi, Shimizu, Taisei, Takenaka, and others. ACS SASSI は耐震SSI詳細解析が必要とされる原子力分野で普及する専用ソフトで、北米、欧州、アジア、南米、アフリカや日本で多くの原子力プロジェクトに使用されています.

In Japan not much known by bridge seismic designers. Bridges have much lower design code requirements on seismic SSI analysis than nuclear structures (ASCE 4 standard). 現状の橋梁設計では原子力施設の設計に比べ耐震SSI解析上の設計要求は低い。

ACS SASSI Application to Bridges

ACS SASSI has been used recently for seismic evaluation of large span concrete highway bridges in US, including New York City, Boston, Washington D.C. and many other places. ACS SASSIはNew York, ボストン,ワシントン D.Cの長スパンコンクリート高速道路橋の耐震評価に用いられています.

The pile foundation ACS SASSI modeling captures the global dynamic SSI structure-pile-group-soil effects including both the *wave scattering and inertial effects*, but also include the *local nonlinear SSI effects* in the vicinity of the piles due to local soil plasticity in the adjacent soil and at pile-soil interface. ACS SASSI杭基礎モデルは巨視的動的SSI構造物-杭群-土壌連成効果を含みます. これには波動散乱と慣性効果を含んでおり、杭に隣接した土壌の塑性による局所的非線形SSI効果も含みます.

In addition, for the entire bridge structure, the site-specific effects of *motion spatial variation (incoherency and wave passage)* is included since it could largely affect bridge-pile seismic responses. さらに, 橋梁全体構造では, 橋-杭の地震応答性に大きく影響するサイト特有の地震波の伝播の変動（インコヒレンシー、地震波通過）特性を考慮します.

Presentation Content

1. Short Introduction to ACS SASSI Seismic SSI Analysis Methodology Applicable to Bridges
   ACS SASSI耐震SSI解析手法の橋梁適用 紹介

2. Specific Bridge-Pile Foundation SSI Modeling Aspects
   個々の橋-杭基礎SSIモデリングの状況

3. Case Studies: ケーススタディ

- Fartec Highway Bridge SSI Analysis… in Europe
- Fukae Bridge Failure Review Including SSI Effects… part of Hanshin Expressway in Kobe

1. Short Introduction to ACS SASSI Seismic SSI Analysis Methodology Applicable to Bridges

ACS SASSI耐震SSI解析手法の橋梁適用 紹介

Seismic Linearized SSI Analysis Problem

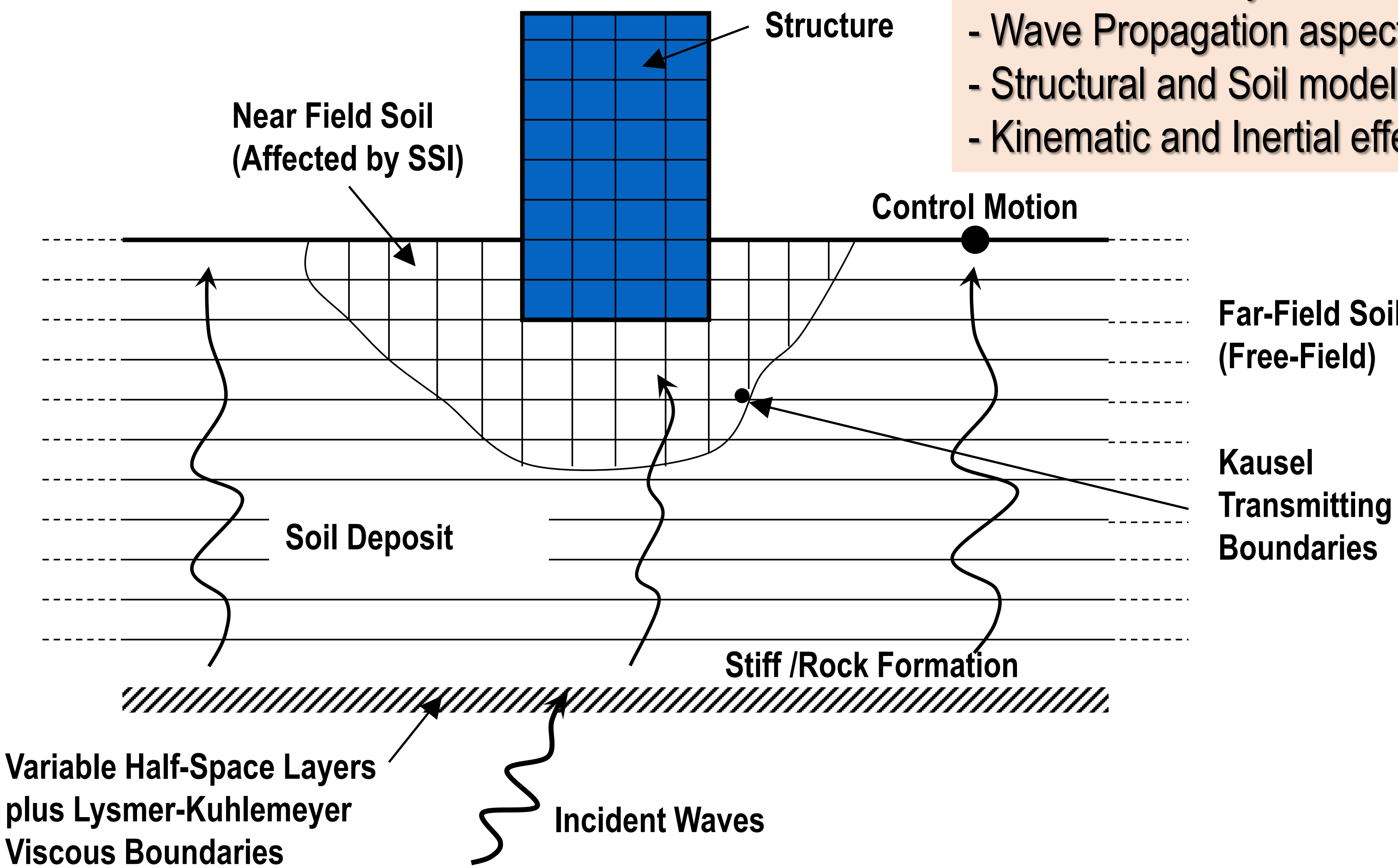

Seismic SSI Analysis includes:
- Wave Propagation aspects
- Structural and Soil modeling
- Kinematic and Inertial effects

Flexible Volume (FV) Substructuring

フレキシブルボリューム部分構造

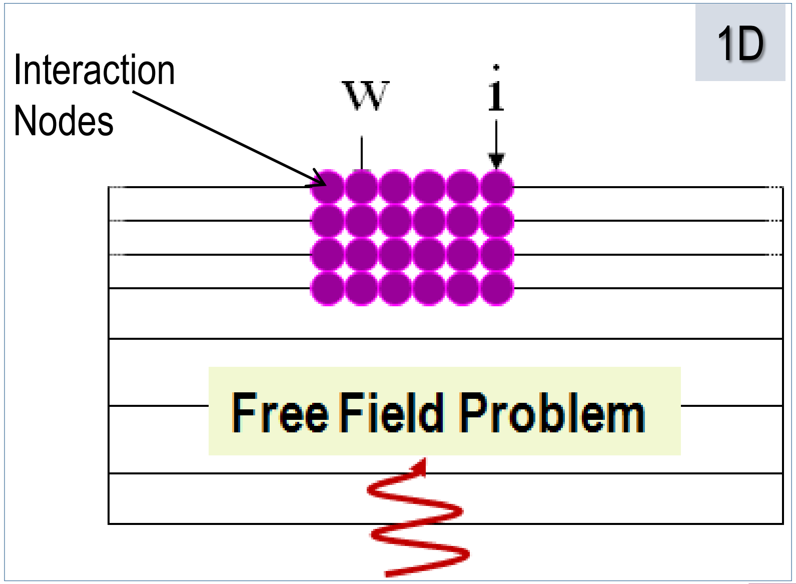

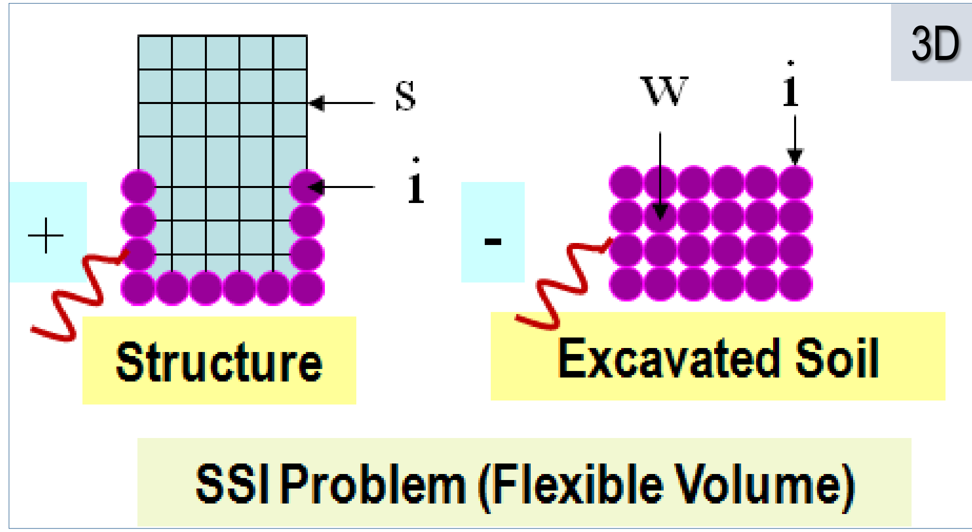

Complex Frequency Domain Formulation:

Complex Dynamic Stiffness

Complex Seismic Load Vector

$$\mathbf{C}(\omega)\mathbf{U}(\omega)=\mathbf{Q}(\omega)$$

Complex Absolute Displacements

Complex Soil Impedance Terms

$$\begin{bmatrix} \mathbf{C}^{s}_{ii}-\mathbf{C}^{e}_{ii}+\mathbf{X}_{ii} & -\mathbf{C}^{e}_{iw}+\mathbf{X}_{iw} & \mathbf{C}^{s}_{is} \\ -\mathbf{C}^{e}_{wi}+\mathbf{X}_{wi} & -\mathbf{C}^{e}_{ww}+\mathbf{X}_{ww} & \mathbf{0} \\ \mathbf{C}^{s}_{si} & \mathbf{0} & \mathbf{C}^{s}_{ss} \end{bmatrix} \begin{Bmatrix} \mathbf{U}_{i} \\ \mathbf{U}_{w} \\ \mathbf{U}_{s} \end{Bmatrix} = \begin{Bmatrix} \mathbf{X}_{ii}\mathbf{U}'_{i}+\mathbf{X}_{iw}\mathbf{U}'_{w} \\ \mathbf{X}_{wi}\mathbf{U}'_{i}+\mathbf{X}_{ww}\mathbf{U}'_{w} \\ \mathbf{0} \end{Bmatrix}$$

REMARK: All Excavated Soil nodes are interaction nodes (include exact equations of motion)

ACS SASSI SSI Model for MHI US-APWR NI

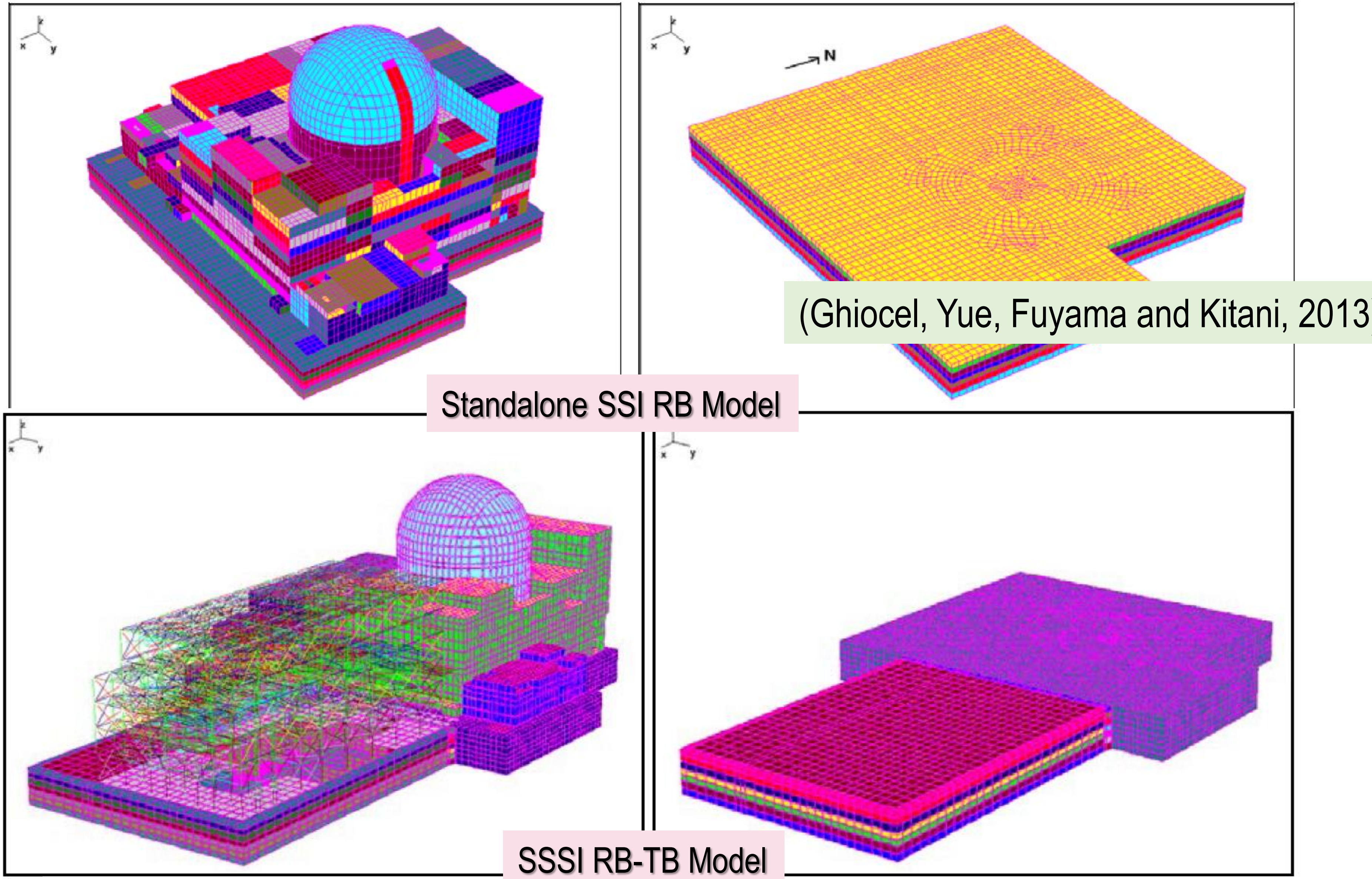

(Ghiocel, Yue, Fuyama and Kitani, 2013)

Standalone SSI RB Model

SSSI RB-TB Model

a) Structural Model

b) Excavated Volume

ACS SASSI NI Pile-Foundation SSI Model

ACS SASSI NI 杭-基礎SSIモデル

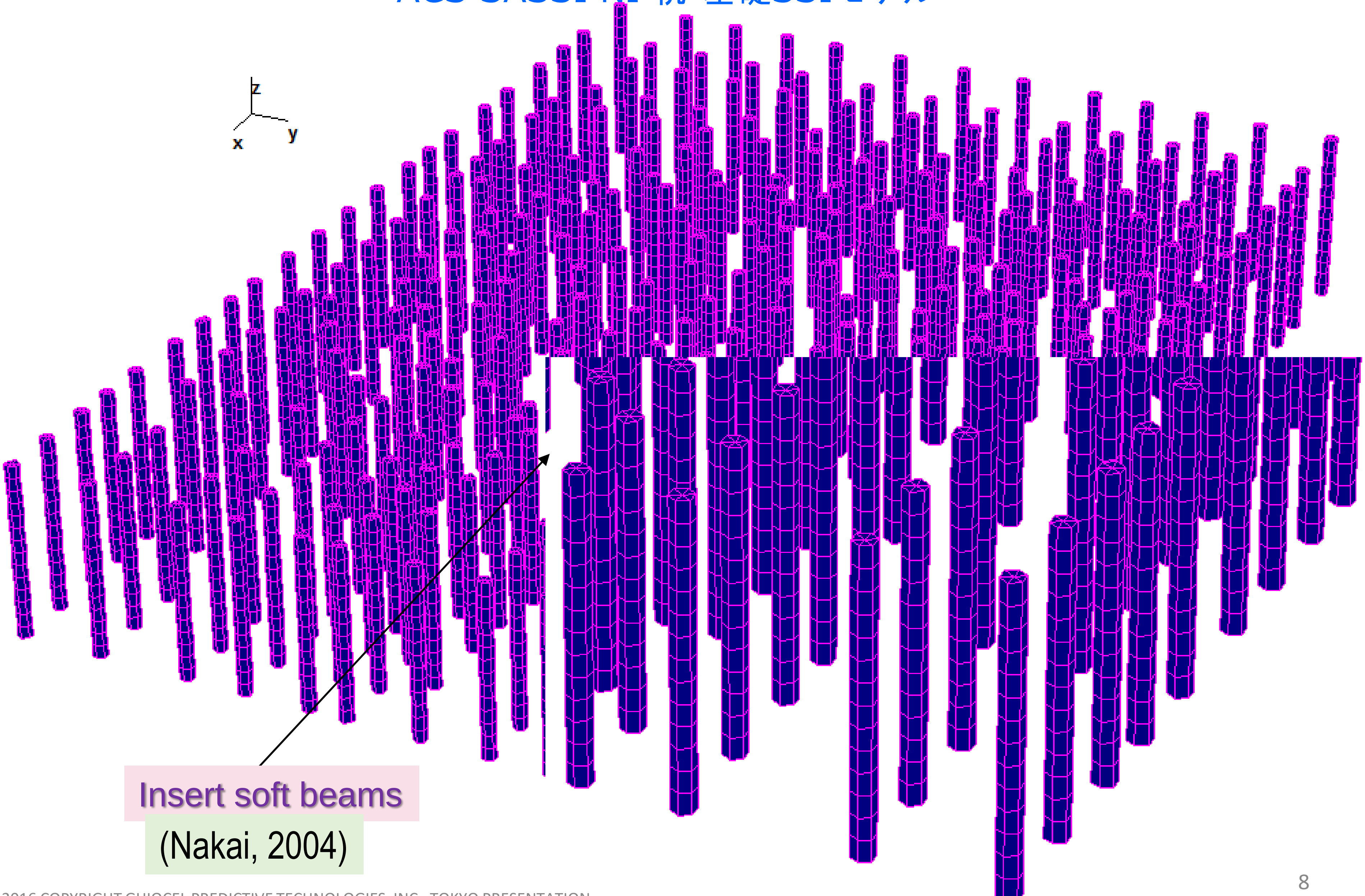

Insert soft beams

(Nakai, 2004)

Coherent vs. Incoherent Wave Propagation Models

地震波伝播モデル比較　コヒレントvs.インコヒレント

3D Rigid Body Soil Motion (Idealized)

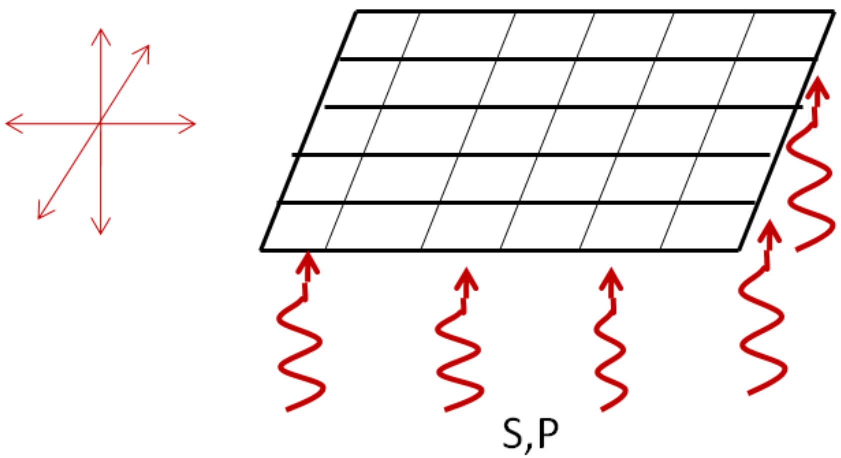

3D Random Wave Field Soil Motion (Realistic)

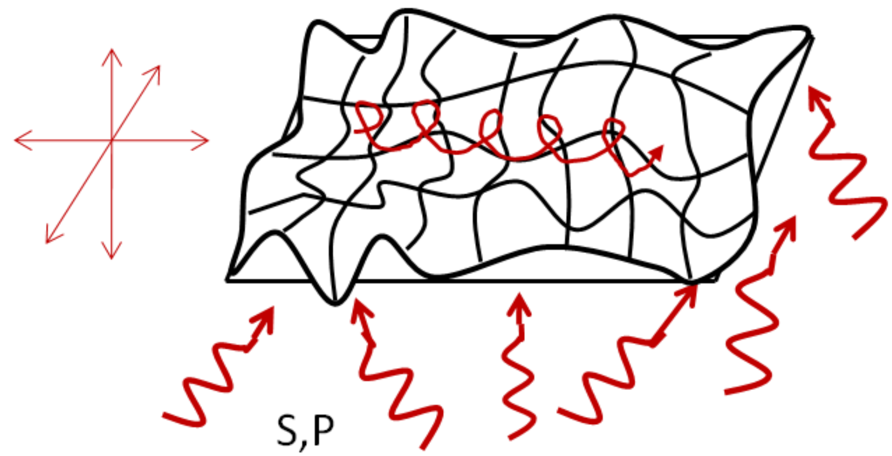

1 D Wave Propagation Analytical Model (Coherent)

Vertically Propagating S and P waves (1D)
- No other waves types included
- No heterogeneity random orientation and arrivals included
- Results in a rigid body soil motion, even for large-size foundations

3D Wave Propagation Data-Based Model (Incoherent – Database-Driven Adjusted Coherent)

Includes real field records information, including implicitly motion field heterogeneity, random arrivals of different wave types under random incident angles.

ANIMATION 1

Modeling of Soil and Structure Hysteretic Behavior

土壌と構造物のヒステリシス挙動モデル化

Linearized Hysteretic Model

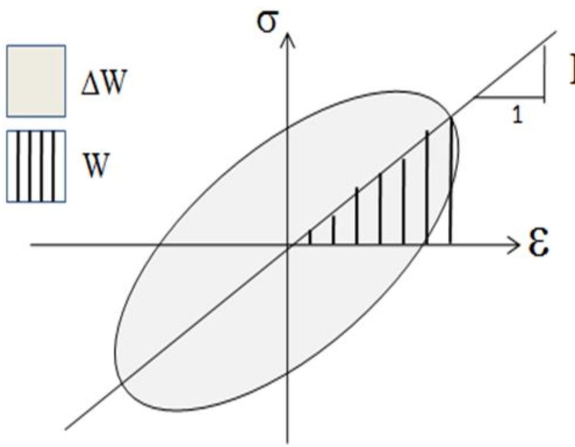

Frequency Domain
Linearized Hysteretic Model

Experimental Hysteretic Model

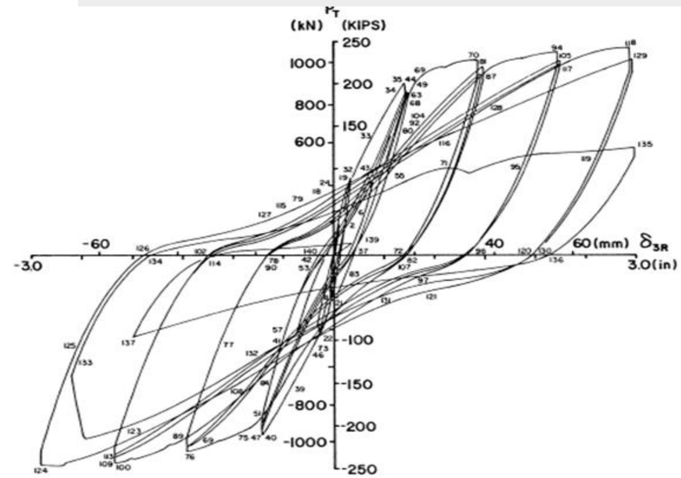

Time Domain
Hysteretic Model

Comparative nonlinear SSI analysis results of the hybrid approach and the "*true*" nonlinear time-integration approach showed a very good matching.

The new nonlinear SSI approach can be used to perform *fast and accurate* nonlinear SSI analyses at a small fraction of the runtime of a time domain nonlinear SSI analysis, about 2-3 times the linear analysis runtime.

Seismic Nonlinear SSI Analysis Methodology

非線形SSI耐震解析手法

Base isolators are modeled as nonlinear spring elements.

ACS SASSI (Option NON) extended the SASSI substructuring methodology to nonlinear SSI using an iterative equivalent linear procedure. Includes shells and springs.

Computational steps:

- For the initial iteration, perform a linear SSI analysis using the initial elastic properties for the nonlinear elements
- Compute the local behavior of nonlinear elements in time domain based on the local relative displacements, that is then used to calibrate the local linearized hysteretic models associated to each nonlinear element in complex frequency
- Perform a new SSI analysis iteration using a fast SSI restart analysis in the complex frequency domain using the linearized hysteretic models computed in Step 2 for nonlinear elements
- Check convergence after new SSI iteration to stop or continue.

Concrete Shearwall Structure SSI Analysis

コンクリート耐震壁構造物のSSI解析

Elastic vs. Nonlinear

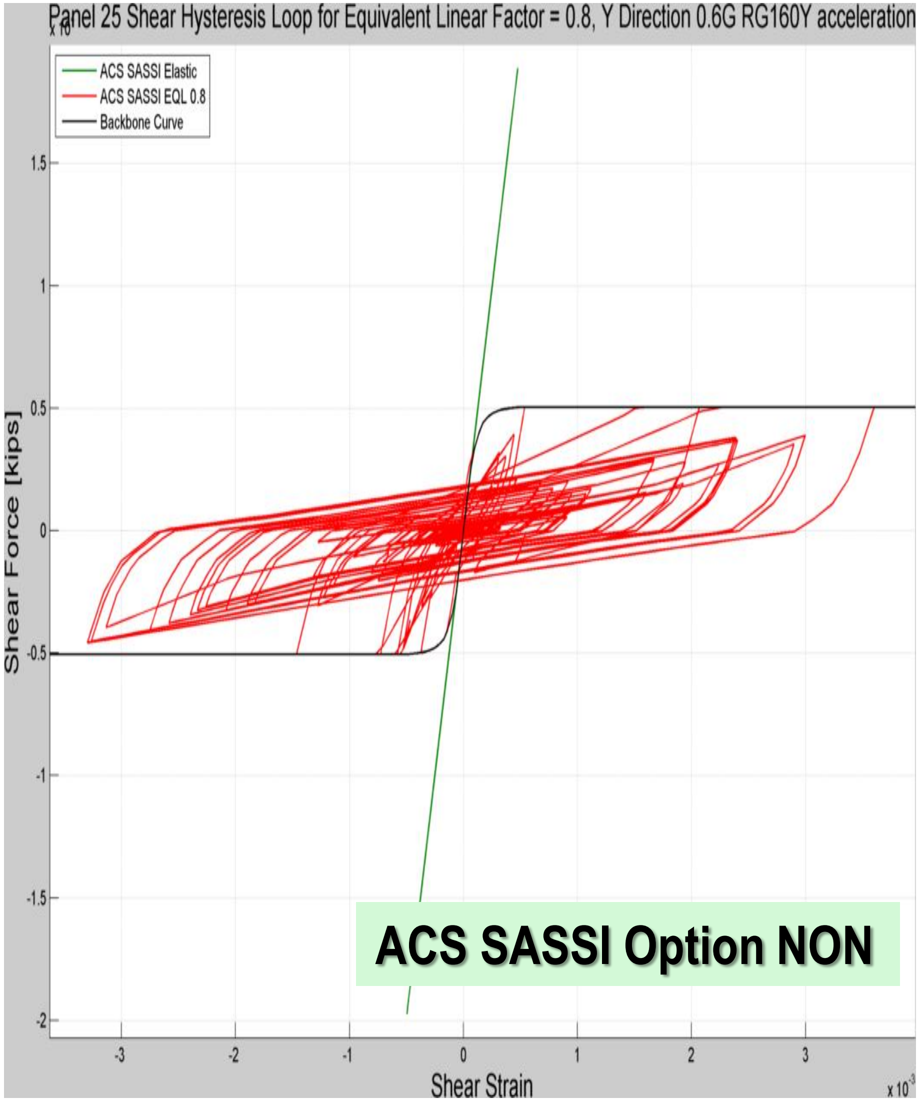

1st Iteration vs. Last Iteration

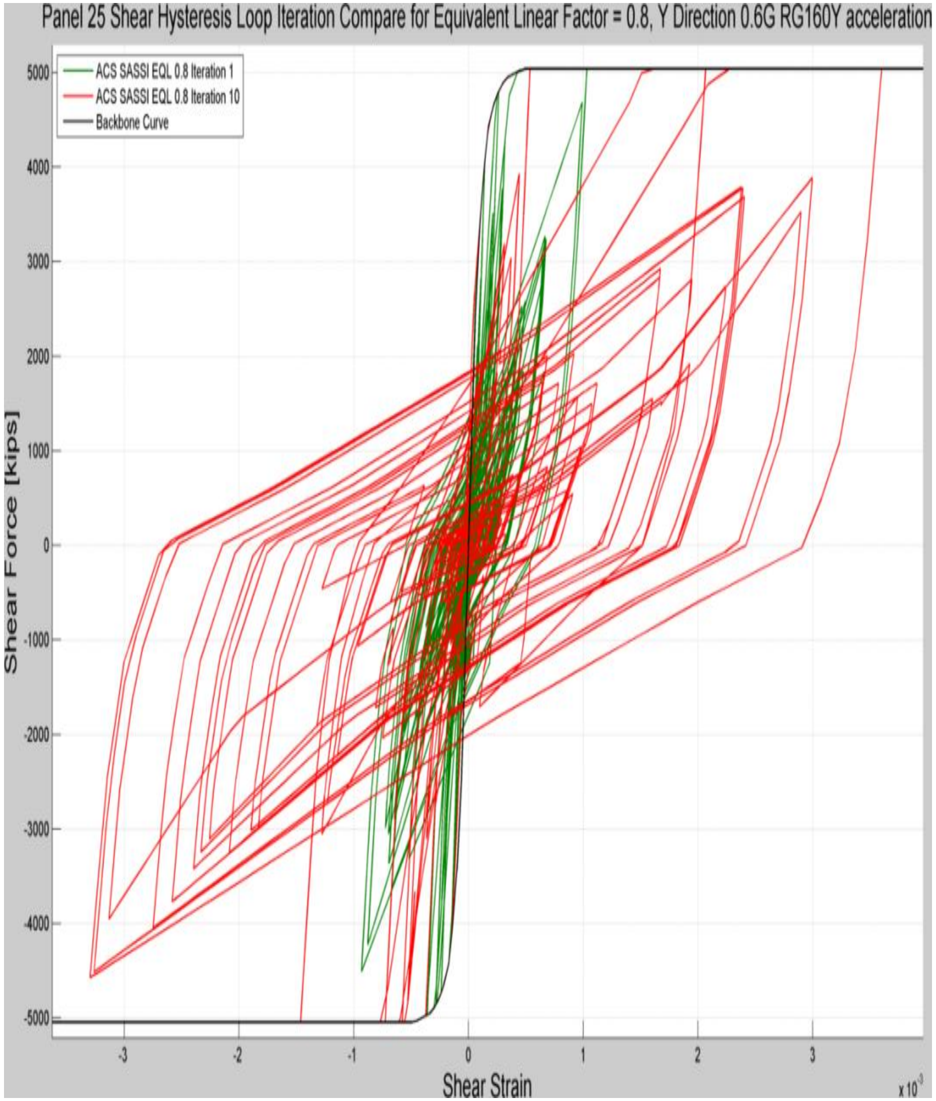

Nonlinear Springs for Modeling Base-Isolators and/or Moderate Building Sliding

基礎アイソレーター、適度な建屋滑りをモデル化する非線形ばね

Base-Isolators

Small-Moderate Sliding

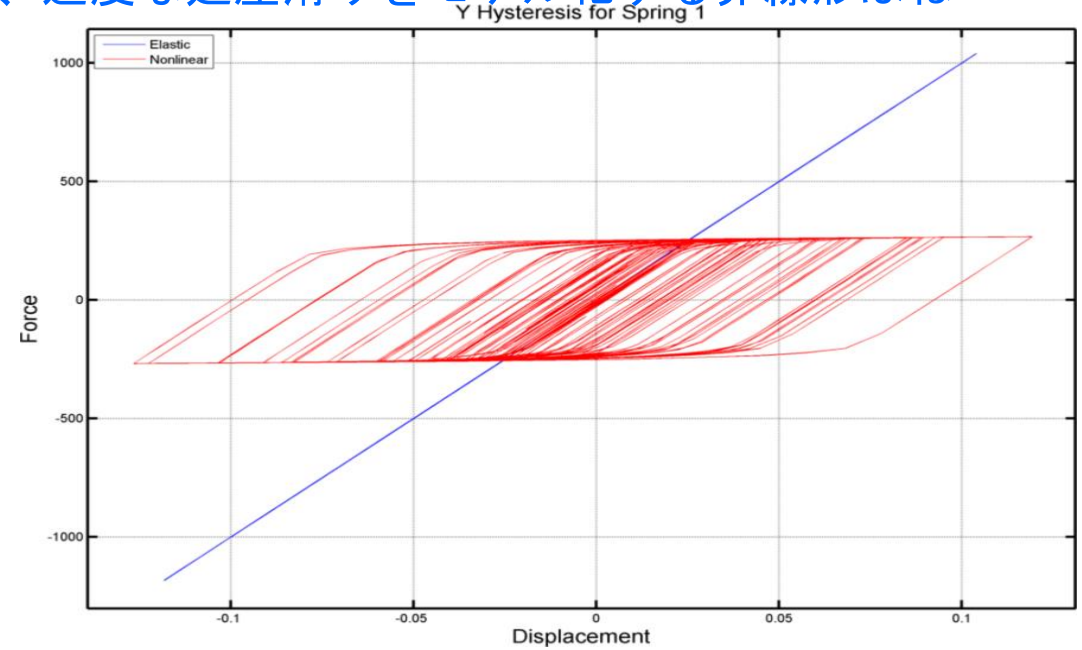

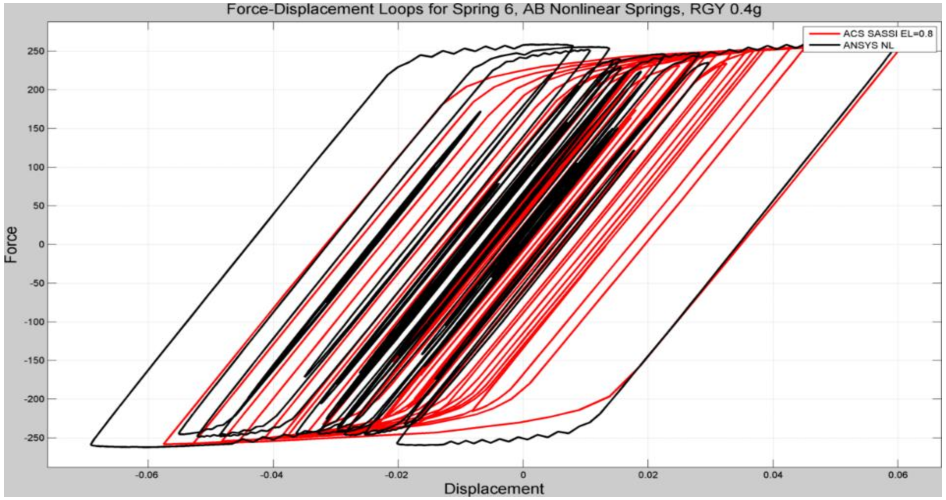

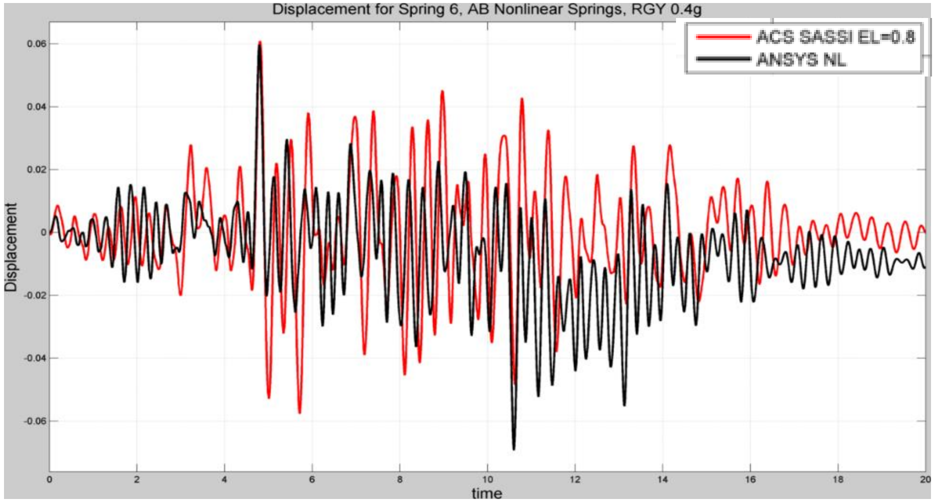

2. Specific Bridge-Pile Foundation SSI Modeling Aspects 個々の橋-杭基礎SSIモデル化の状況

Highway Bridge Model (Stiff)

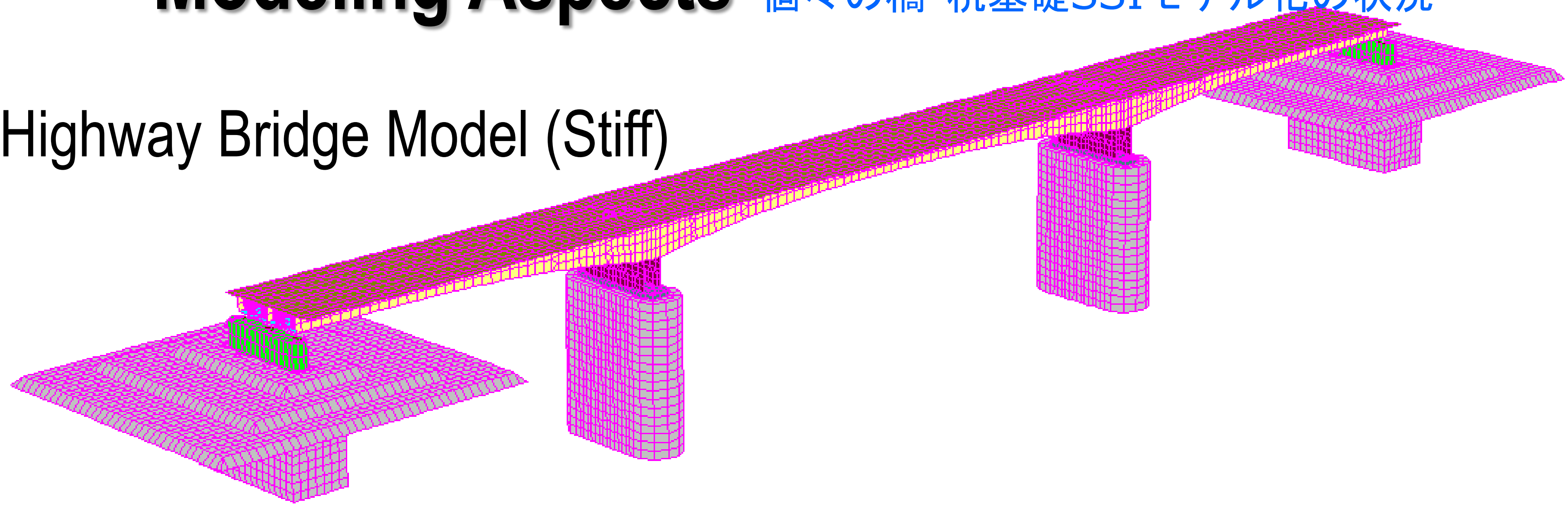

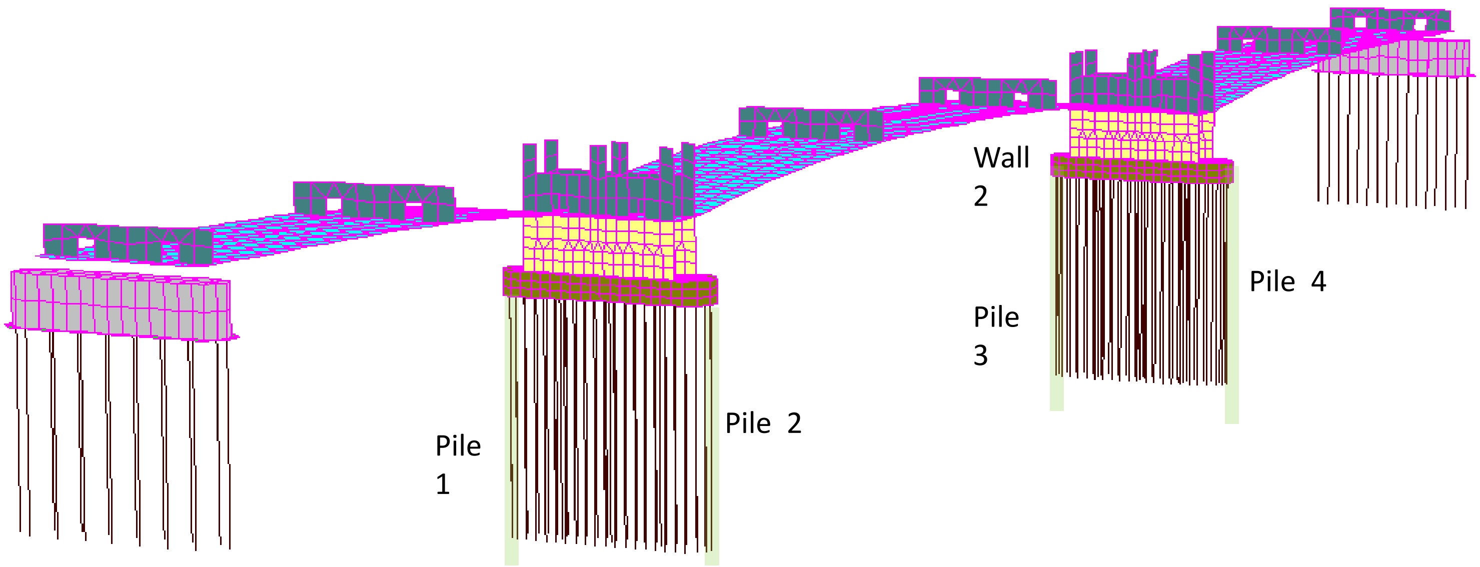

Bridge-Pile Foundation SSI Modeling

橋-杭基礎SSIモデル化

Highway Bridge Model (Flexible)

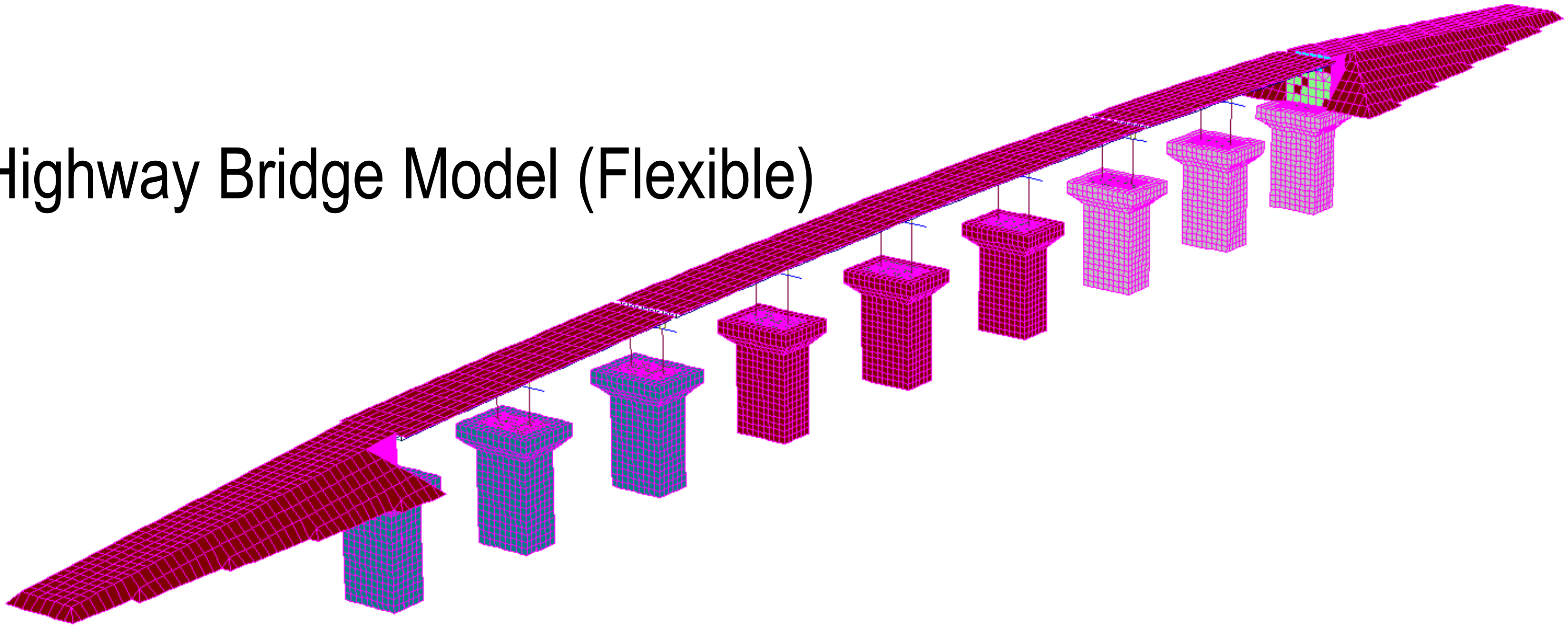

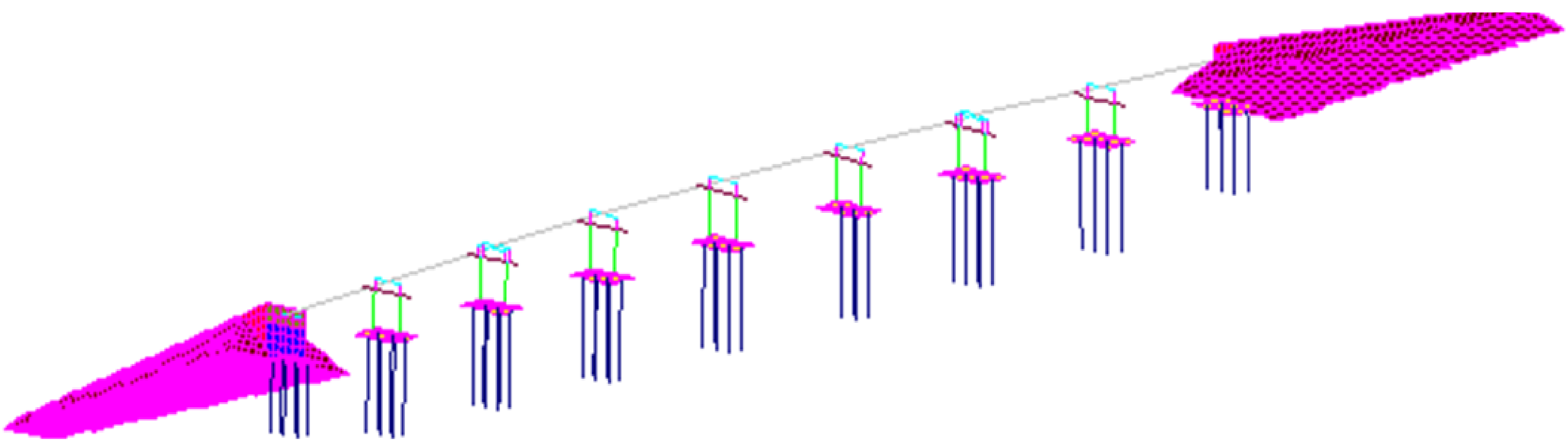

ACS SASSI Pier Pile-Foundation Models

ACS SASSI 橋脚 杭-基礎モデル

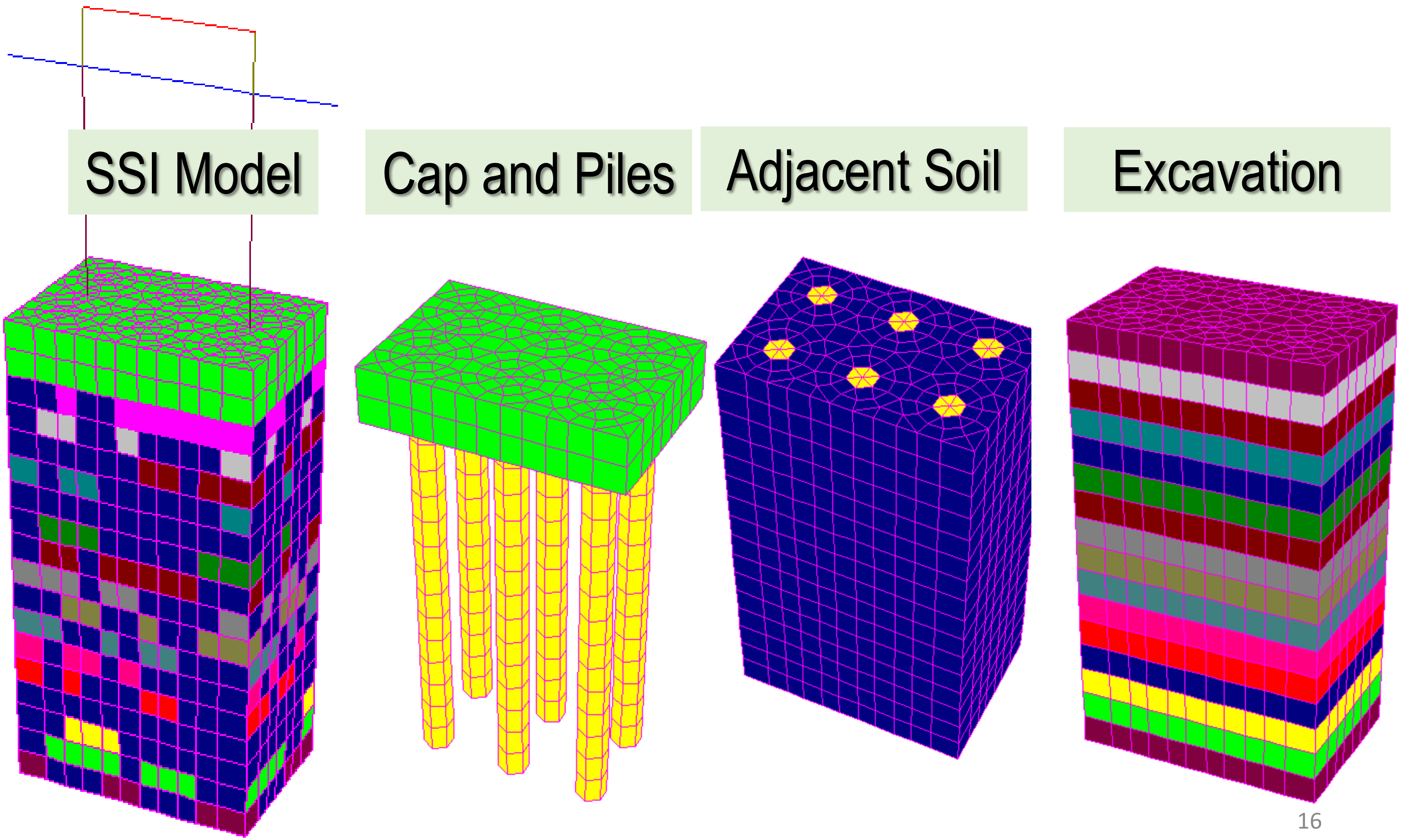

Local Pile Foundation (Hexagon Section)

ローカル杭基礎（六角形断面）

Stress outputs:
Group 5, e1
Group 3, e1-5
Group 7, e1-14

Rdisp outputs:
Node 31, 73, 115, 157, 199, 241, 283, 325, 367, 409, 451, 493, 535, 577, 725, 869, 1059, 1157, 1159, 1161, 1164, 1170

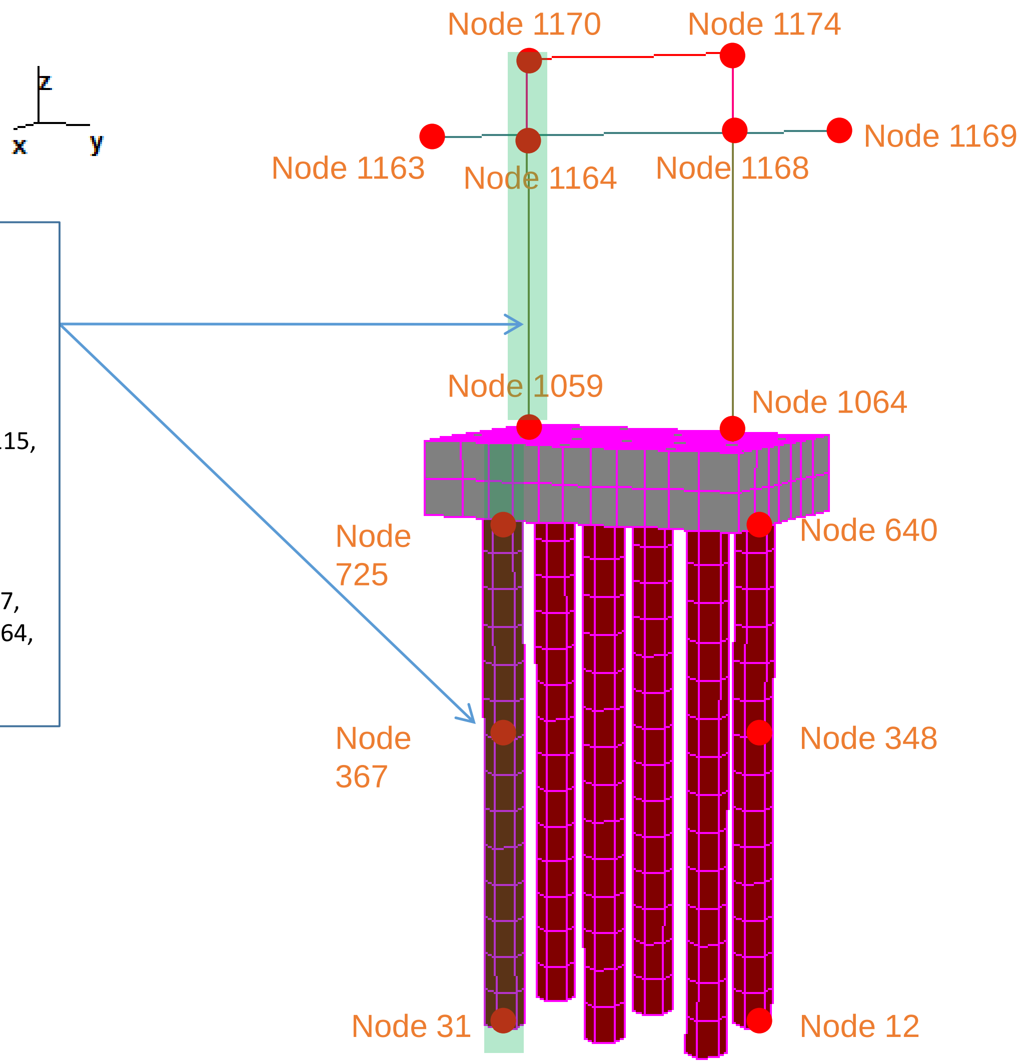

Local Pile Foundation (Square Section)

ローカル杭基礎（四角形断面）

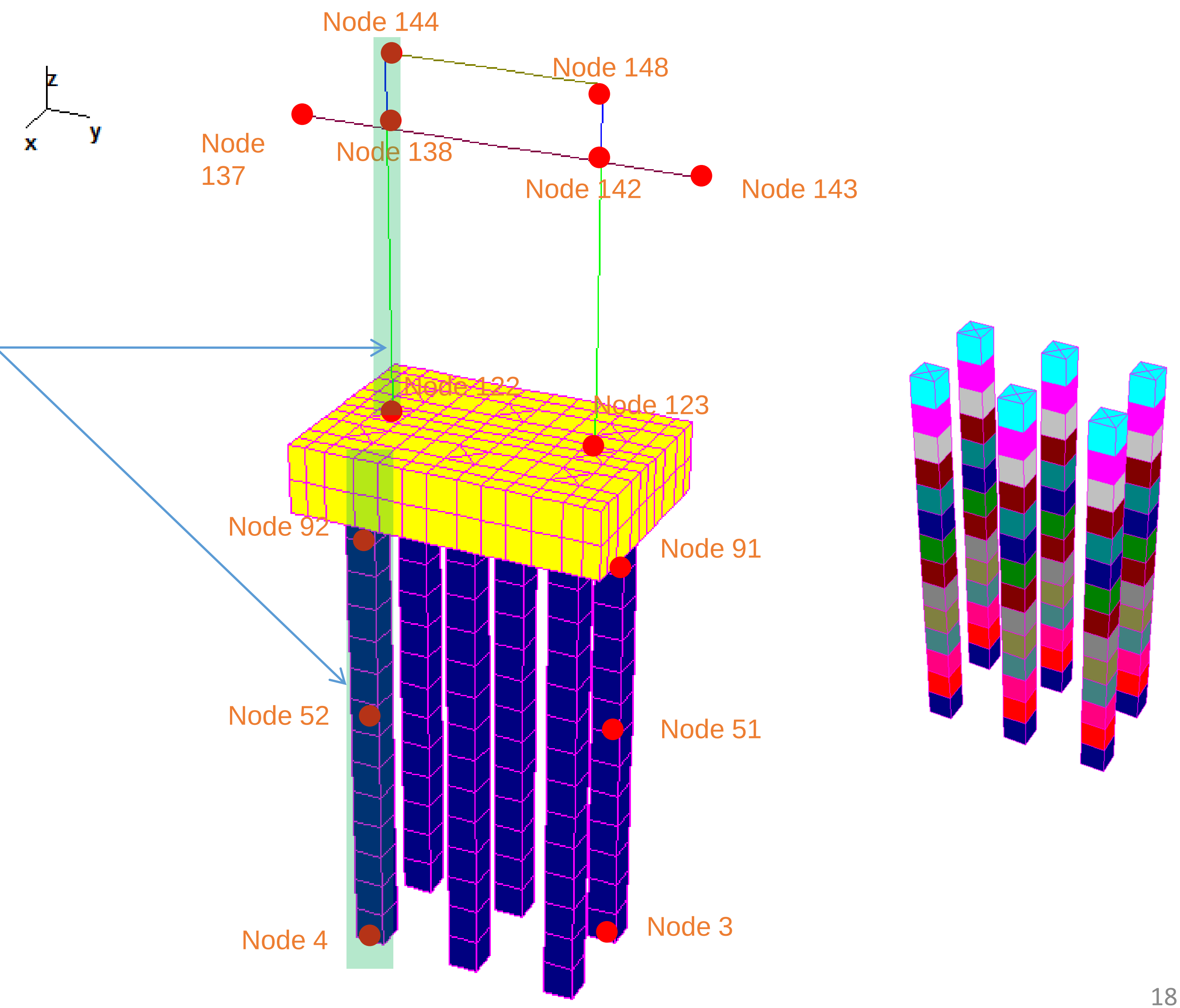

Stress outputs:
Group 5, e1
Group 3, e1-5
Group 7, e1-14

Rdisp outputs:
Node 4, 10, 16, 22, 28, 34, 40, 46, 52, 58, 64, 70, 76, 82, 92, 106, 122, 131, 133, 135, 138, 144

Local Pile Foundation Including Adjacent Soil

周辺土壌を含むローカル杭基礎

Stress outputs:
Group 6, e1
Group 4, e1-5
Group 8, e1-16

Rdisp outputs:
Node 137, 325, 513, 701, 889, 1077, 1265, 1453, 1641, 1829, 2017, 2205, 2393, 2581, 2769, 2957, 3145, 3289,3479, 3577, 3579, 3581, 3584, 3590

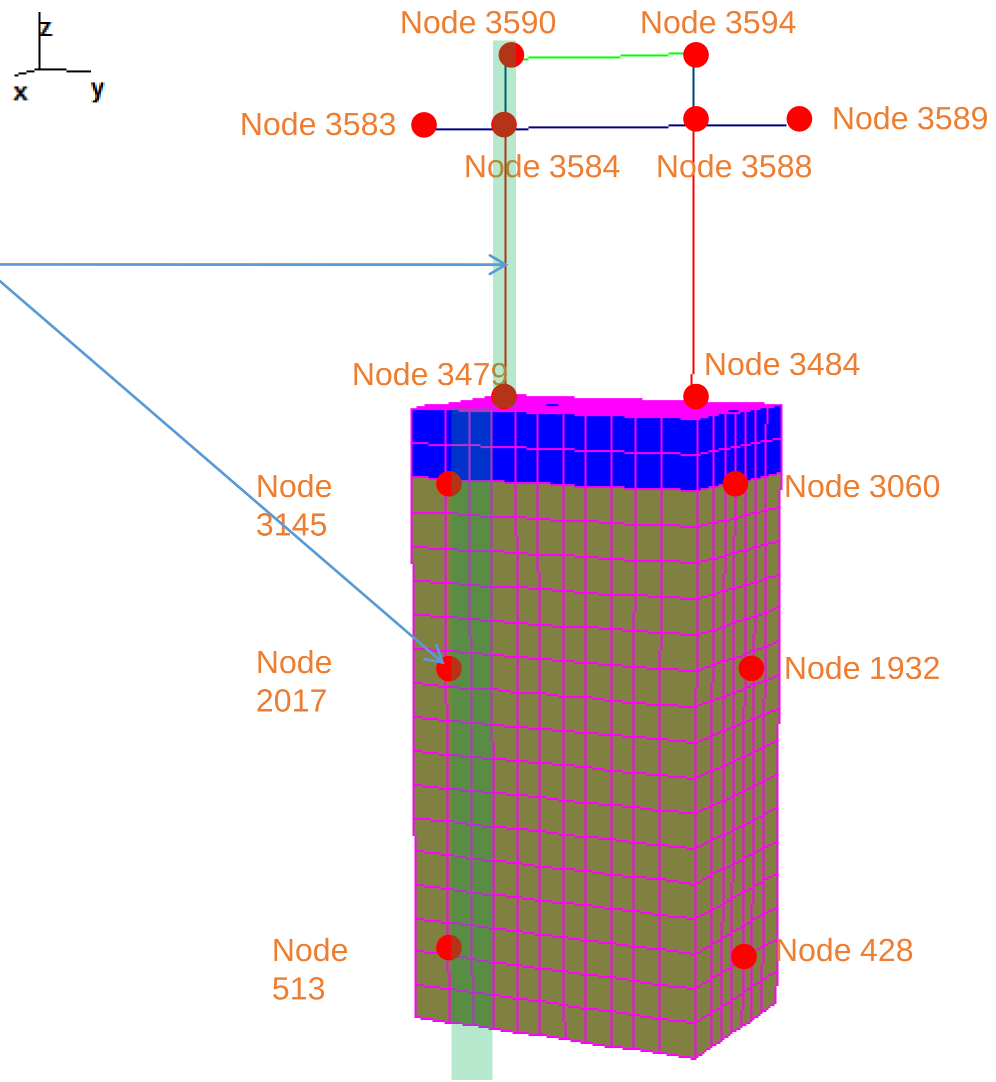

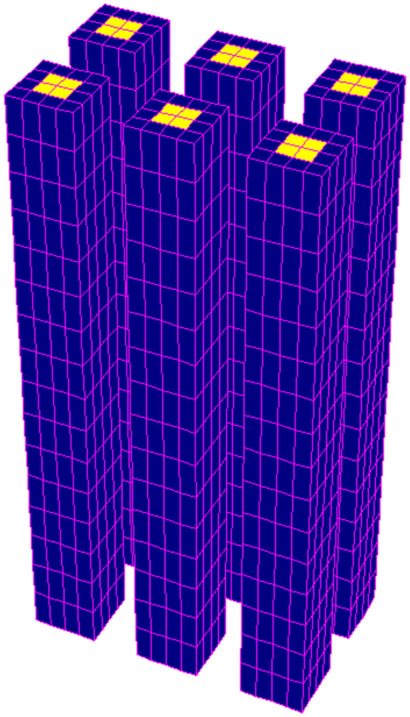

Single Pile Modeling Using Solid Elements

ソリッド要素を用いた単一の杭モデル化

Horizontal Motion

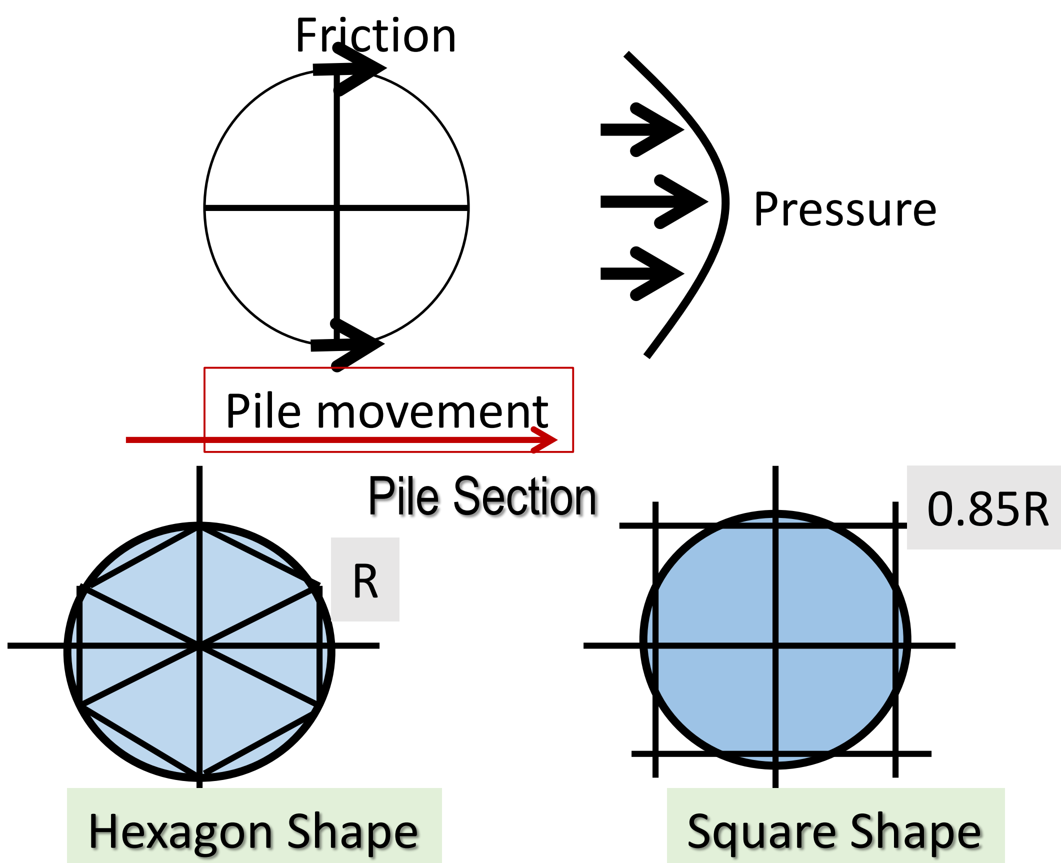

Pile-Soil Interface Modeling Using Option NON

オプションNONを用いた杭-土インターフェースのモデル化

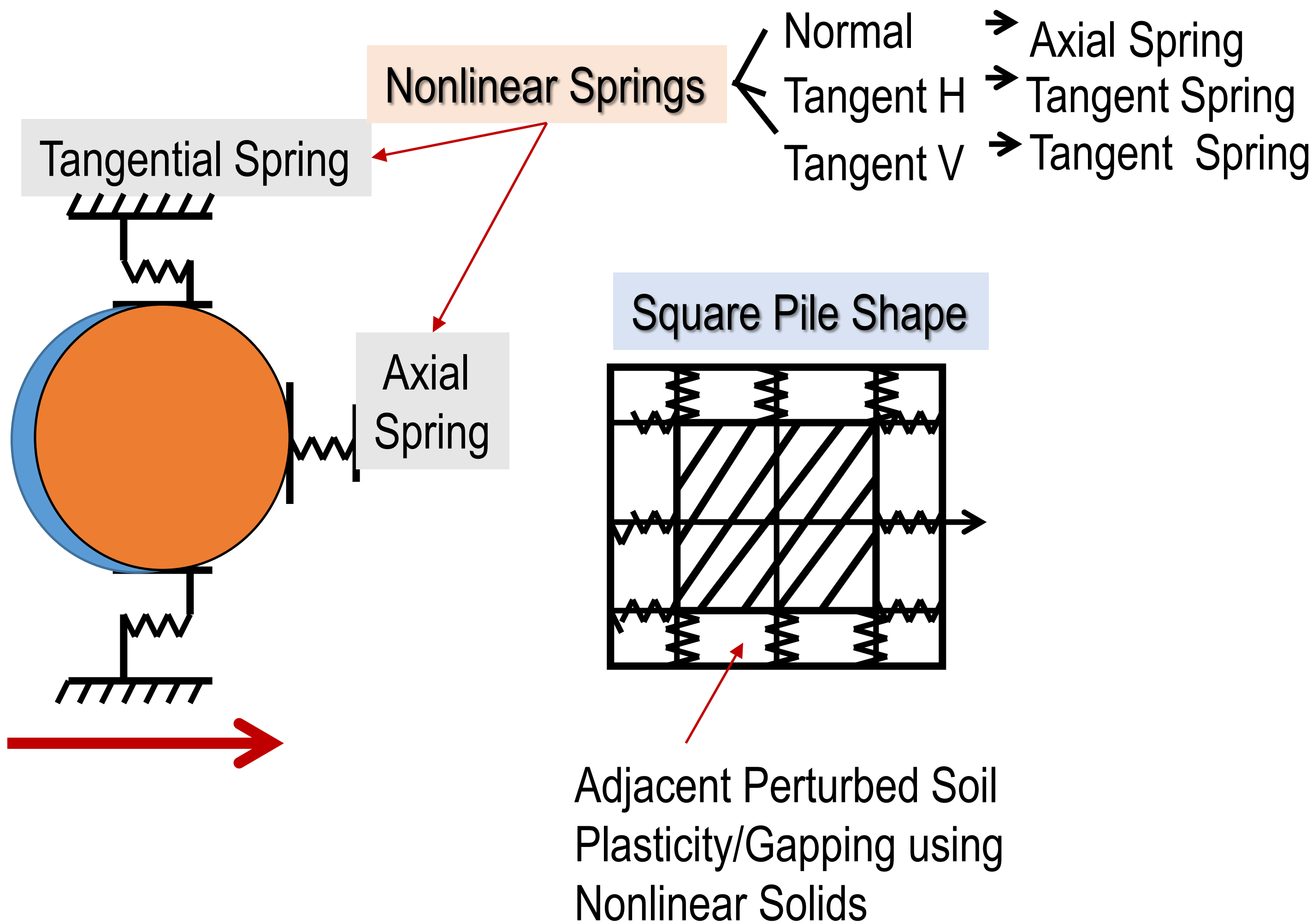

Adjacent Soil Local Plasticity Using Nonlinear Solid Elements 非線形ソリッド要素を用いた周辺土壌の塑性

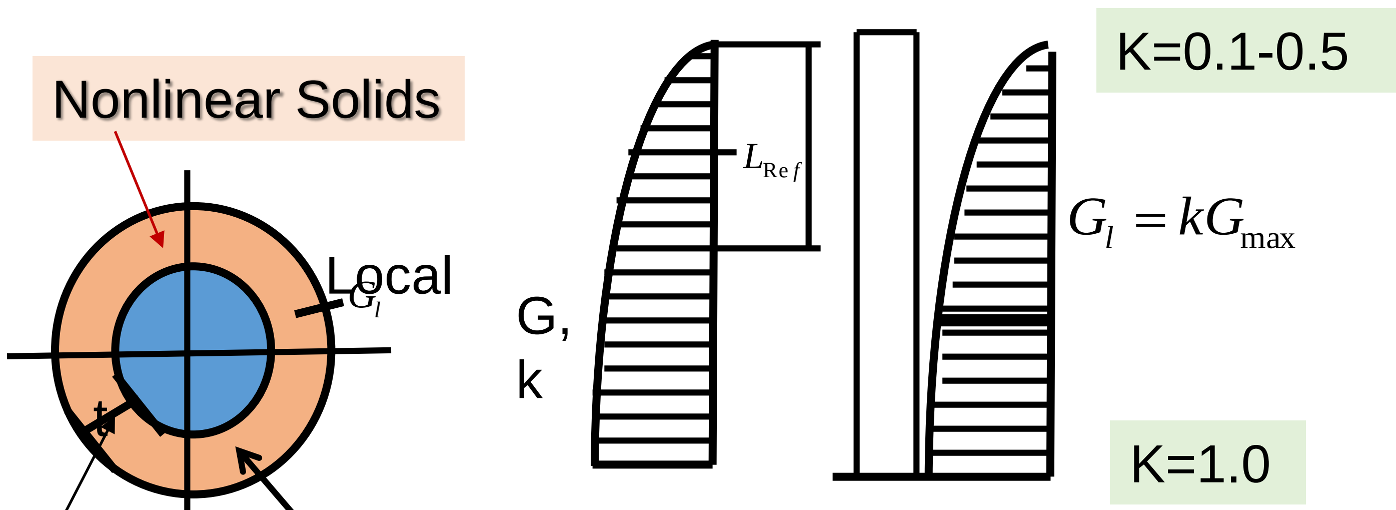

$t = 0.25 - 1.0R$

$G_l = kG_{max}$

$k = f(depth)$

$$G_l = G_{max}\left(\frac{X}{L_{Ref}}\right)^n$$

$$n \sim 0.5$$

Pile Group Modeling Including Nonlinear Soil

非線形土壌を含む杭群モデル化

Horizontal Motion

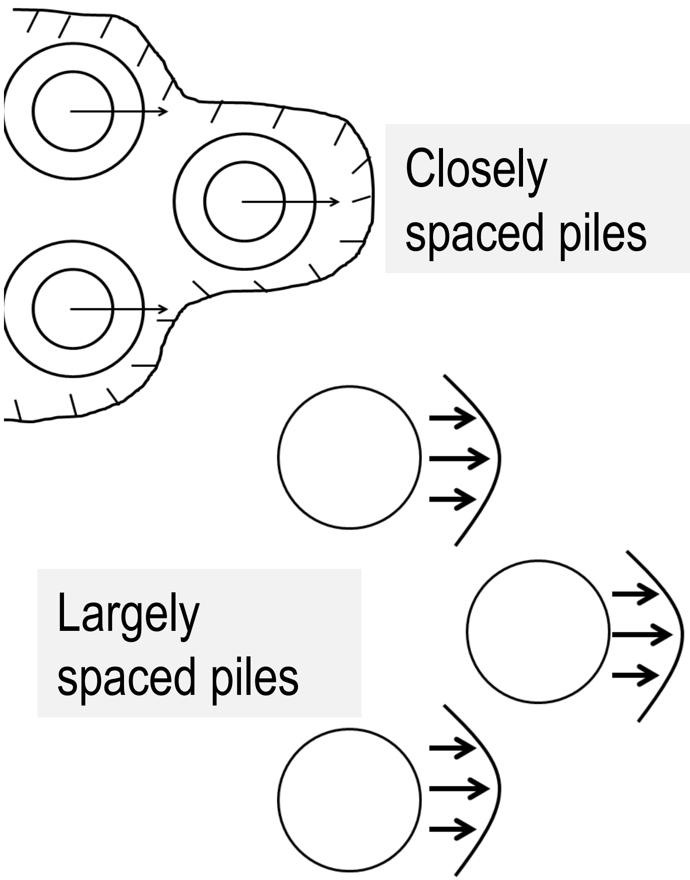

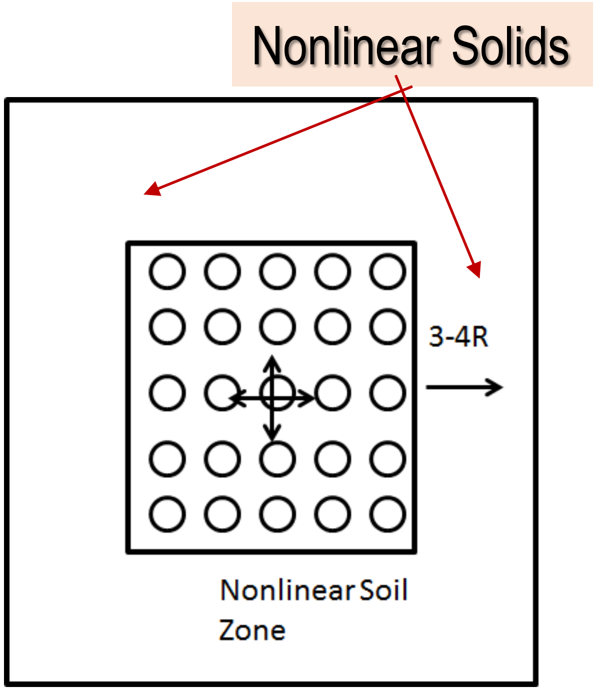

Pile Vertical Motion Including Slipping

すべりを含む杭の垂直モーション

Vertical Motion

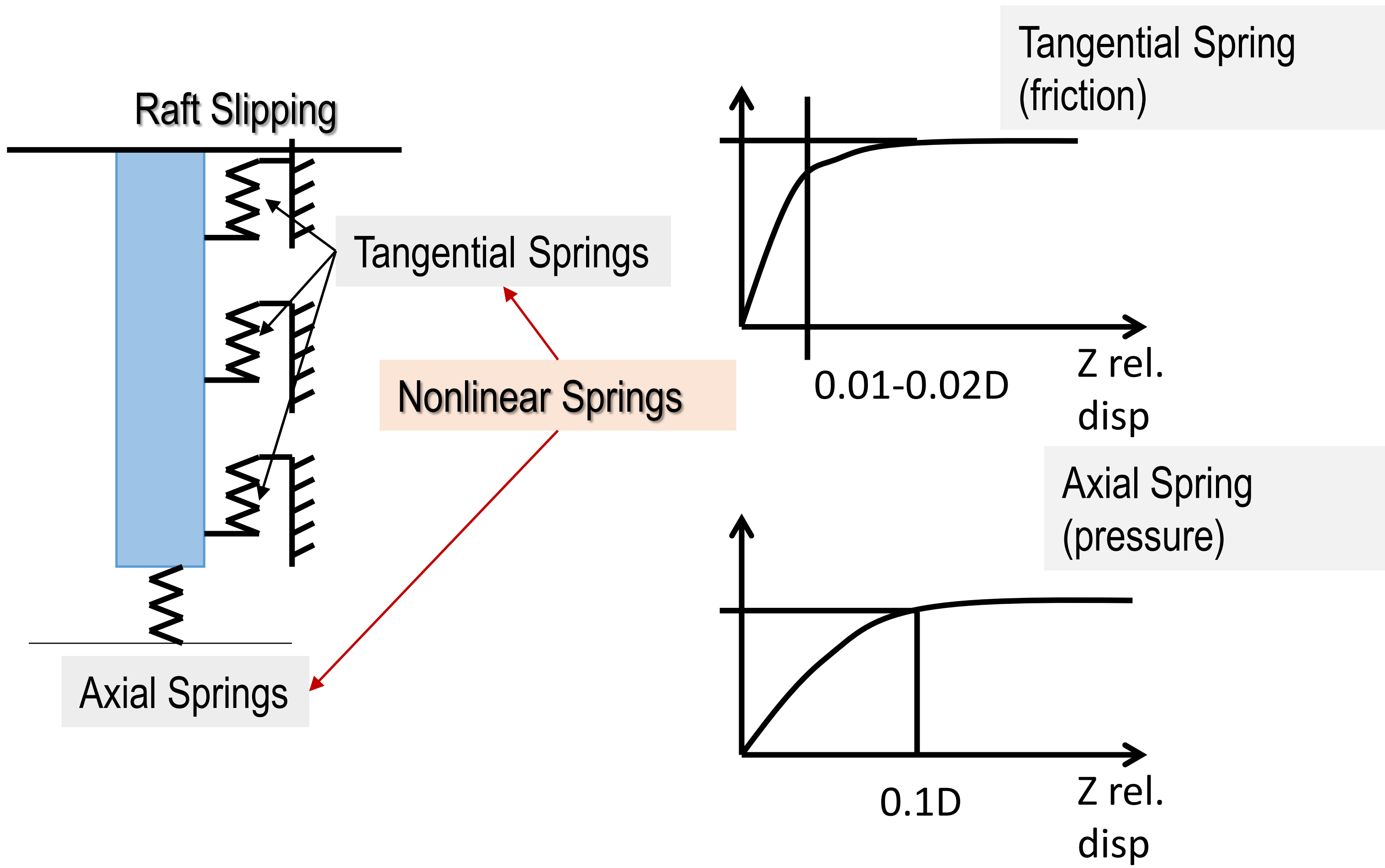

Pile Vertical Motion at Bottom

底部の杭の垂直モーション

Vertical Motion

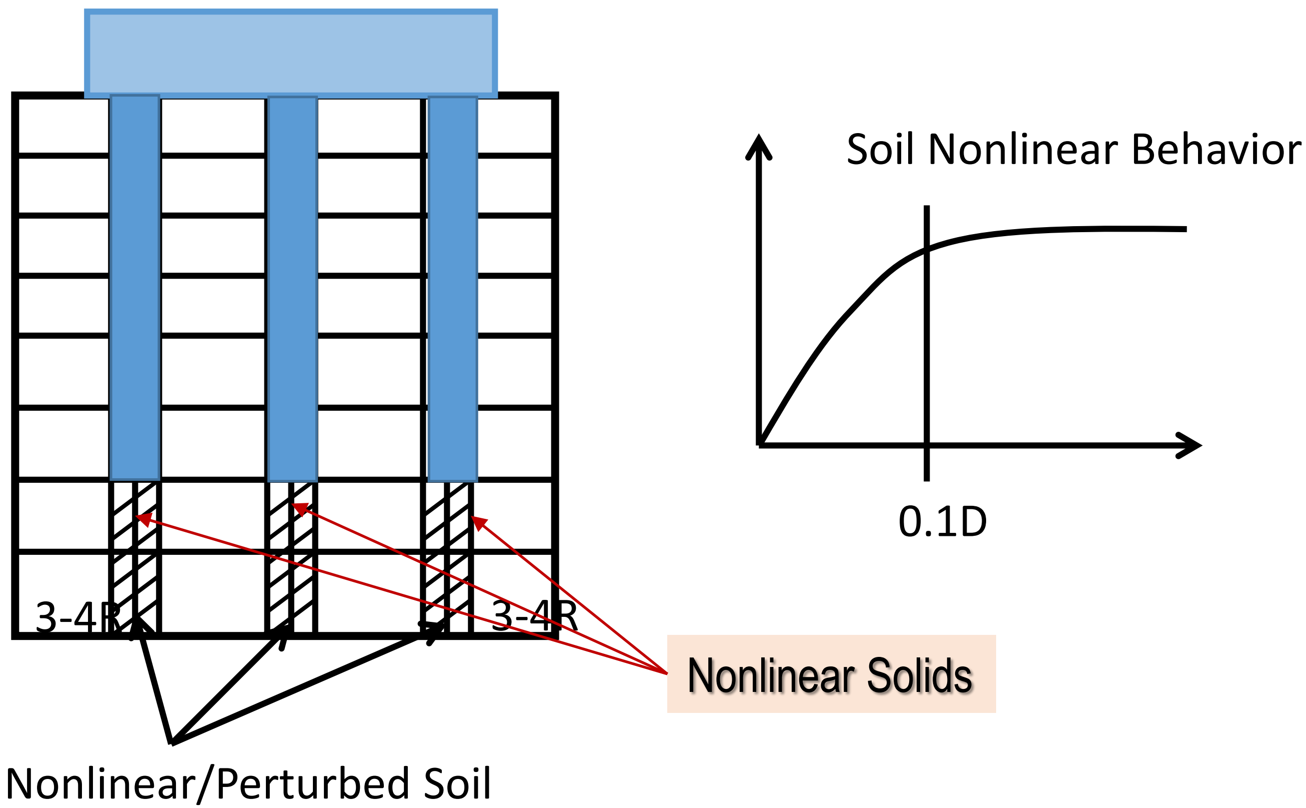

3. Case Studies: Fartec Highway Bridge SSI Analysis
ケーススタディ：ファーテック高速道路橋のSSI解析

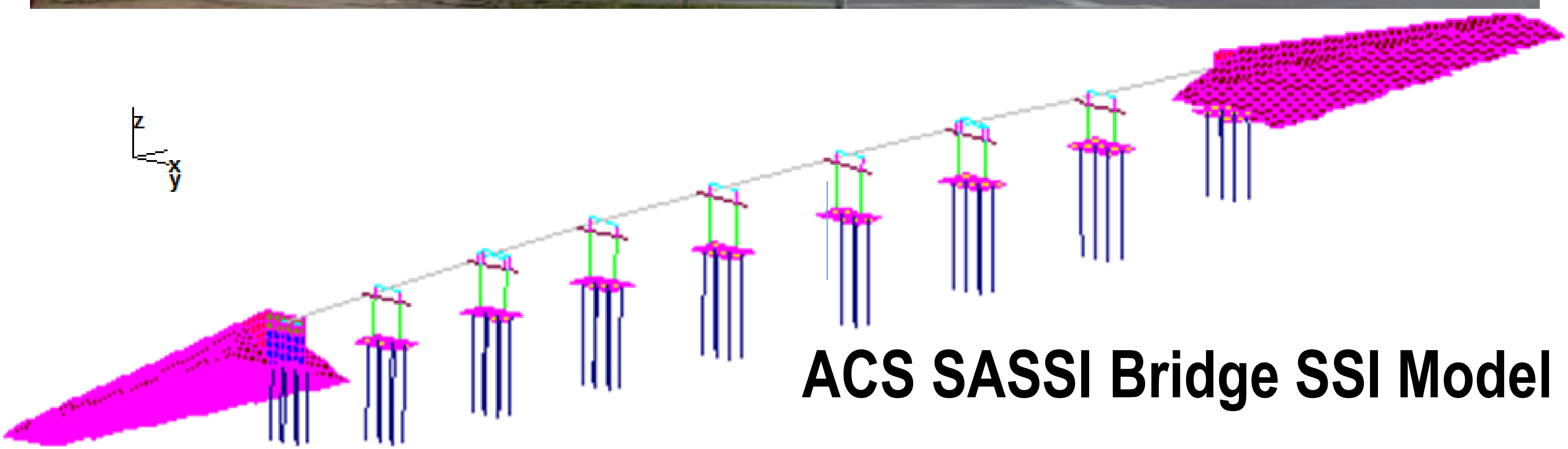

ACS SASSI Bridge SSI Model

Seismic SSI Analysis Inputs

SSI耐震解析の入力データ

Seismic Input Motion at Ground Surface:

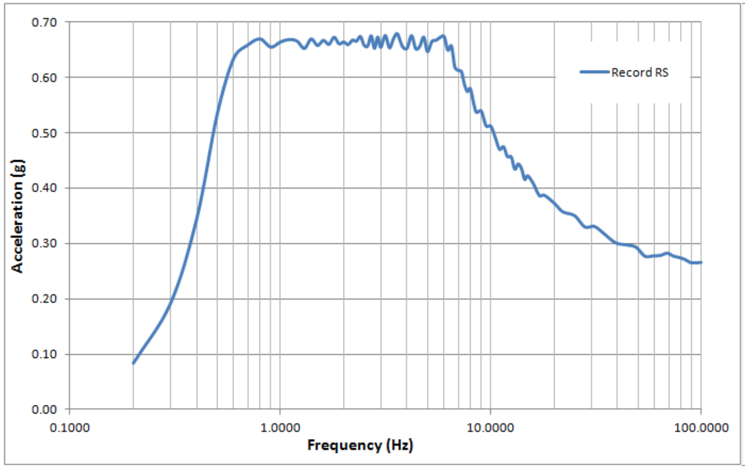

Design Spectrum (0.25g)

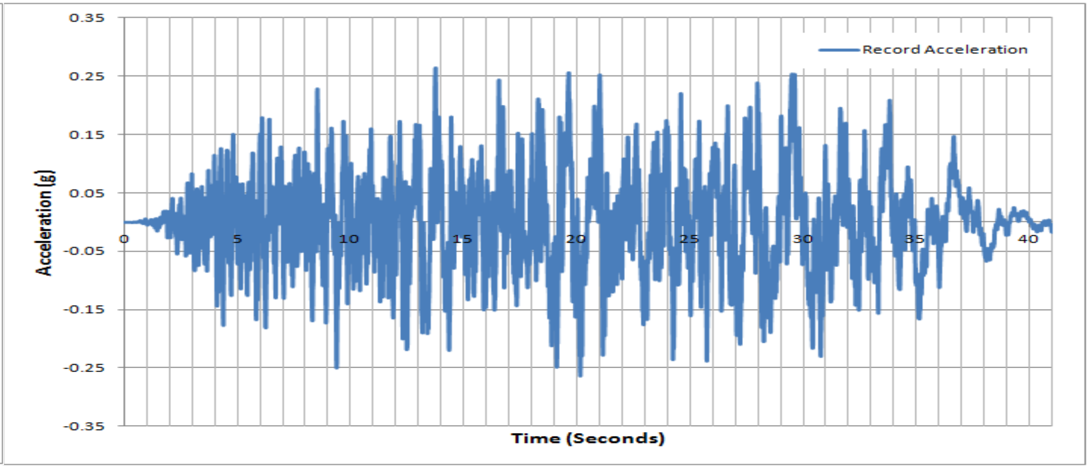

Simulated Acceleration Input (0.25g)

Incoherent Motion:

2005 Abrahamson coherency model, with wave passage Va=1,300m/s

Soil Layering:

Hard Soil: Vs=1,300m/s, Uniform Profile

Soft Soil: Vs=200m/s, Uniform Profile

SSI Response Locations

SSI応答位置

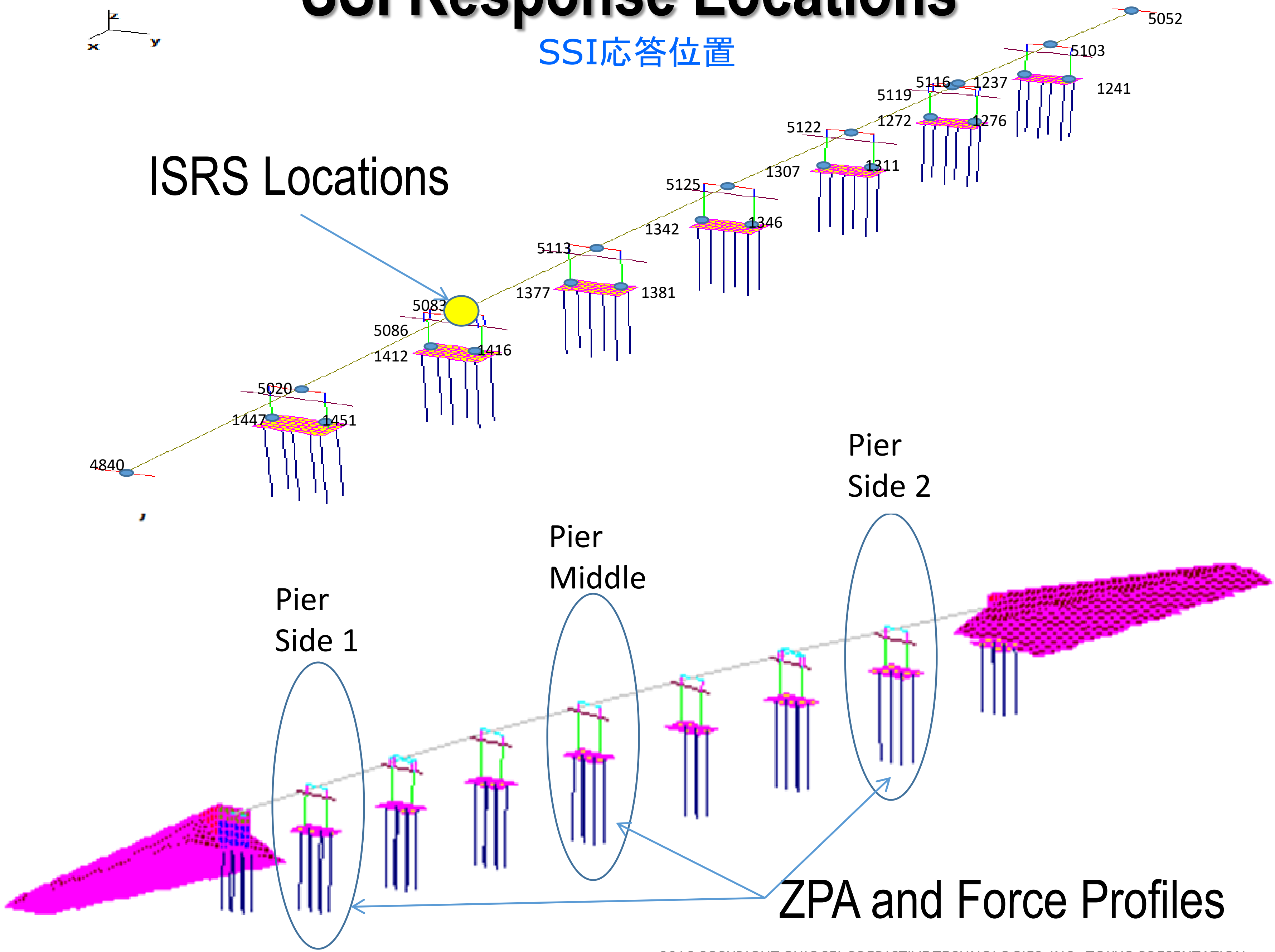

SSI Response Acceleration Transfer Functions

SSI応答加速度伝達関数

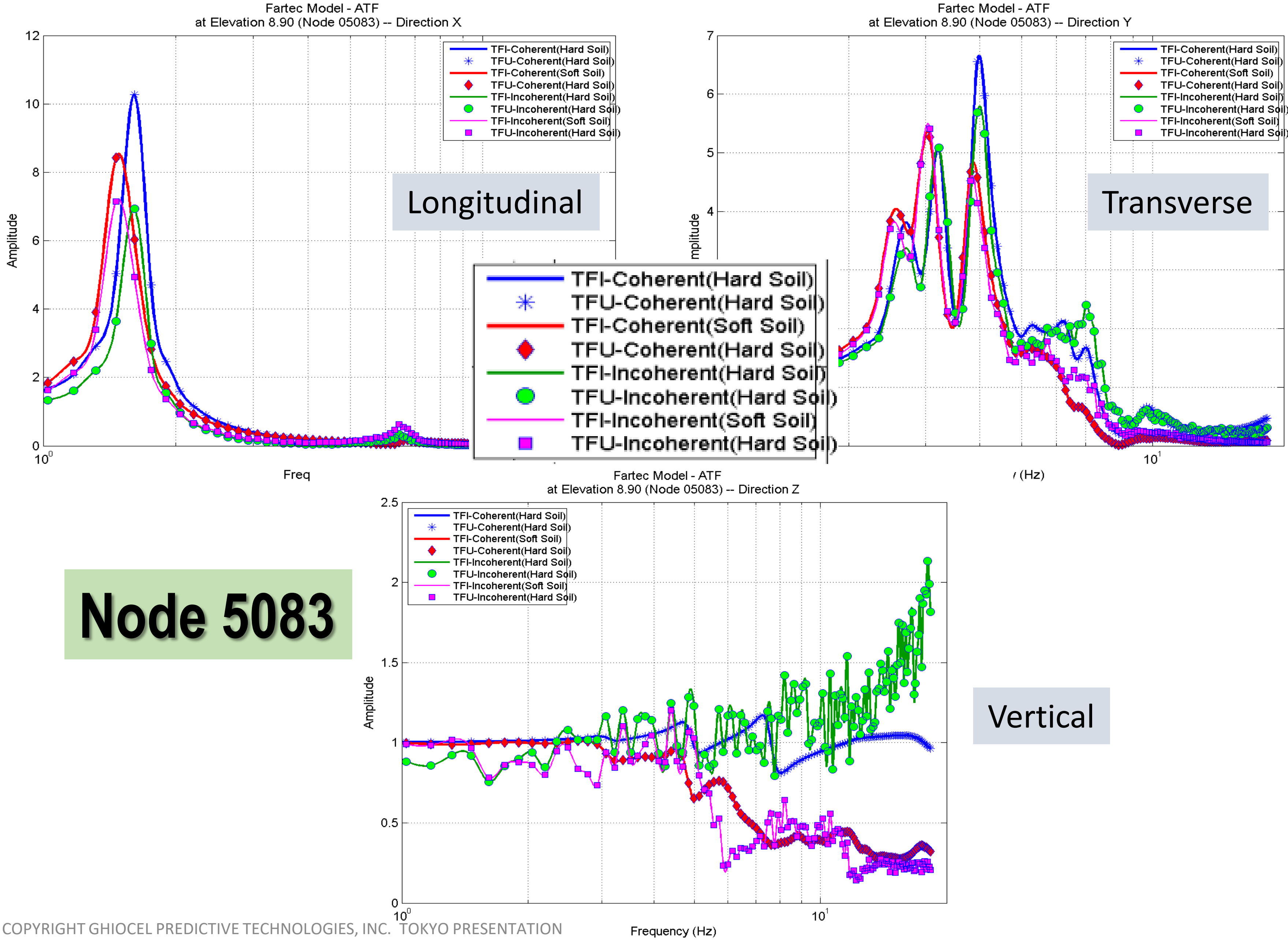

SSI Response Acceleration Response Spectra

SSI応答加速度スペクトル

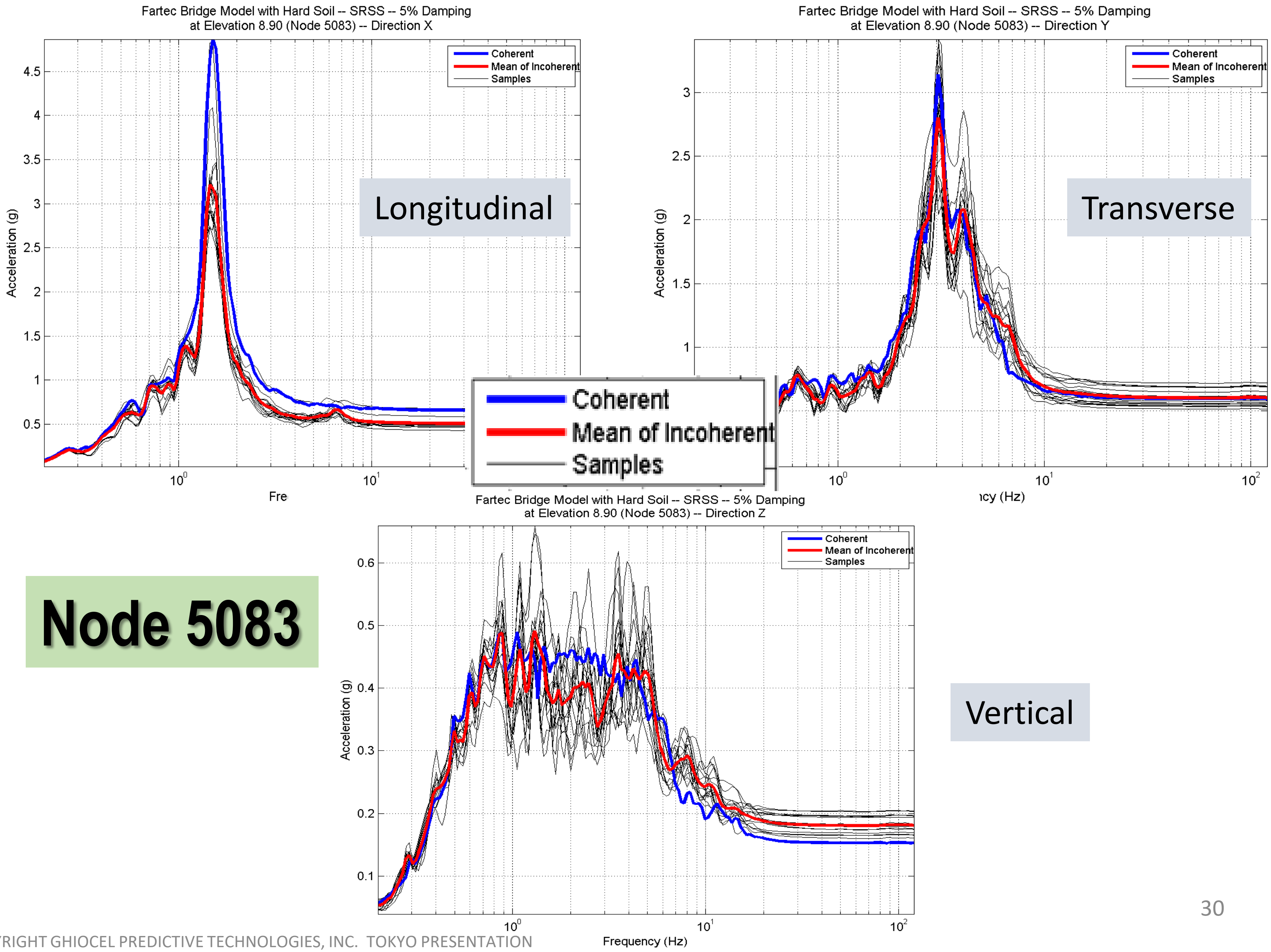

SSI Maximum Acceleration Profile at Pier Side 1

SSI最大加速度プロファイル、橋脚サイド１

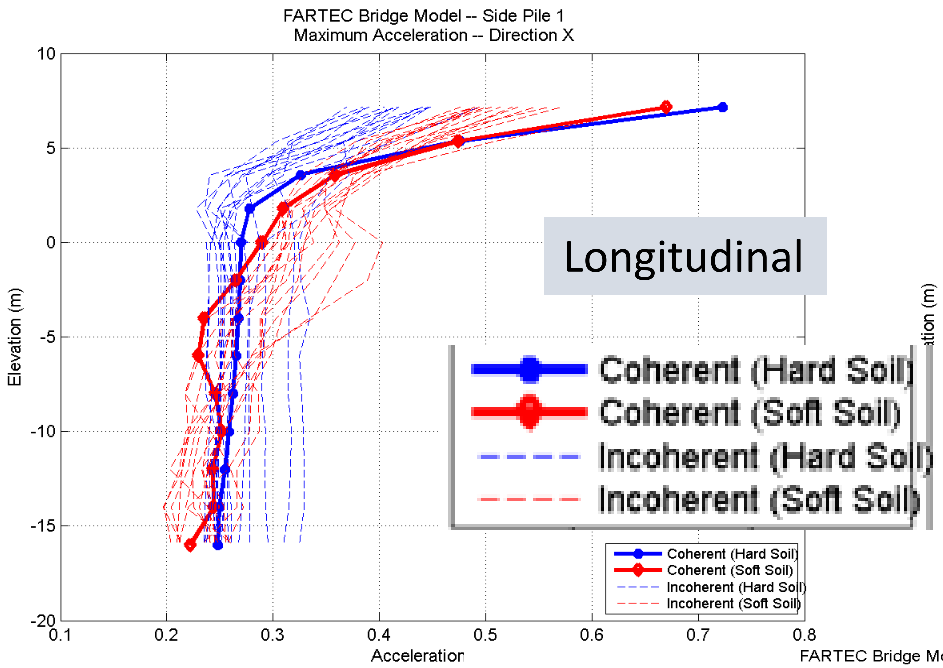

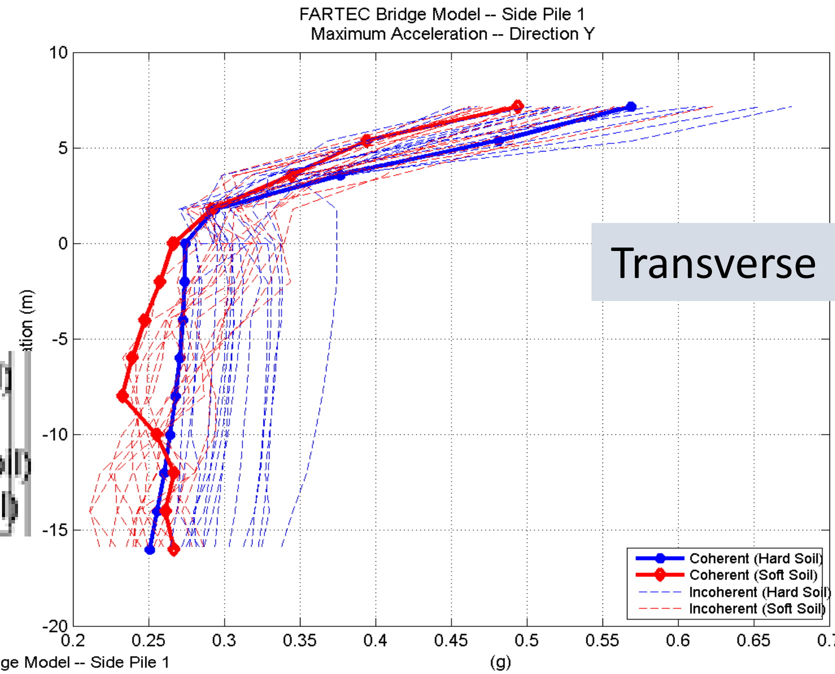

Pier Side 1

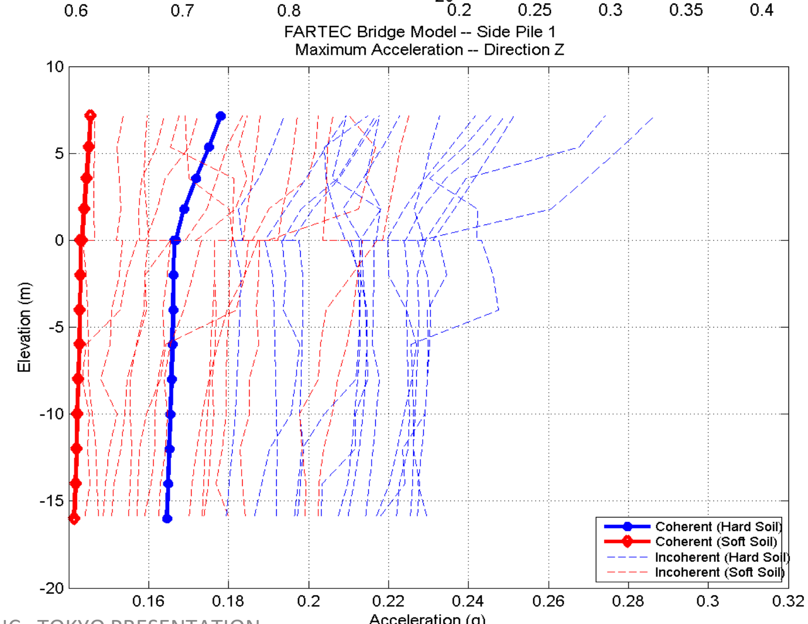

SSI Maximum Displacement Profile at Pier Side 1

SSI最大変位プロファイル、橋脚サイド１

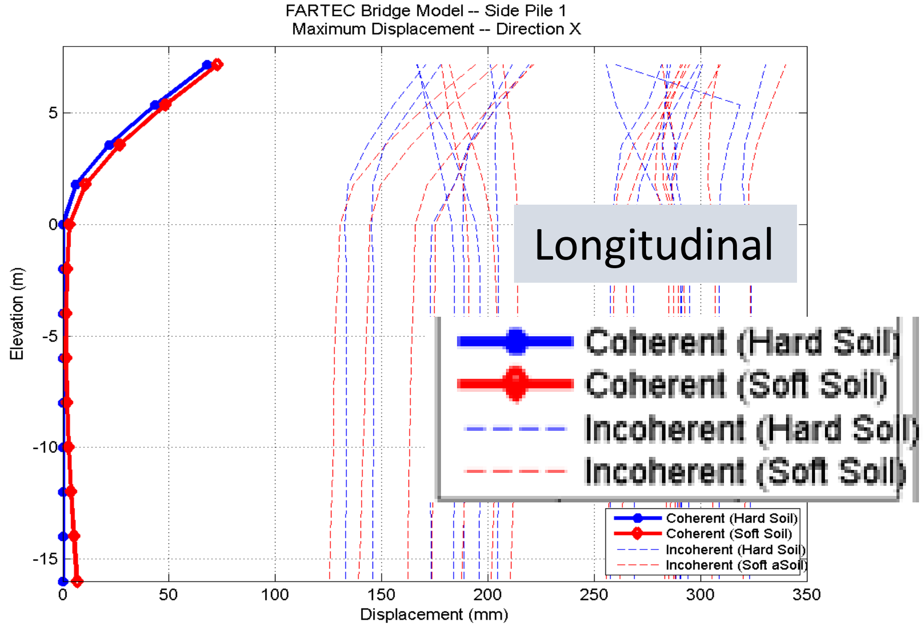

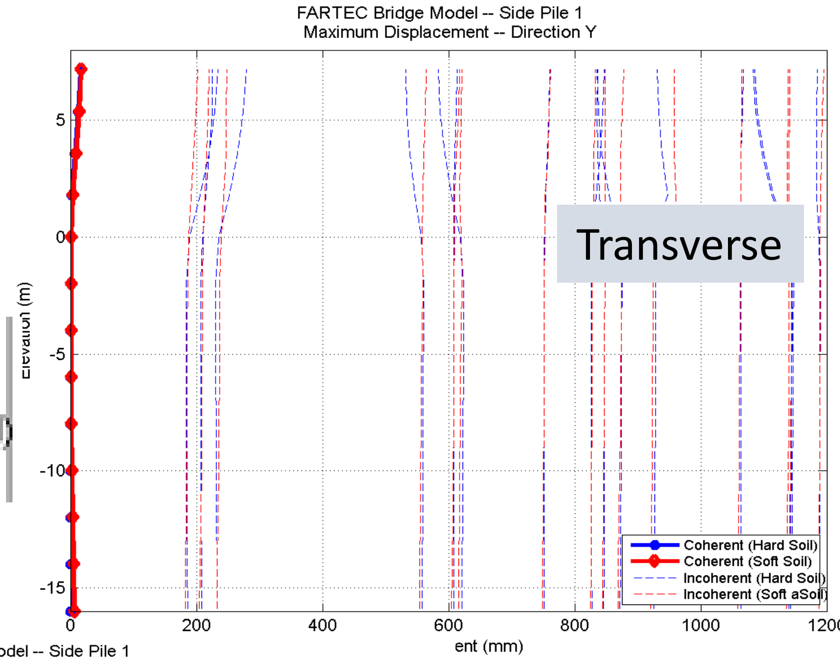

Pier Side 1

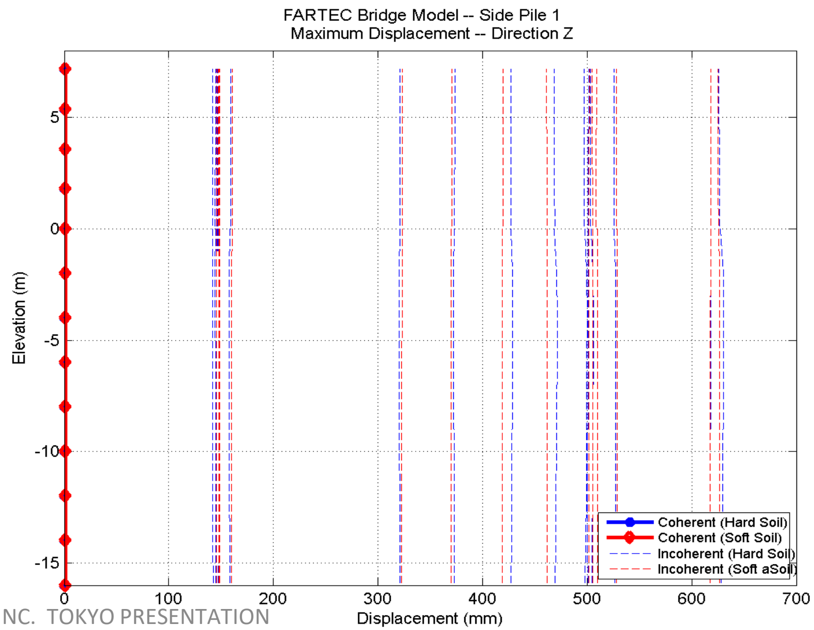

Vertical

SSI Response ZPA Profile at Pier Side 2

SSI応答ZPAプロファイル、橋脚サイド２

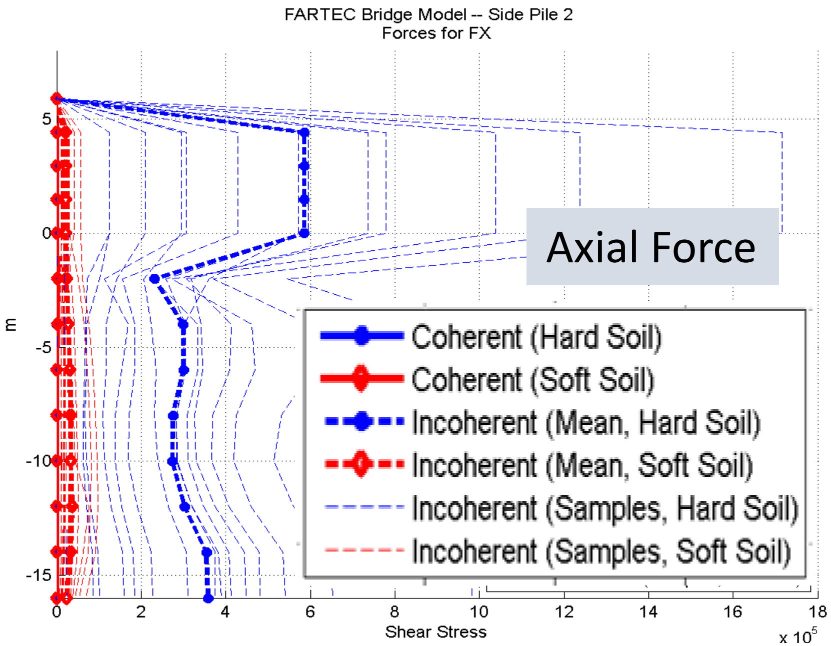

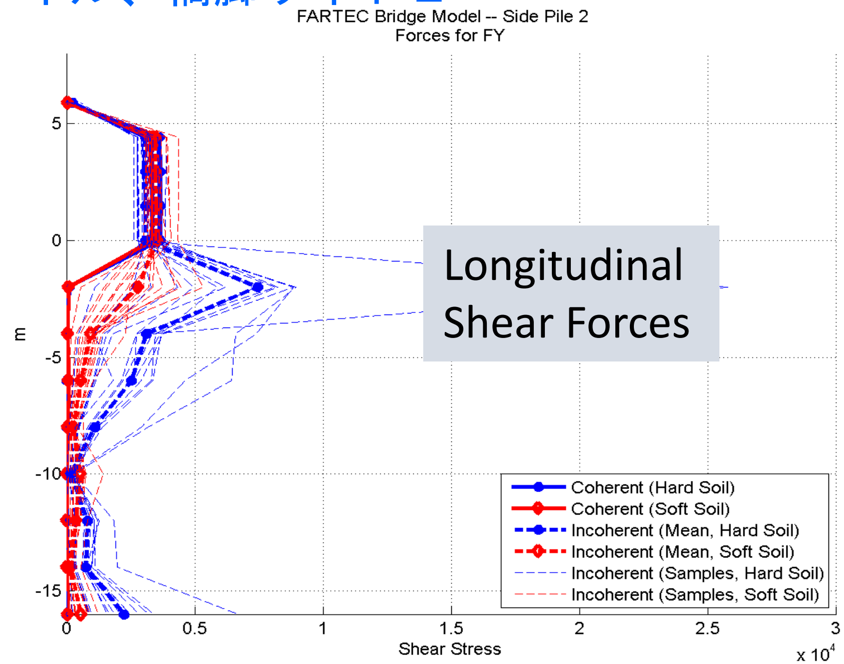

Pier Side 2

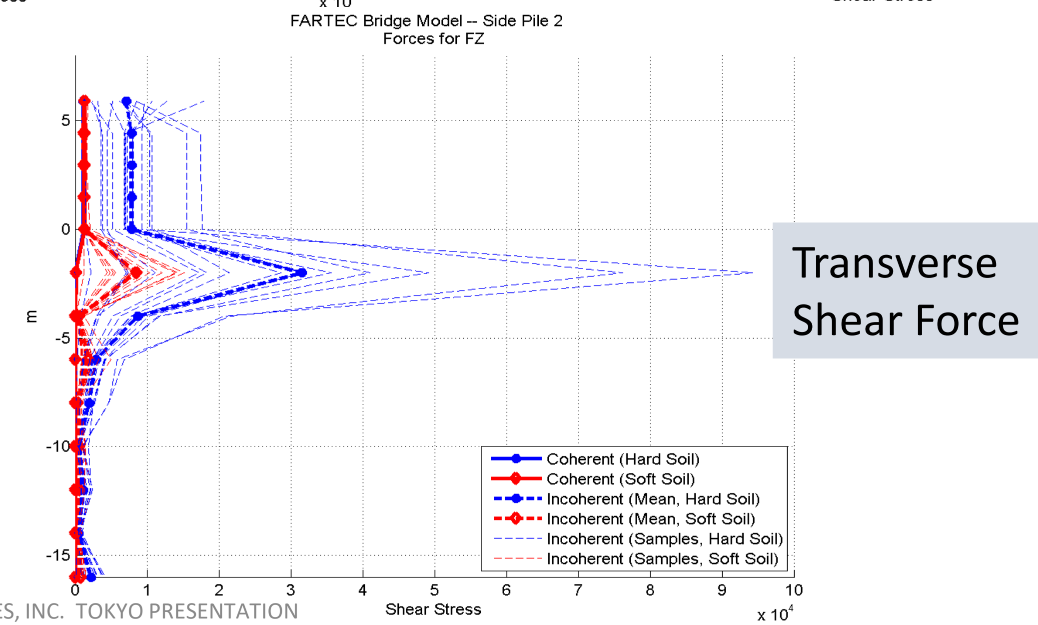

SSI Response ZPA Profile at Pier Side 2

SSI応答ZPAプロファイル、橋脚サイド２

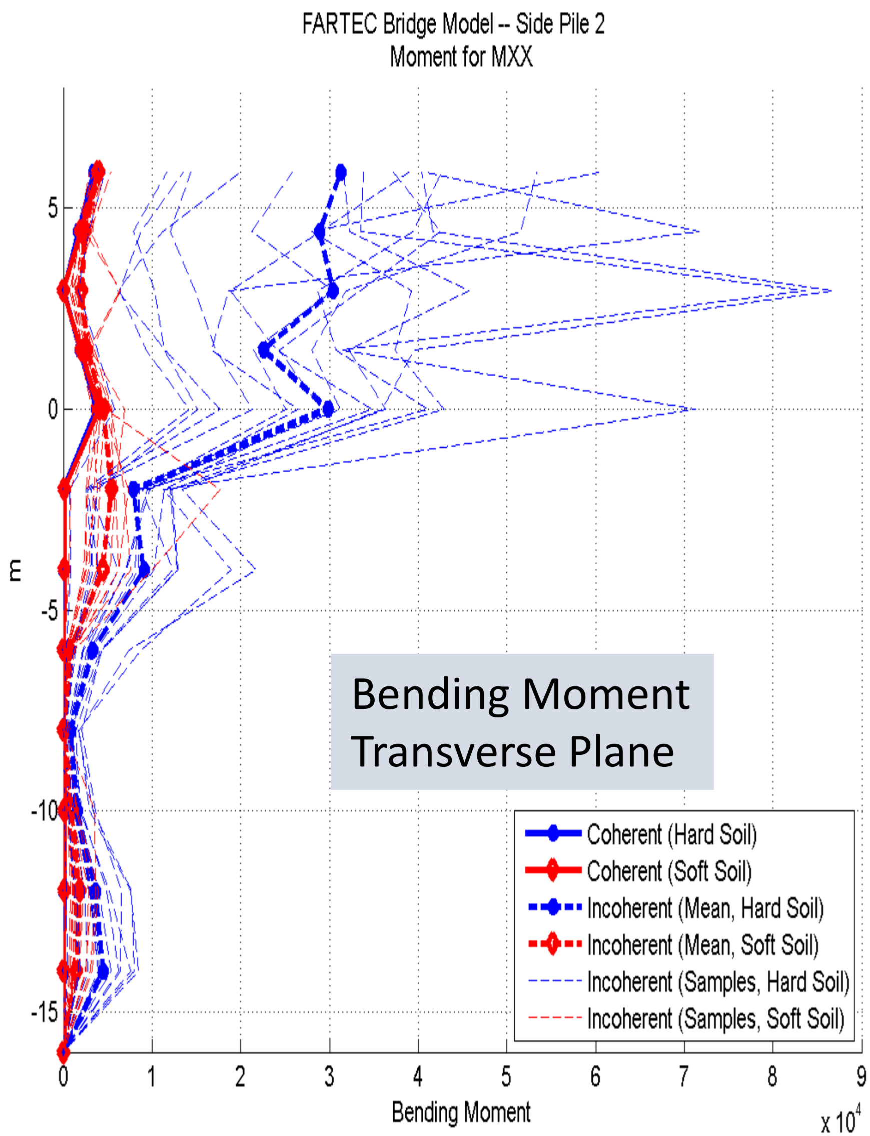

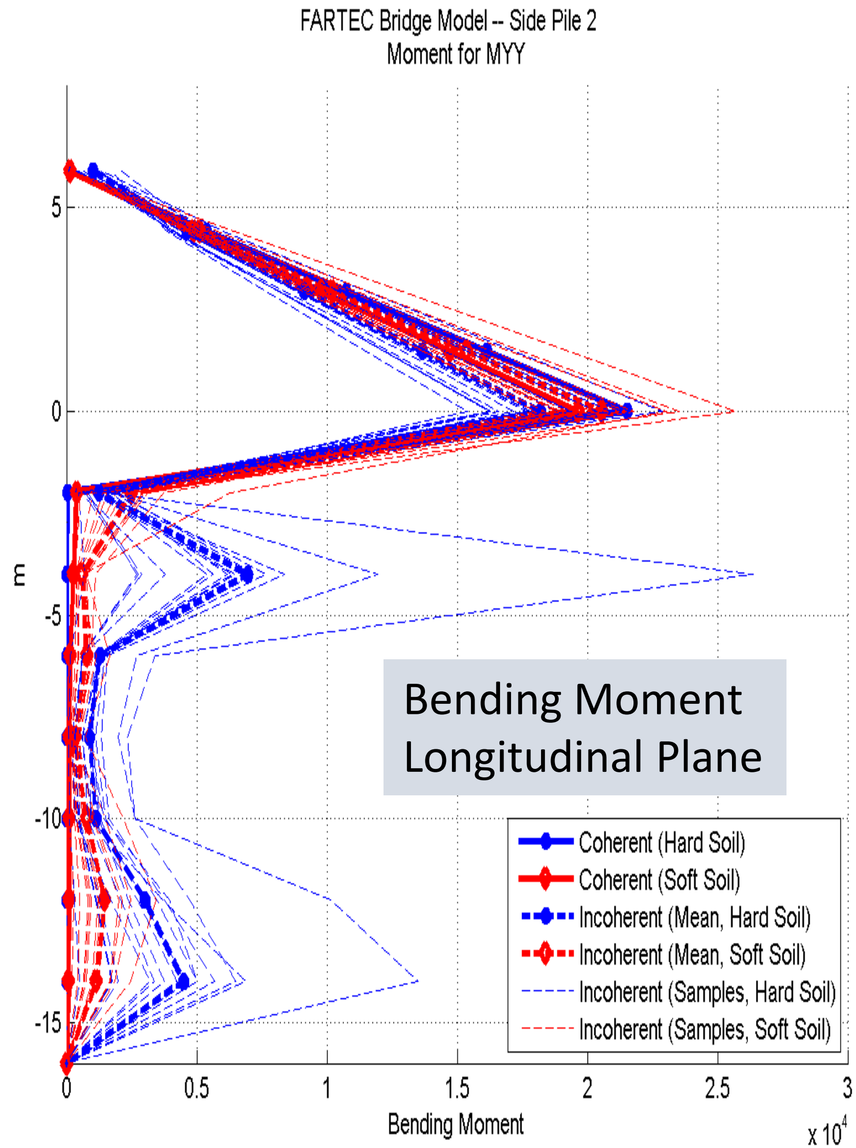

Comparison of SSI Analysis and Design Analysis Results Using Eurocode 8

SSI解析とEurocode8を用いた設計解析結果比較

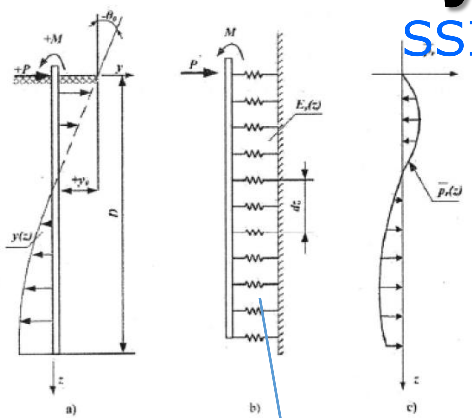

Design Model

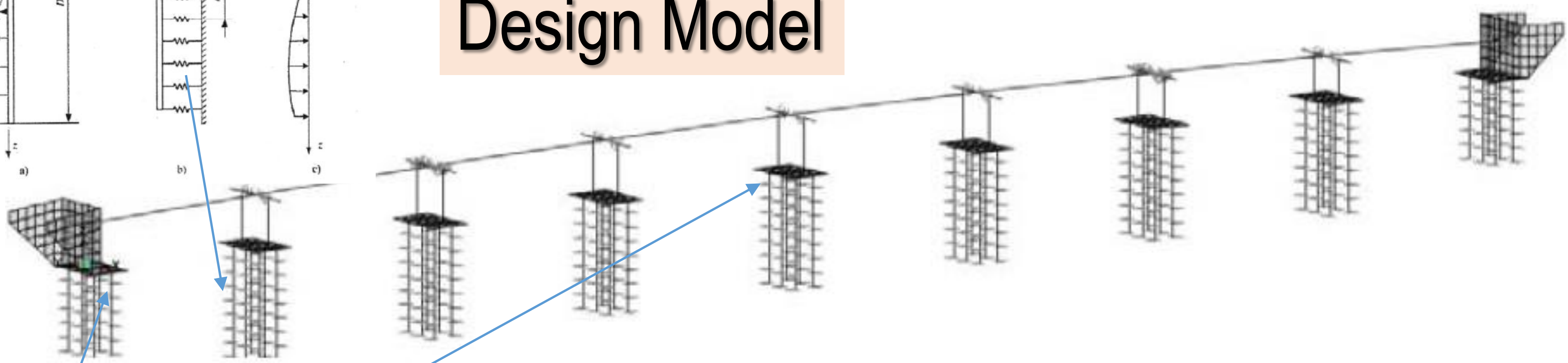

SSI Model

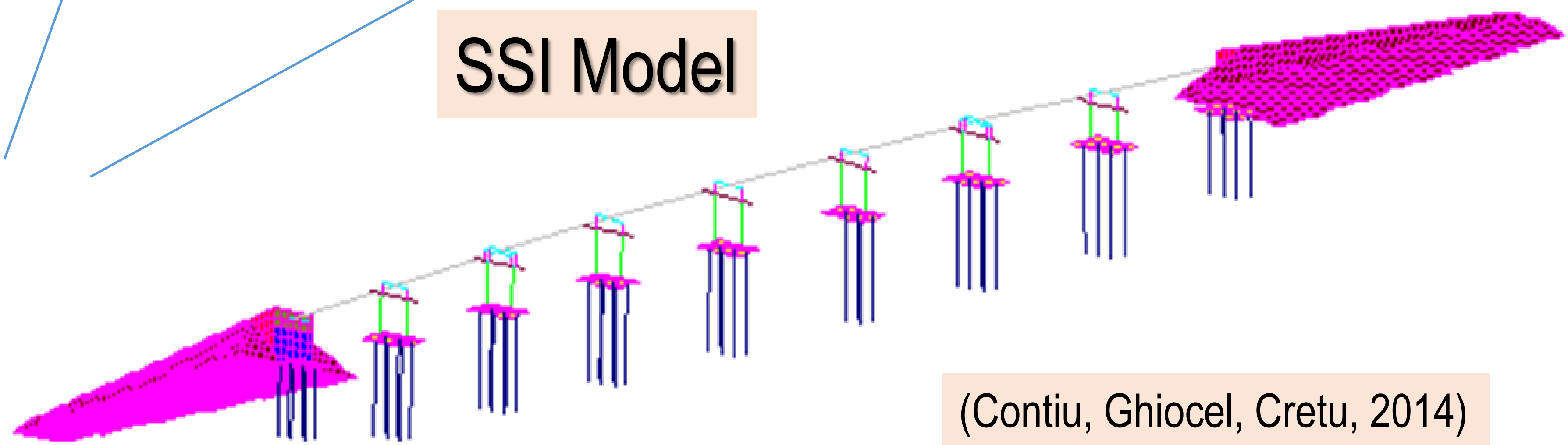

(Contiu, Ghiocel, Cretu, 2014)

X-Input (Long) SSI Analysis and Eurocode 8

X方向-入力SSI解析とEurocode8

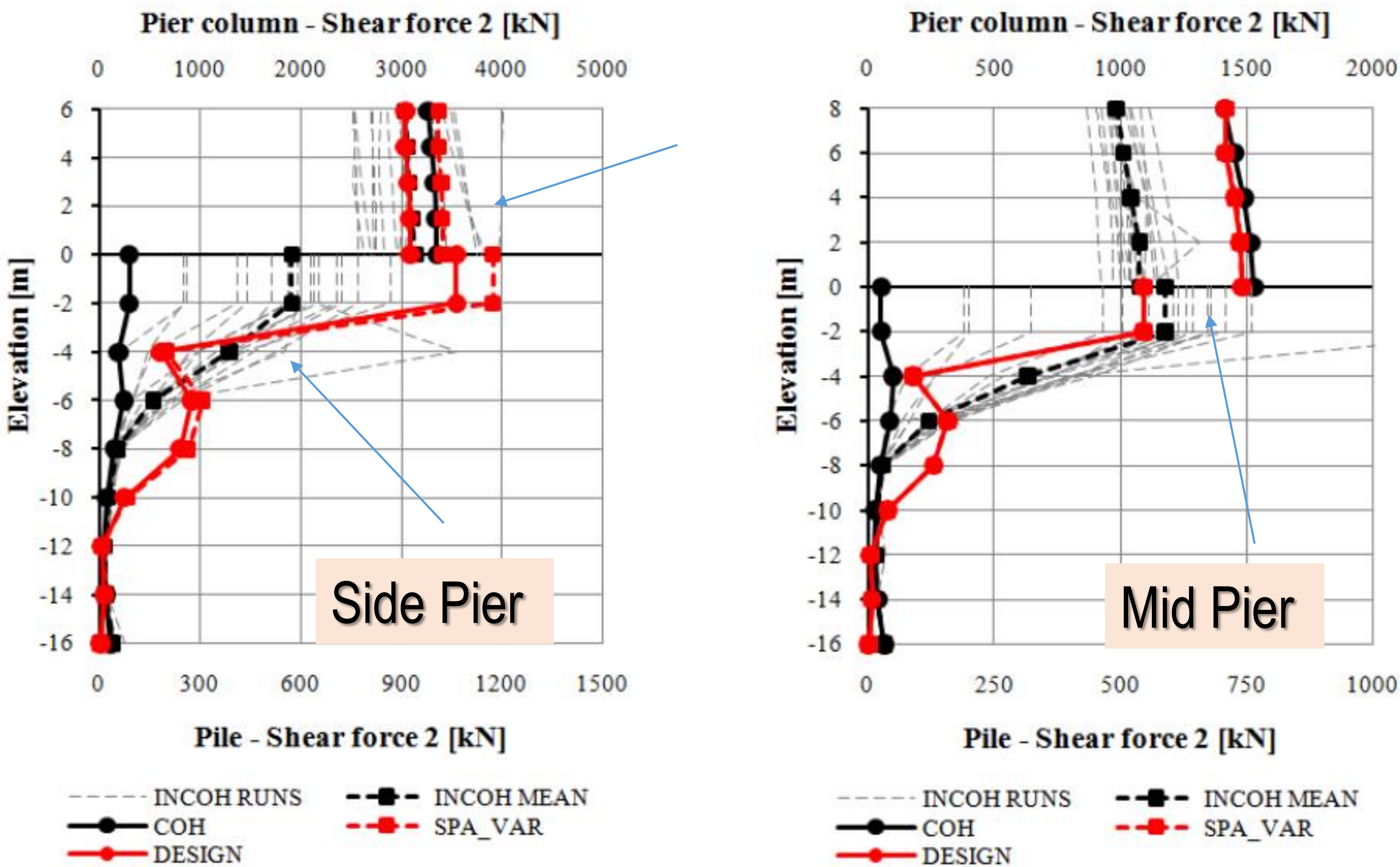

X-Input (Long) SSI Analysis and Eurocode 8

X方向-入力SSI解析とEurocode8

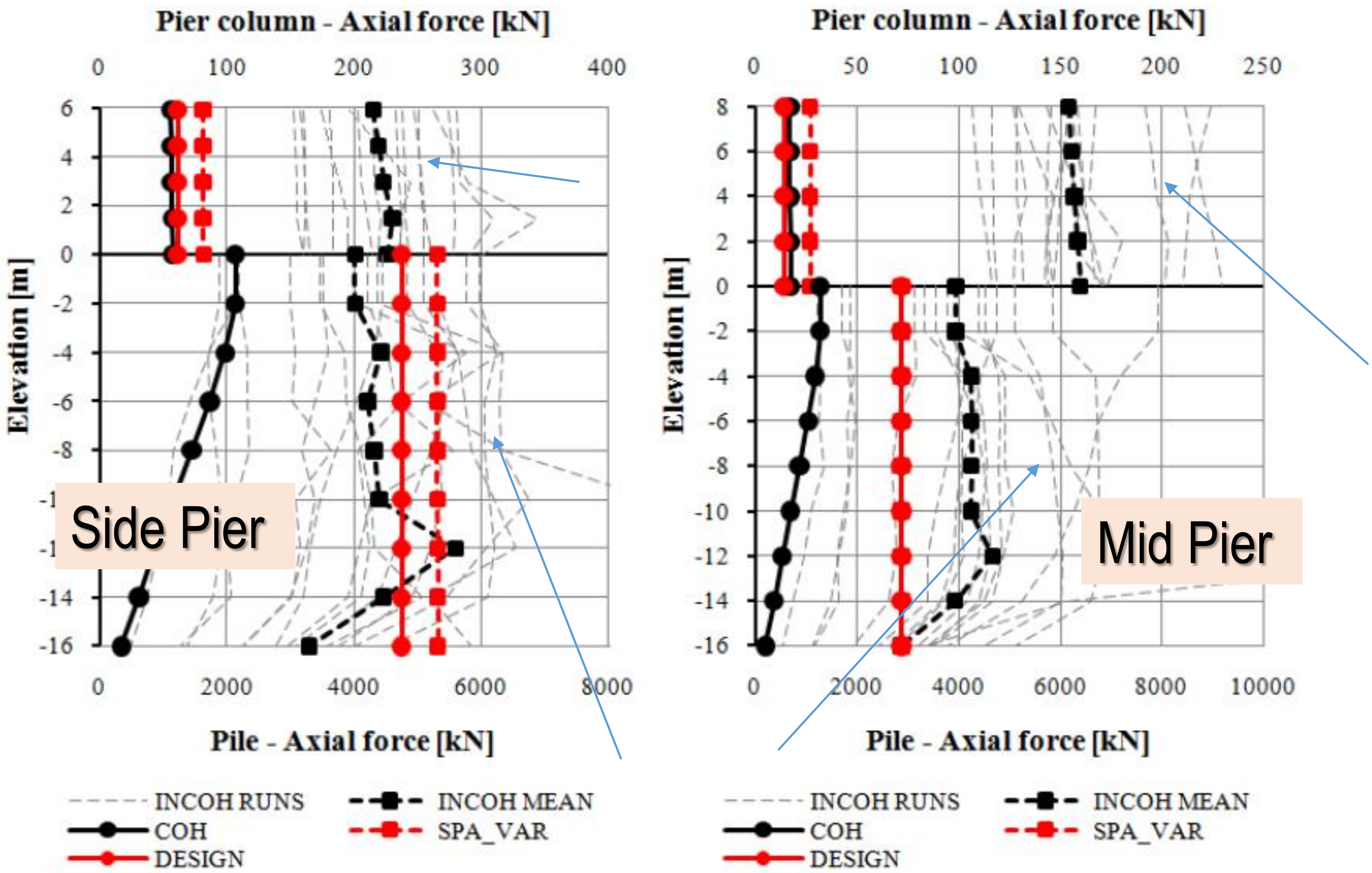

X-Input (Long) SSI Analysis and Eurocode 8

X方向-入力SSI解析とEurocode8

Table 1. Stress comparison for earthquake loading in X direction

Pier position	Structural element	Stress	DESIGN	SPA_ _VAR	% INCREASE (SPA_VAR to DESIGN)	COH	INCOH_ _MEAN	% increase (INCOH_ MEAN to COH)
Side pier	Pier column	M3	18247	20194	10.7%	19660	18226	-7.3%
		V2	3088	3412	10.5%	3354	3140	-6.4%
	Pile	M3	1394	1518	8.9%	573	1747	204.9%
		V2	1064	1172	10.2%	90	573	536.7%
		N	4753	5318	11.9%	334	3294	886.2%
Mid pier	Pier column	M3	11700	11718	0.2%	11970	8430	-29.6%
		V2	1482	1484	0.1%	1527	1075	-29.6%
	Pile	M3	663	664	0.2%	314	1420	352.2%
		V2	545	546	0.2%	27	588	2077.8%
		N	2874	2880	0.2%	200	2870	1335.0%

Y-Input (Long) SSI Analysis and Eurocode 8

Y方向-入力SSI解析とEurocode8

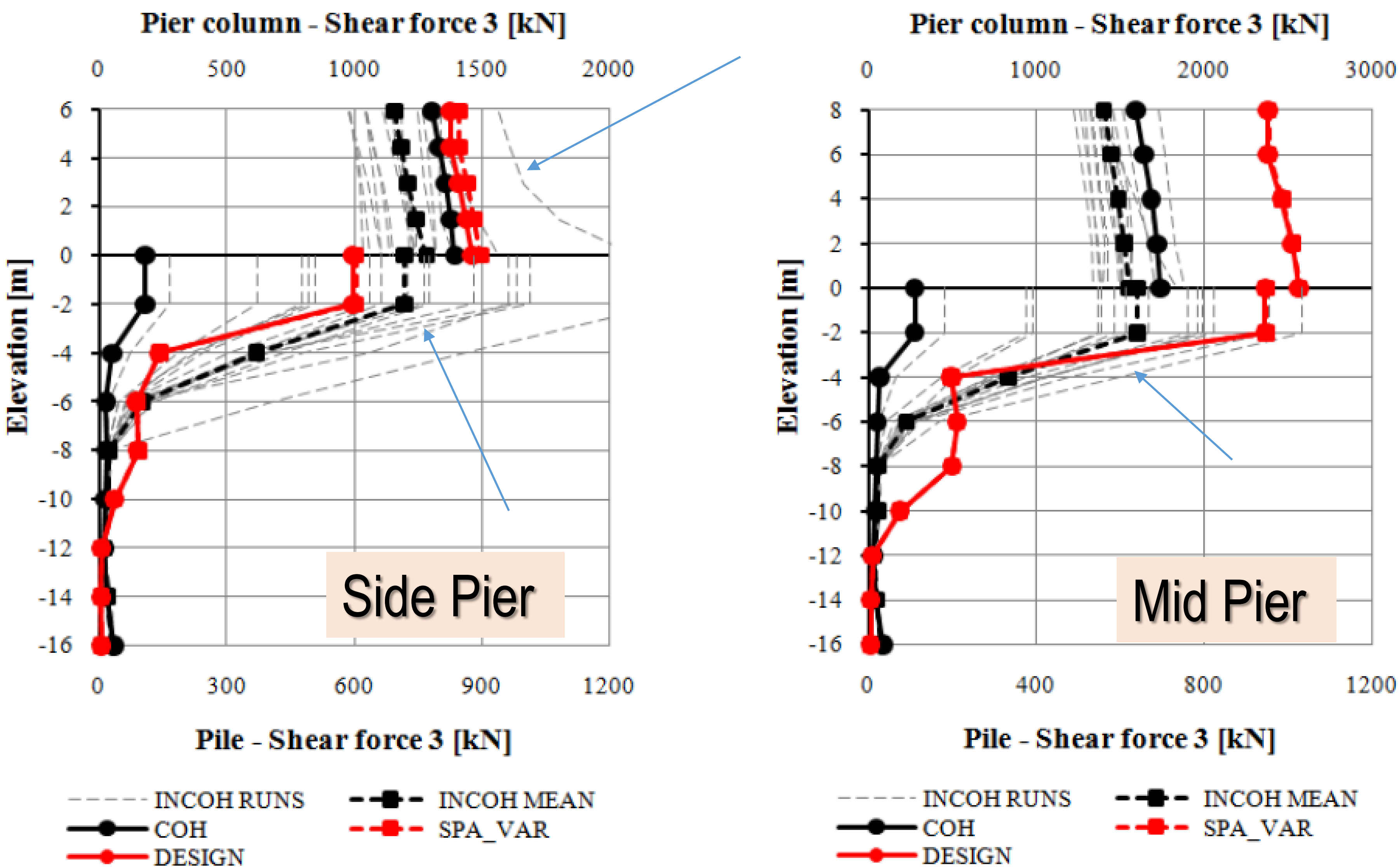

Y-Input (Long) SSI Analysis and Eurocode 8

Y方向-入力SSI解析とEurocode8

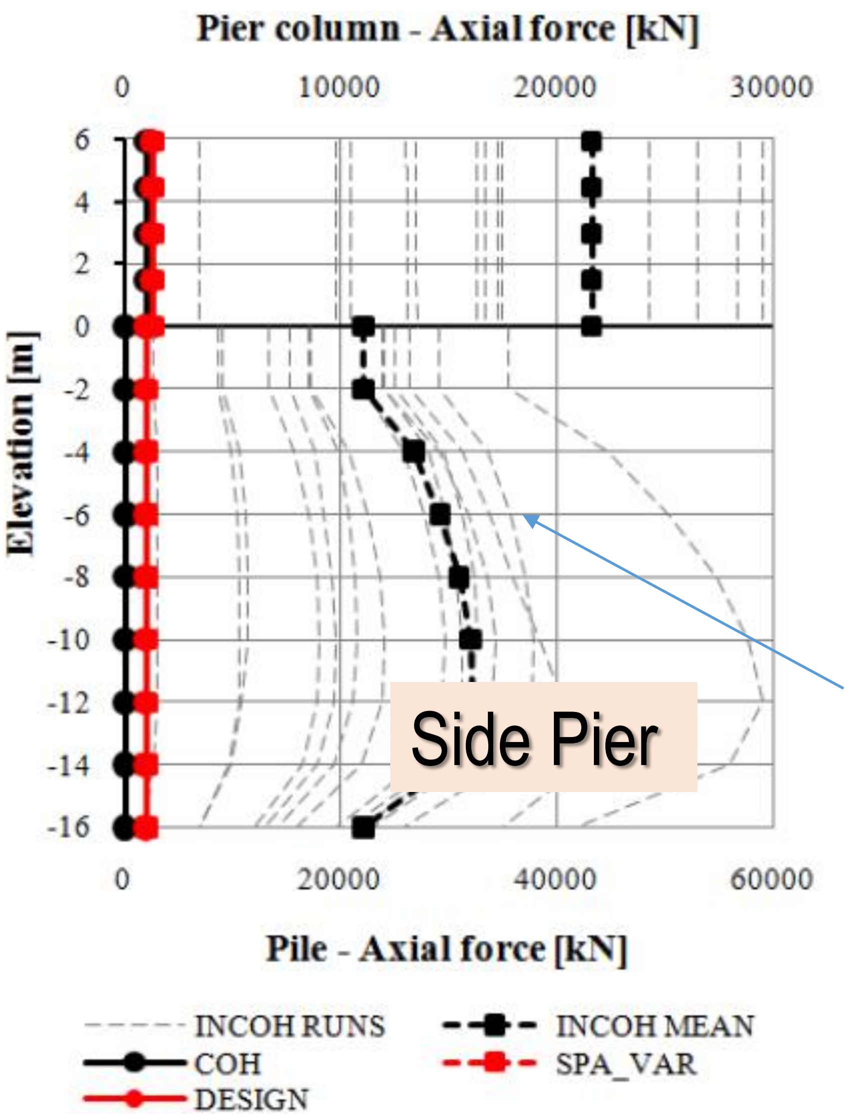

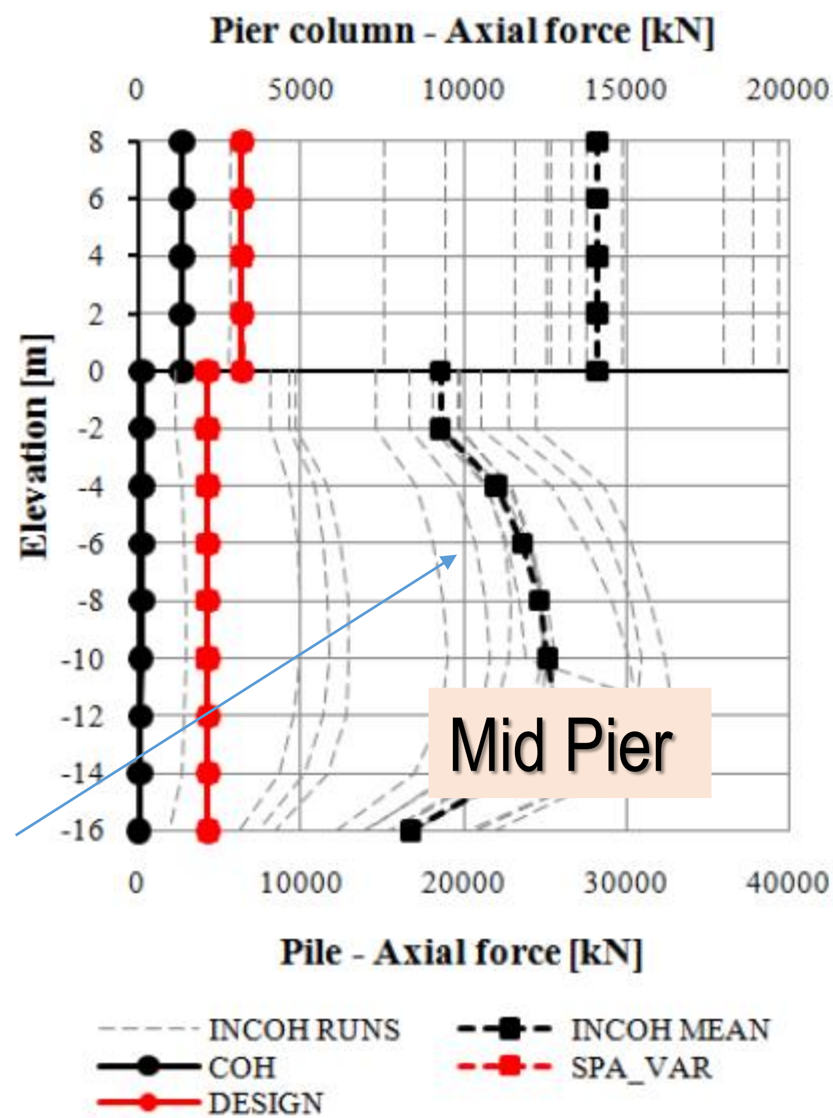

Y-Input (Long) SSI Analysis and Eurocode 8

Y方向-入力SSI解析とEurocode8

Table 2. Stress comparison for earthquake loading in Y direction

Pier position	Structural element	Stress	DESIGN	SPA_ _VAR	% INCREASE (SPA_VAR to DESIGN)	COH	INCOH_ _MEAN	% increase (INCOH_ MEAN to COH)
Side pier	Pier column	M2	4683	4791	2.3%	4087	4213	3.1%
		V3	1461	1494	2.3%	1394	1283	-8.0%
	Pile	M2	888	903	1.7%	327	1380	322.0%
		V3	596	604	1.3%	107	720	572.9%
Mid pier	Pier column	M2	10913	10942	0.3%	6890	6676	-3.1%
		V3	2562	2569	0.3%	1737	1548	-10.9%
	Pile	M2	1689	1691	0.1%	342	1534	348.5%
		V3	944	946	0.2%	110	640	481.8%

Z-Input (Long) SSI Analysis and Eurocode 8

Z方向-入力SSI解析とEurocode8

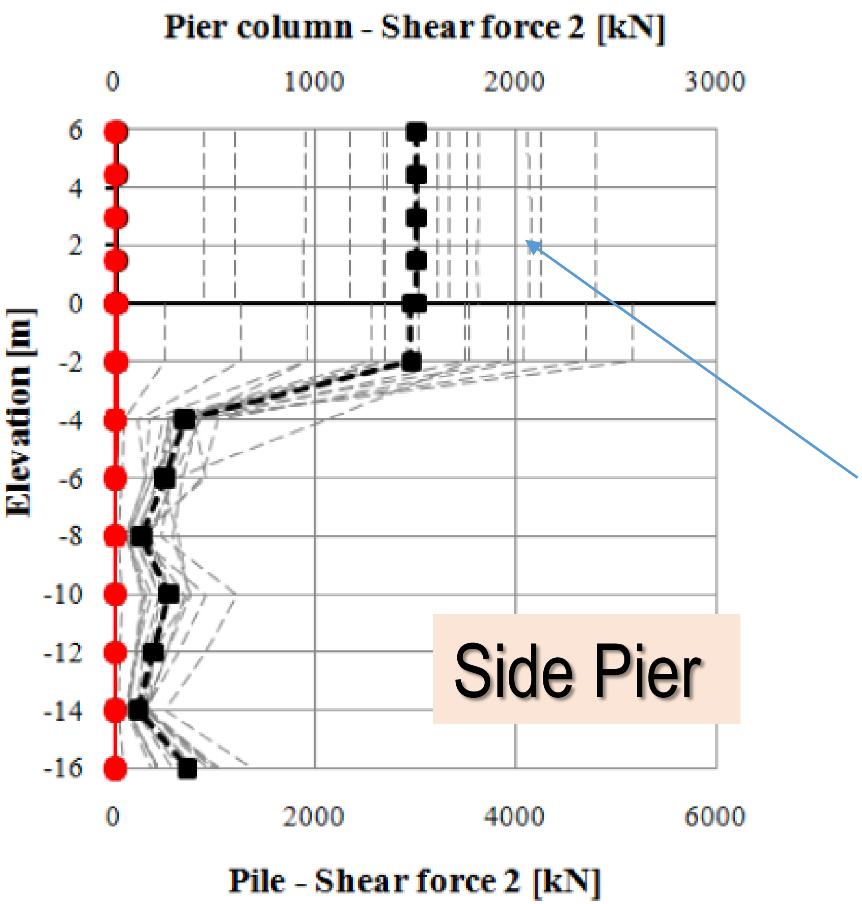

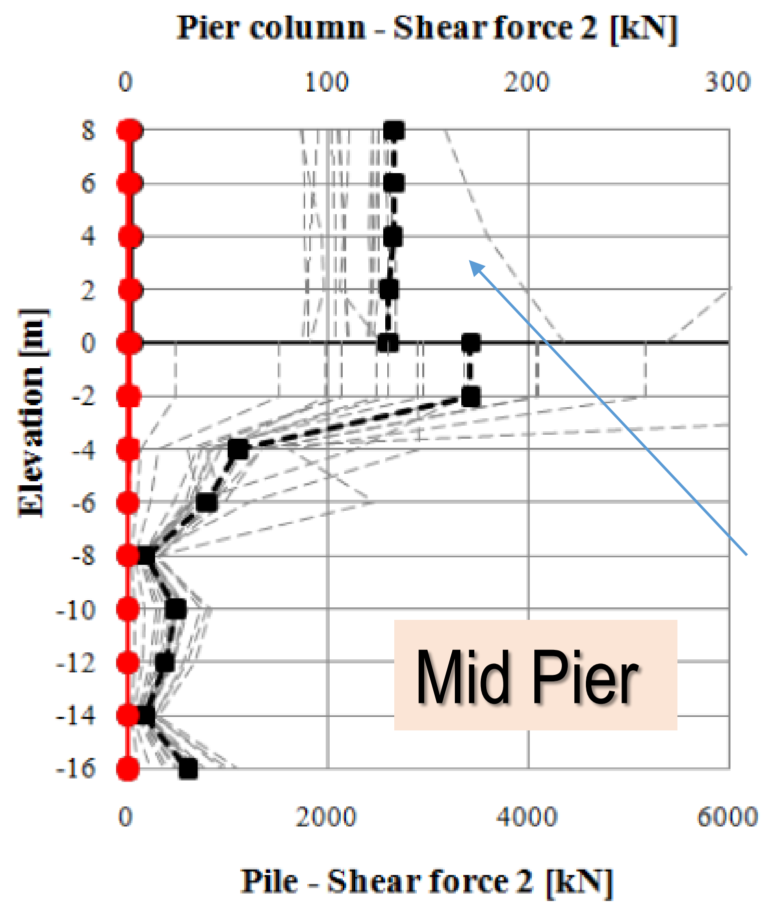

Z-Input (Long) SSI Analysis and Eurocode 8

Z方向-入力SSI解析とEurocode8

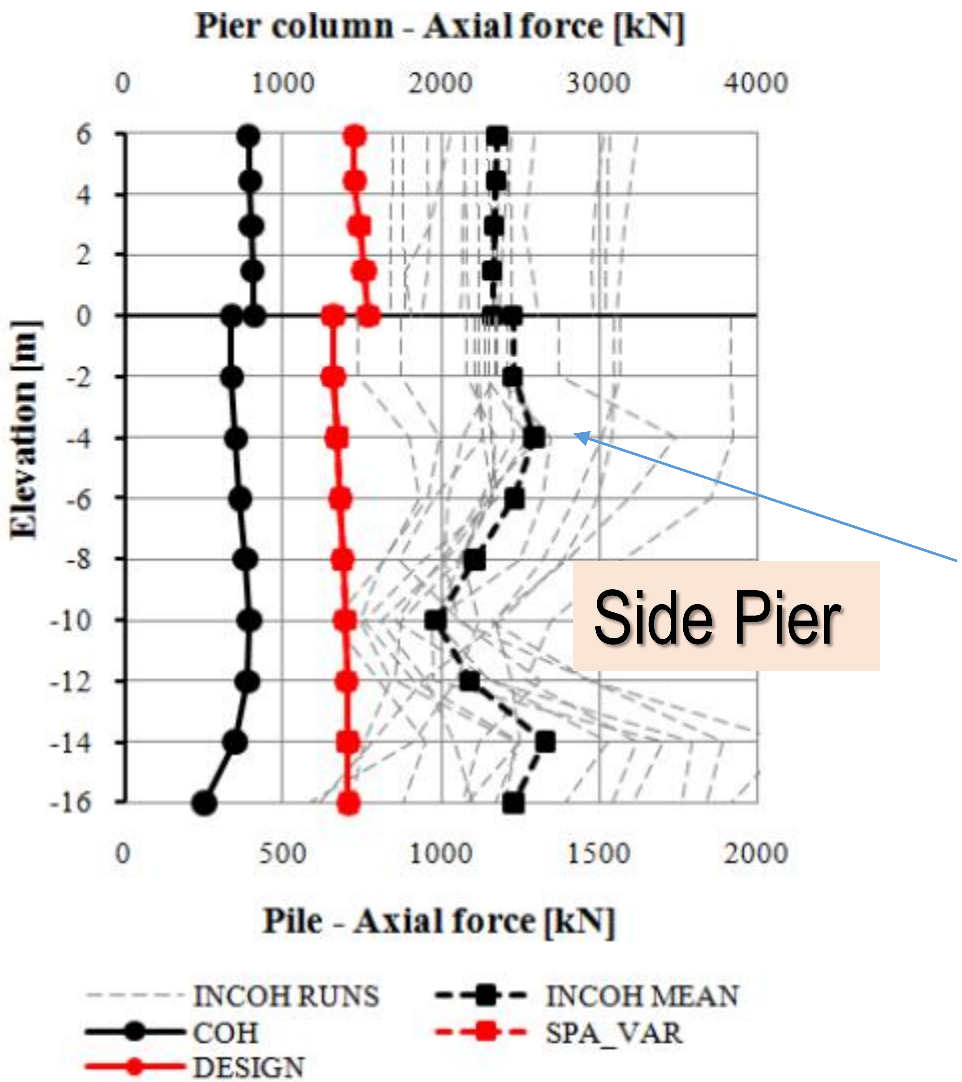

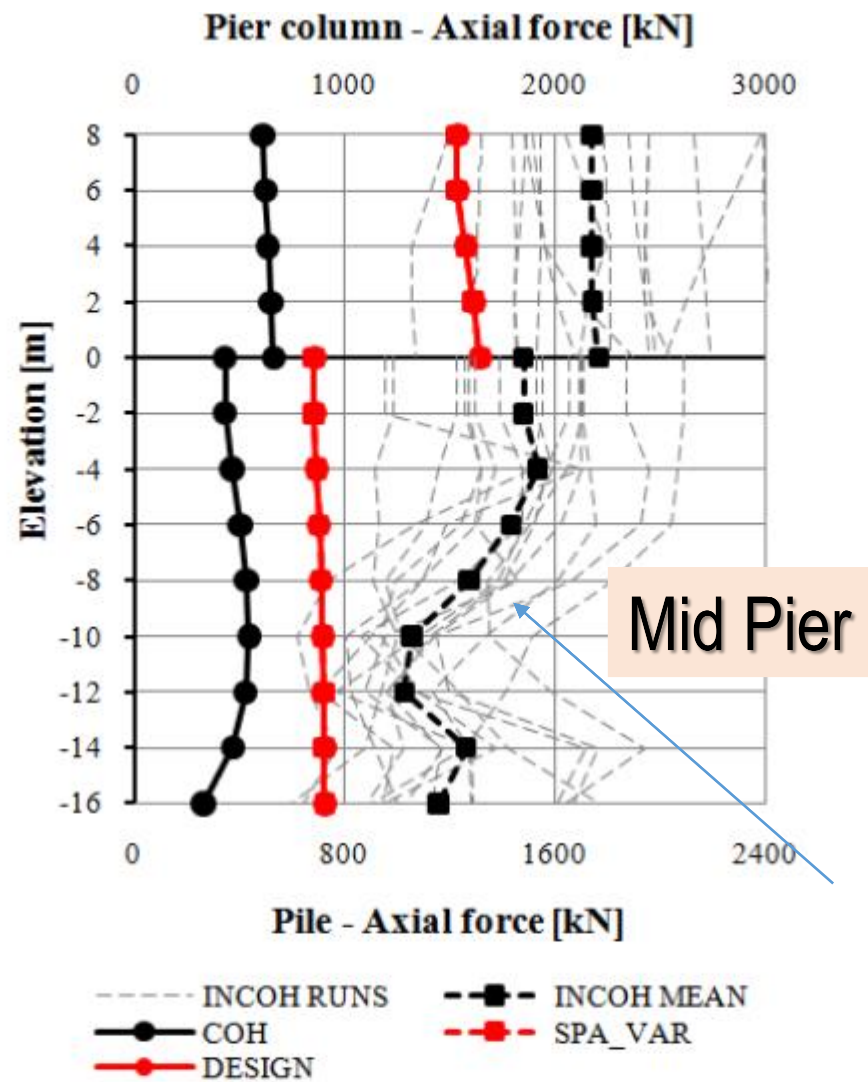

Z-Input (Long) SSI Analysis and Eurocode 8

Z方向-入力SSI解析とEurocode8

Table 3. Stress comparison for earthquake loading in Z direction

Pier position	Structural element	Stress	DESIGN	SPA_ _VAR	% INCREASE (SPA_VAR to DESIGN)	COH	INCOH_ _MEAN	% increase (INCOH_MEAN to COH)
Side pier	Pier column	N	1538	1538	0.0%	820	2325	183.5%
		V2	2	2	0.0%	10	1503	14930.0%
	Pile	N	707	707	0.0%	250	1230	392.0%
		V2	13	13	0.0%	5	2960	59100.0%
Mid pier	Pier column	N	1643	1643	0.0%	660	2206	234.2%
		V2	1	1	0.0%	2	130	6400.0%
	Pile	N	683	683	0.0%	345	1480	329.0%
		V2	14	14	0.0%	8	3420	42650.0%

Coherent and Incoherent Instant Bridge Acceleration Deformed Shape

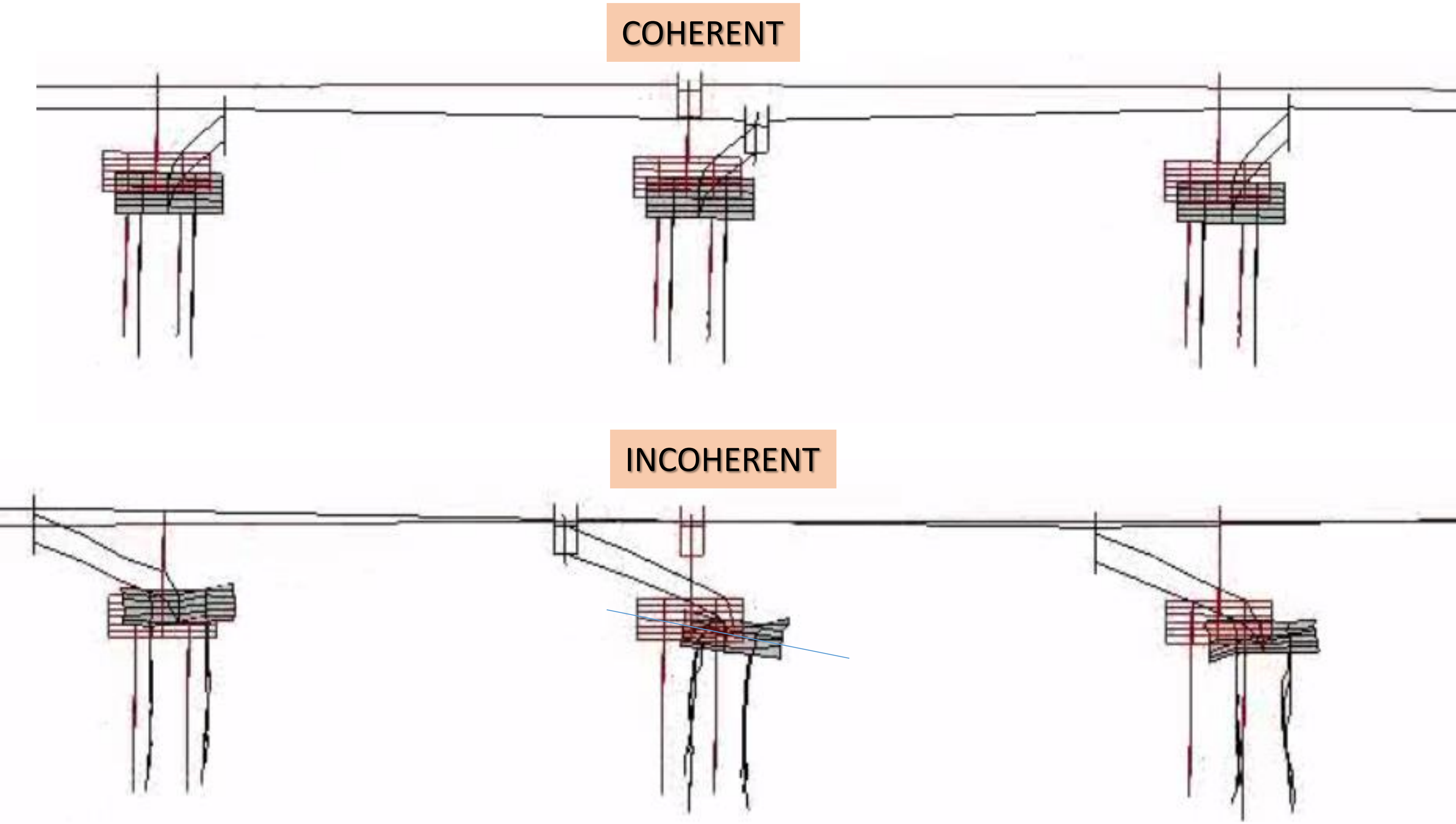

Motion Incoherency Effects on Concrete Bridges

コンクリート橋に対するインコヒレンシーの影響

This study shows that the effects of motion incoherency and wave passage can increase the maximum forces in the bridge pier columns and piles by up to 200 or even more in the transverse direction. 本研究では、インコヒレンシーと地震波通過の効果により橋の橋脚柱と杭にかかる横方向の最大の力が200%～500%増加した.

It should be noted that the SSI effects are highly amplified due to motion spatial variation in horizontal direction, i.e. motion incoherency, that creates random differential phasing between neighbor building motions. 水平方向の地震波伝播の変動（インコヒレンシー）によってSSI効果が大きく増幅された。インコヒーレントは、隣接する建物の振動にランダムな位相差を発生させる.

Design analysis has deficiency since its neglects the dynamic SSI effects due to the differential seismic soil motions produced by the motion spatial variation. The vertical input motion induces SSI effects which are much larger for the SSI analysis than Design analysis. 設計解析では、地震波伝播の変動に由来する地盤震動による動的SSI効果を考慮しておらず、不十分である.垂直方向の地震波入力がSSI効果を生じ、SSI解析では設計解析よりもはるかに大きなSSI効果を再現している.

Fukae Bridge Failure at 1995 Kobe Earthquake

1995年兵庫県南部地震で倒壊した深江橋

Failed Bridge Indicates Large Transverse Seismic Shear Force Loads

倒壊した橋の様子から、地震によって大きなせん断力が水平方向に加わったことがわかります.

Fukae Bridge Location in Kobe, Japan

深江橋の場所

Recorded locations at MOTOYAMA and HIGASHI at about 10-15m Depths

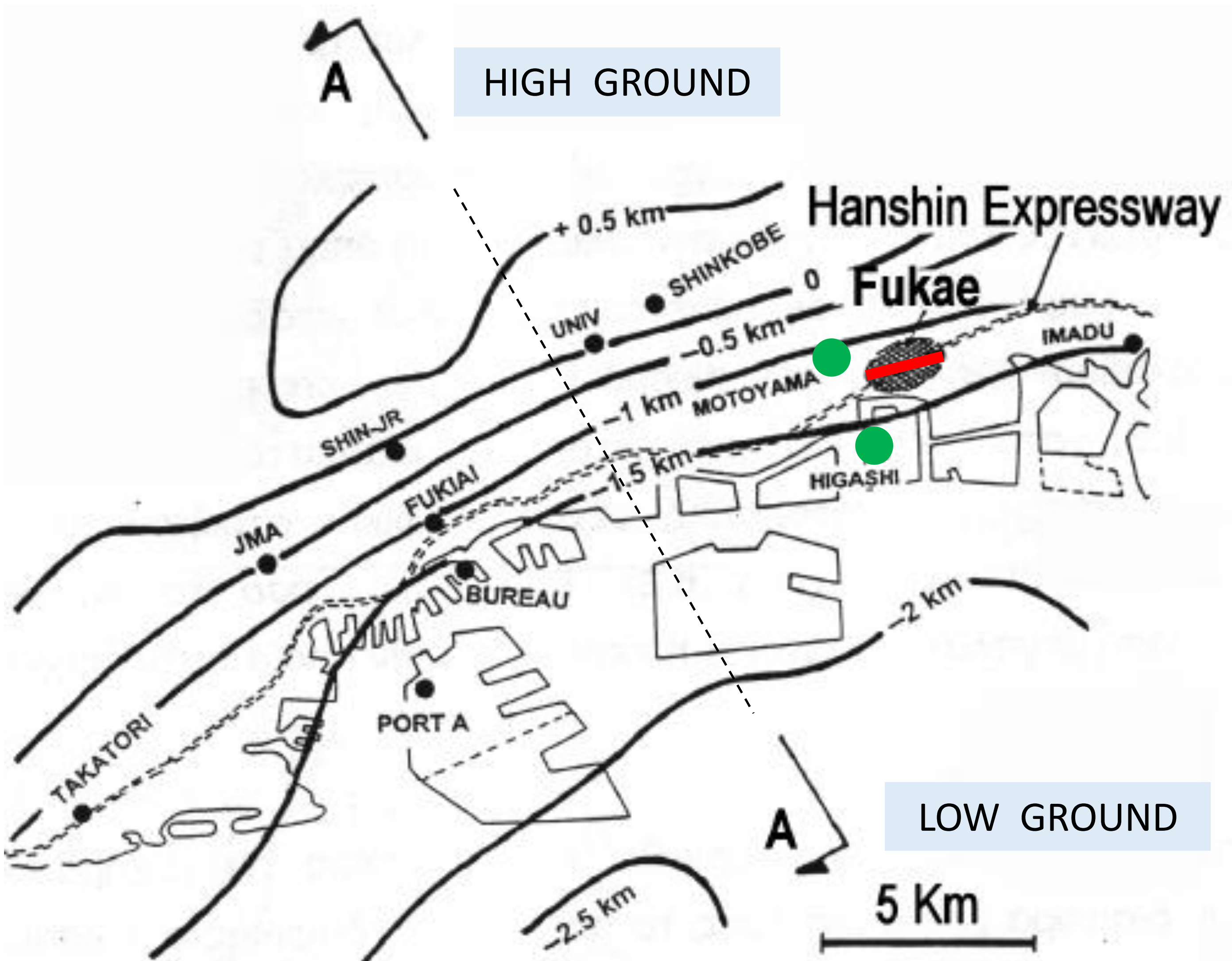

Normal and Parallel Motion Components of Kobe 1995 Earthquake (FN and FP) 法線方向/水平方向の振動

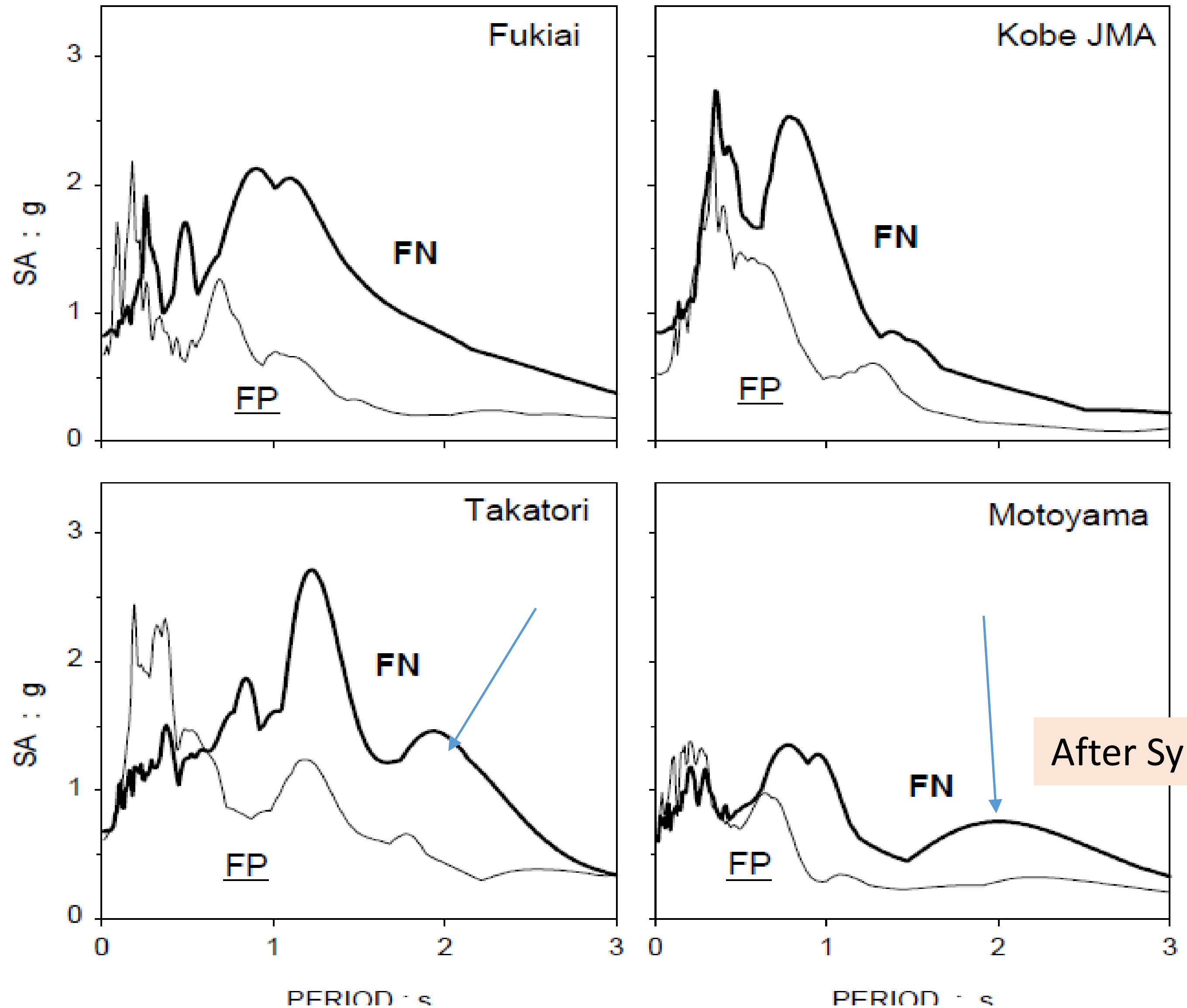

After Syngros, 2004)

Kobe 1995 Quake Records at Different Locations

地震動記録

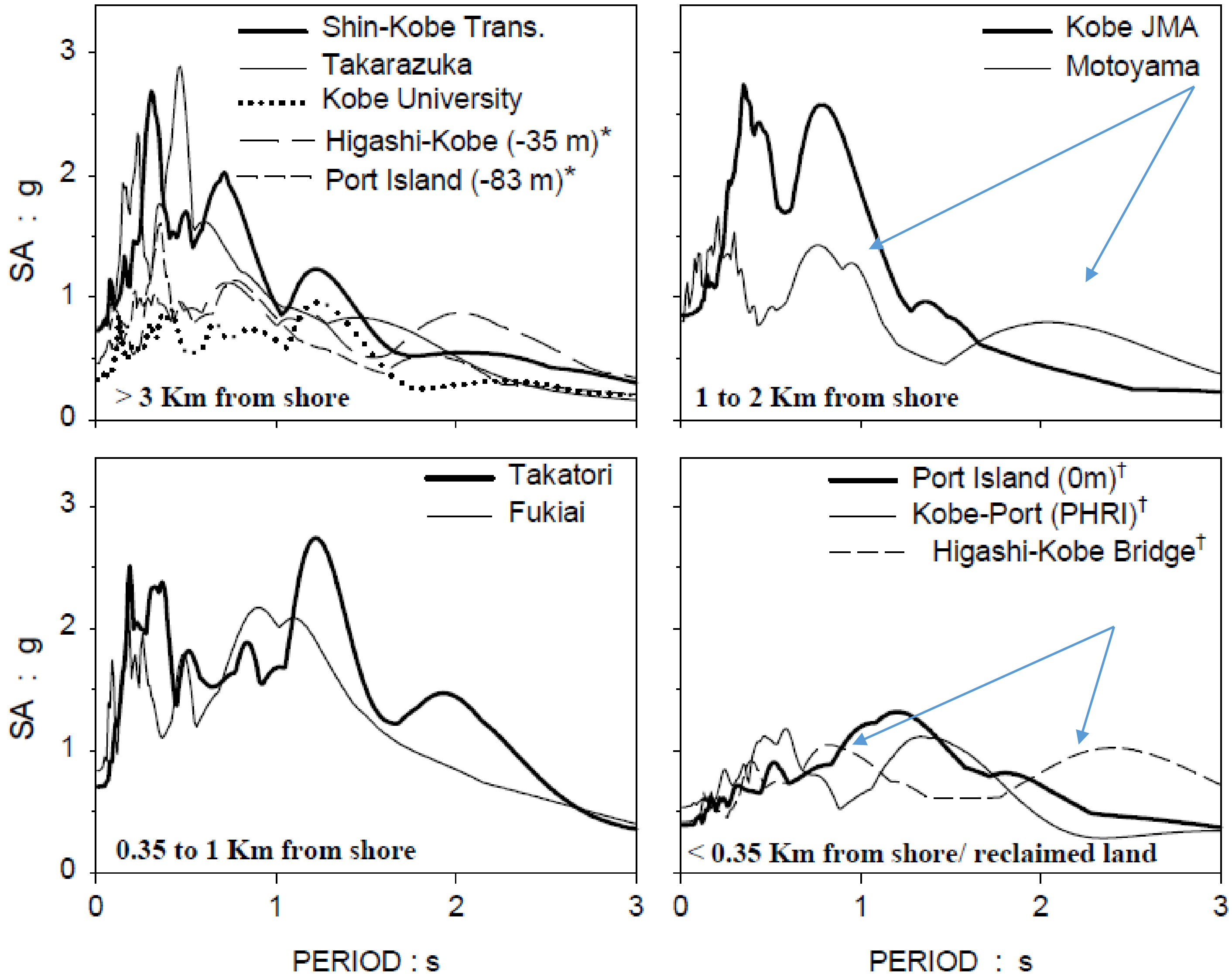

After Syngros, 2004)

Section A-A of the Kobe Soil Profile

A-A断面の神戸地盤プロファイル

Recorded locations at MOTOYAMA and HIGASHI at about 10-15m Depths

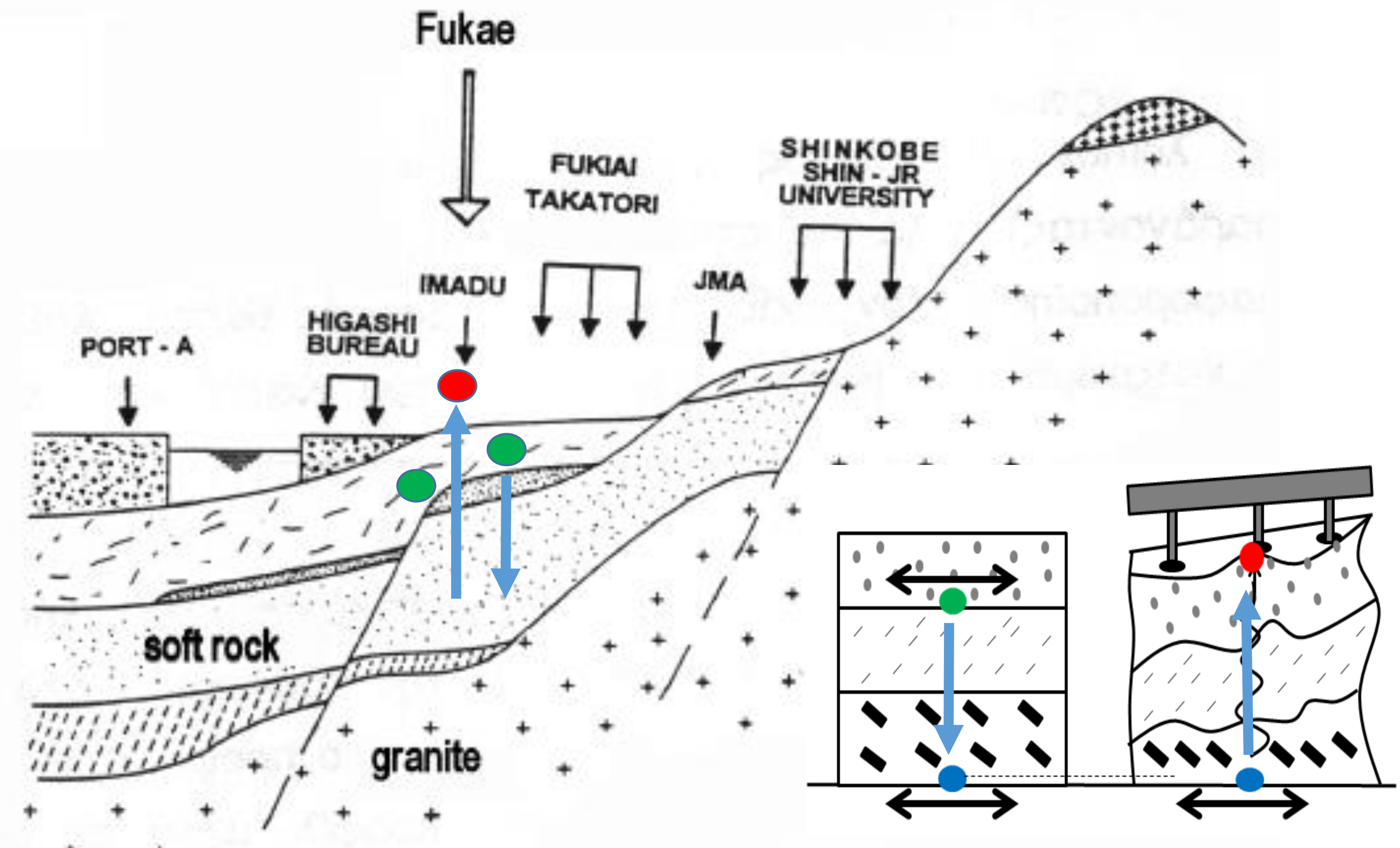

Computed Surface Motions Near Fukae Bridge

計算された表層の地震動、深江橋近辺

1D Nonlinear Convolutions Using SHAKE Methodology – as SOIL Module

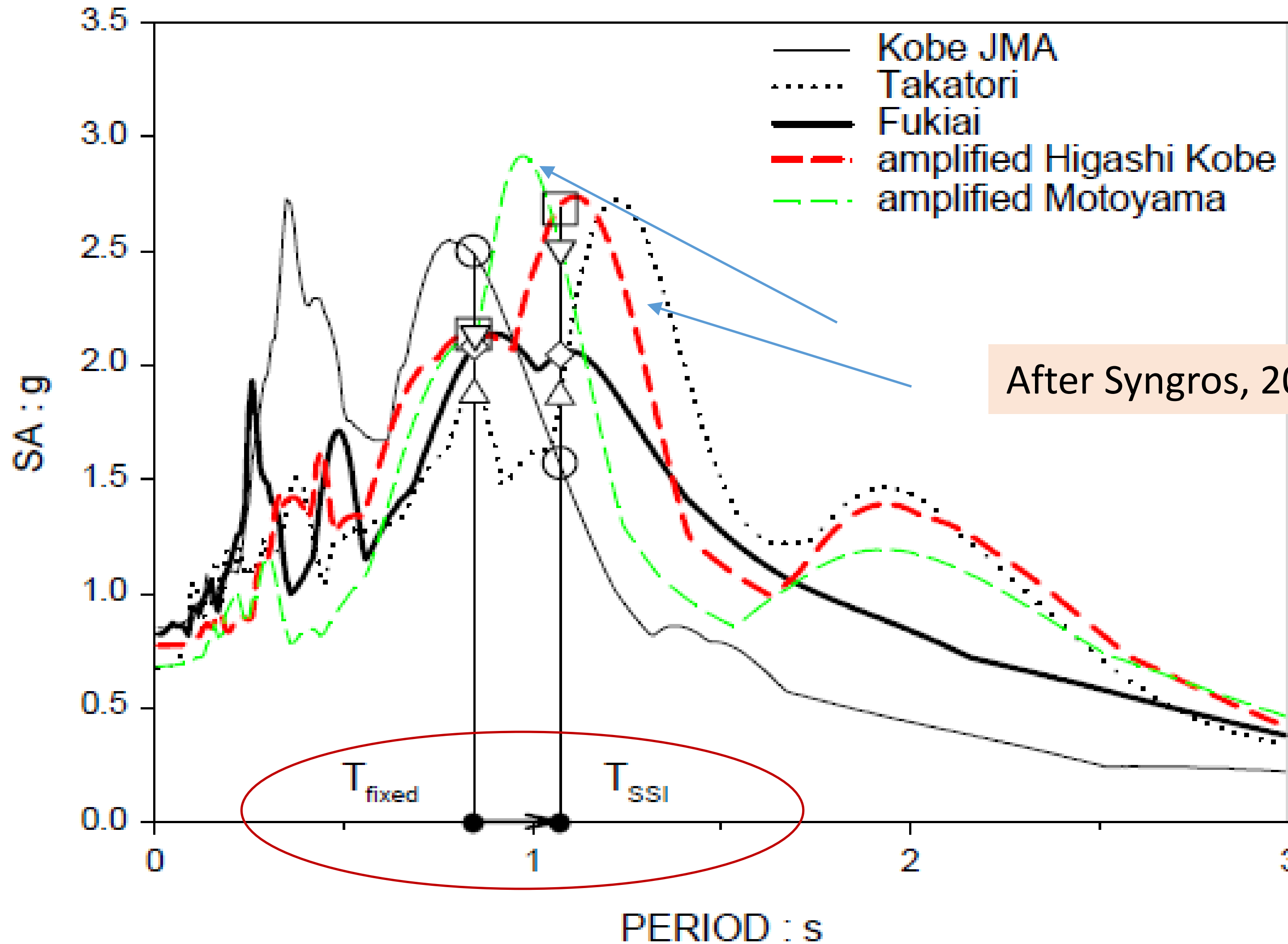

After Syngros, 2004)

Equivalent-Linear Soil Vs and Damping Profiles

等価線形土壌のVsと減衰プロファイル

1D Deconvolution-Nonlinear Convolutions Using the SOIL Module

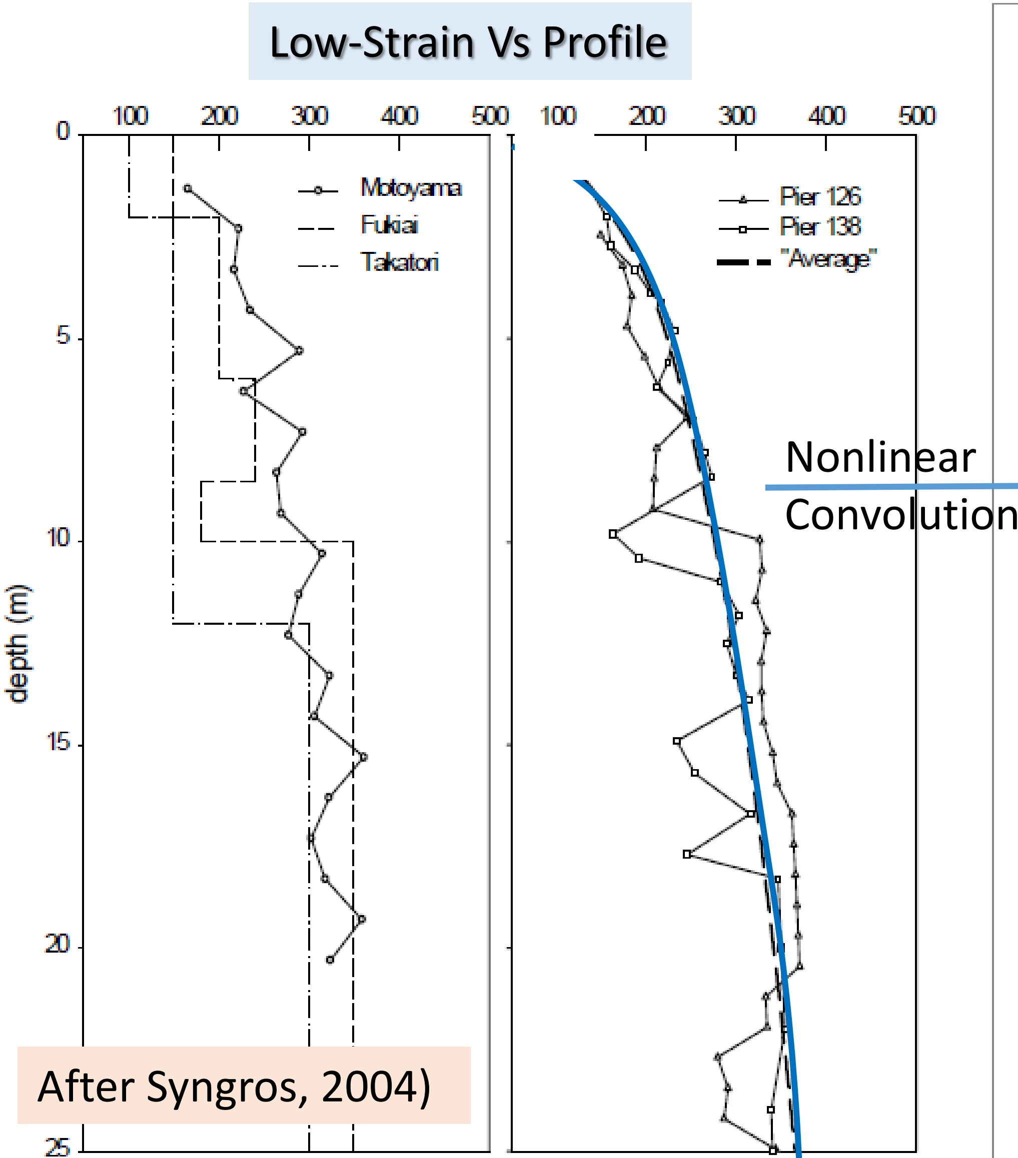

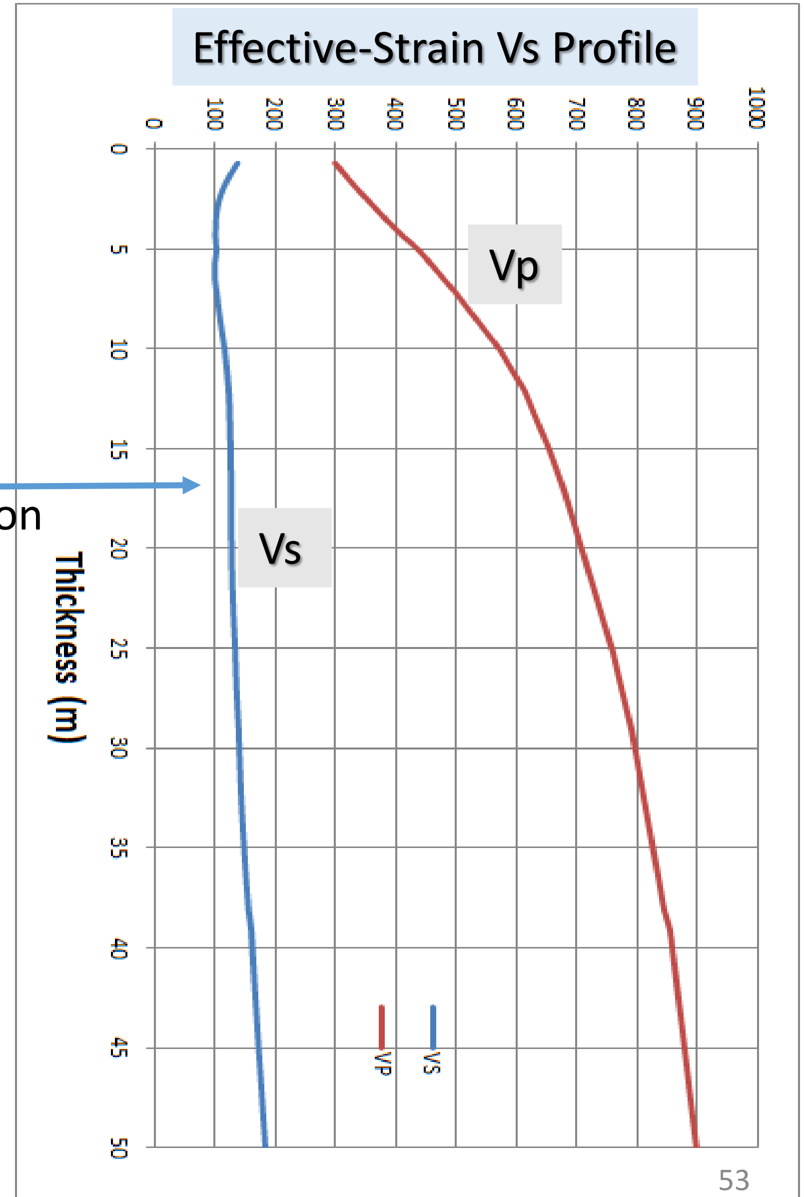

Final Fukae Bridge Transverse Acceleration Input

JMA Acceleration Used As Input Record in the SOIL Module

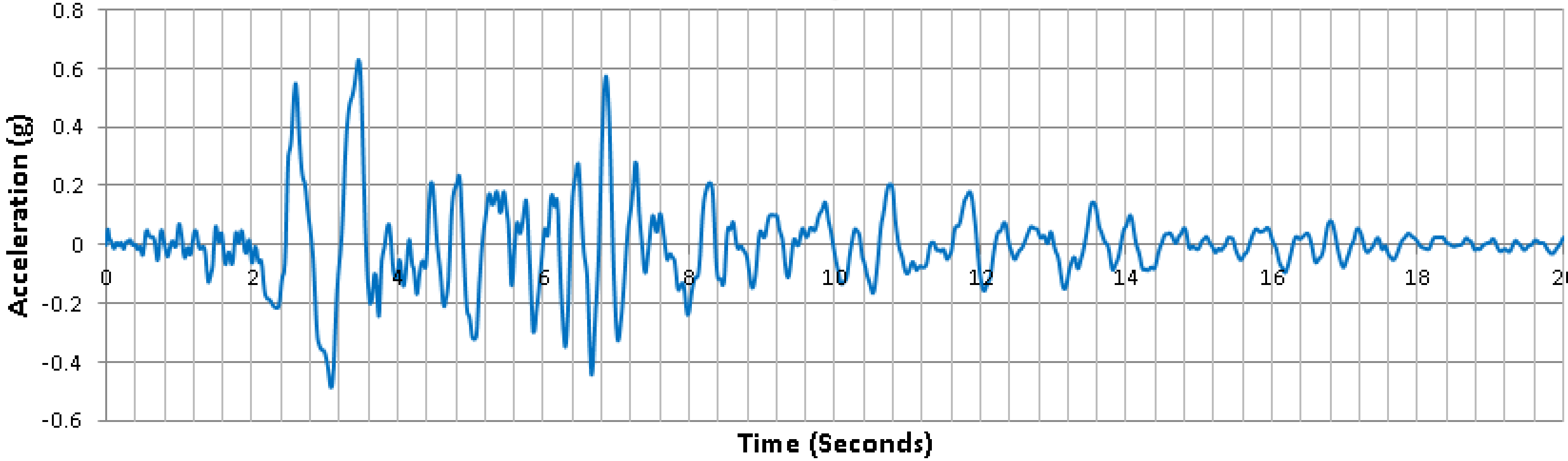

Final Acceleration Input for Fukae Bridge Using EQUAKE with SEED Record from SOIL

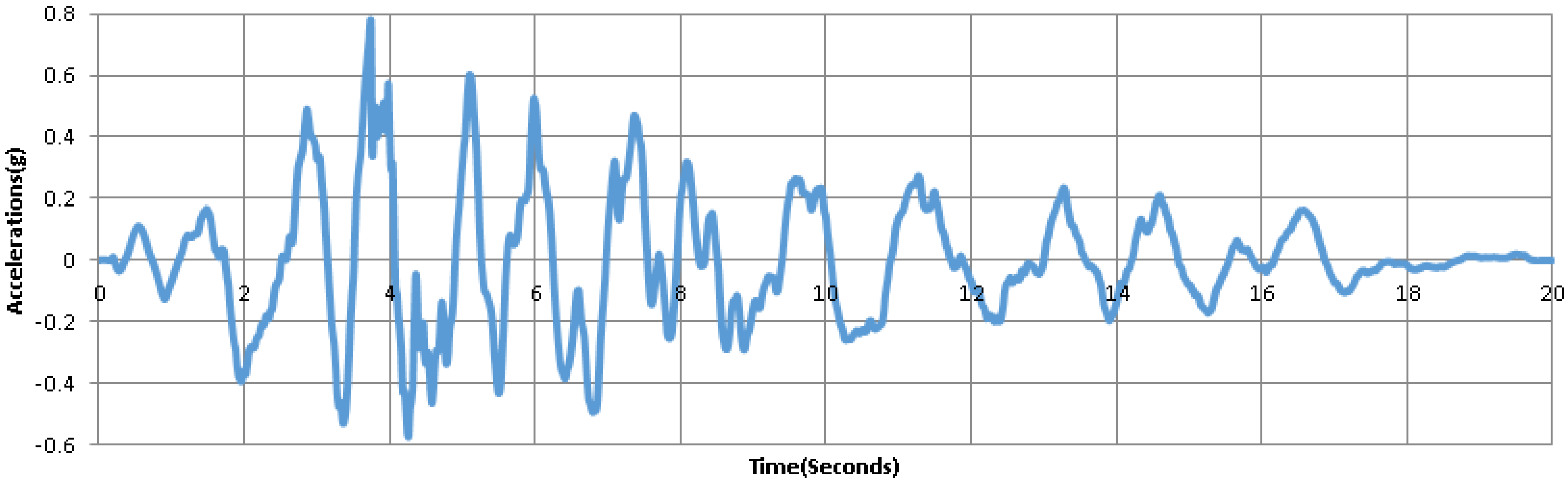

Final Fukae Bridge Transverse Input Acceleration

深江橋　地震動入力（直交方向）

Final Acceleration Computed Using EQUAKE with Input Seed Record from SOIL

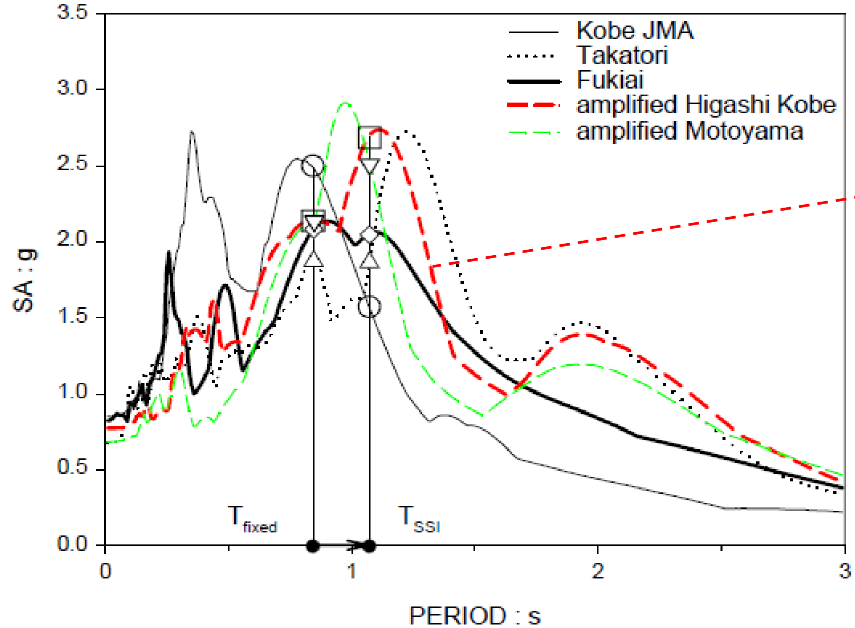

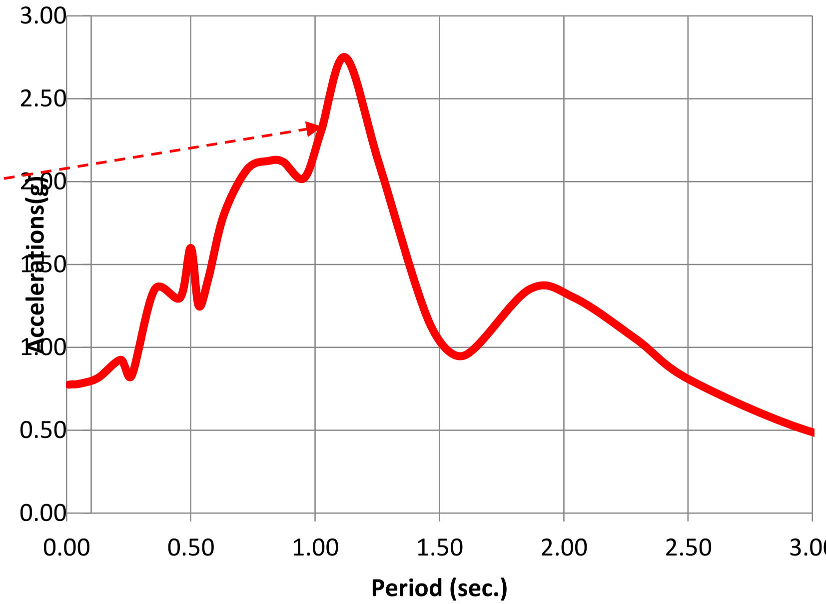

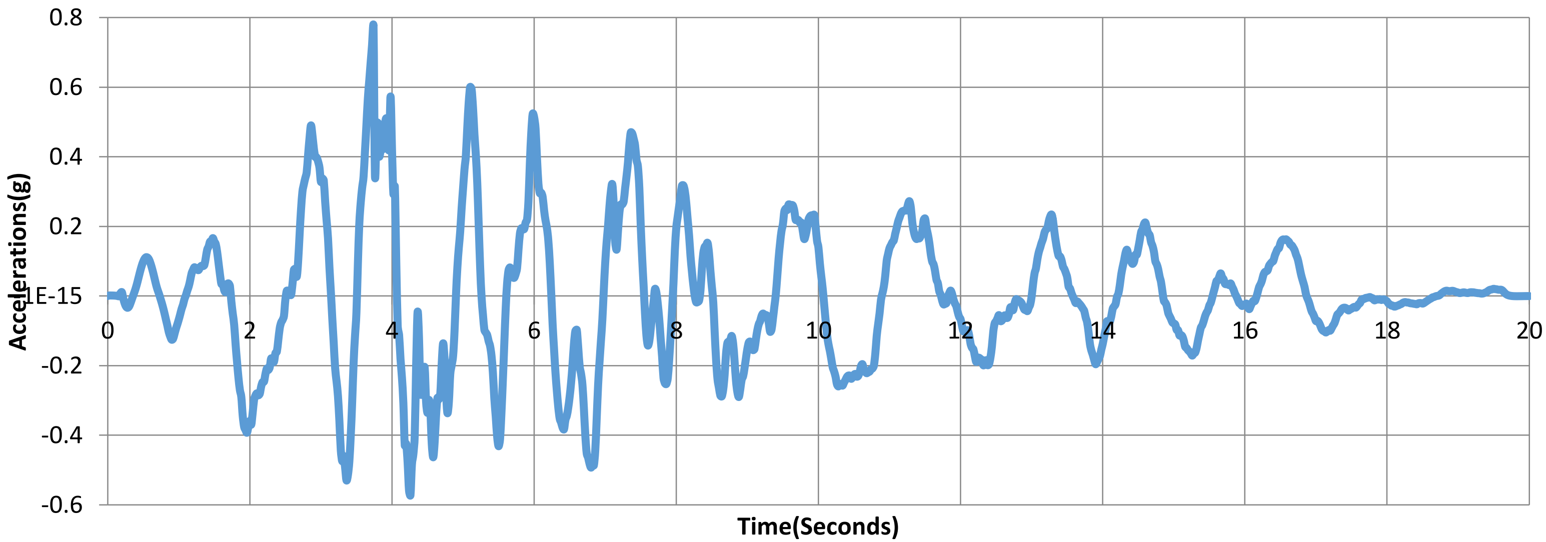

ACS SASSI SSI Model for the Fukae Bridge

ACS SASSI 深江橋SSIモデル

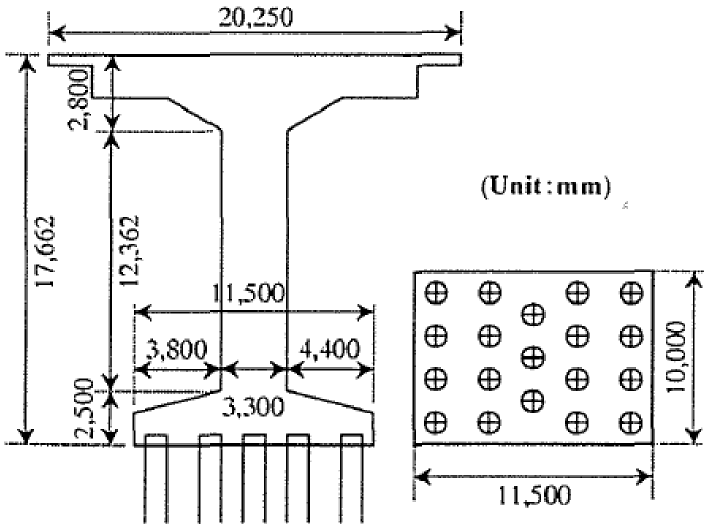

Fukae Bridge Model
Developed by Terrabyte

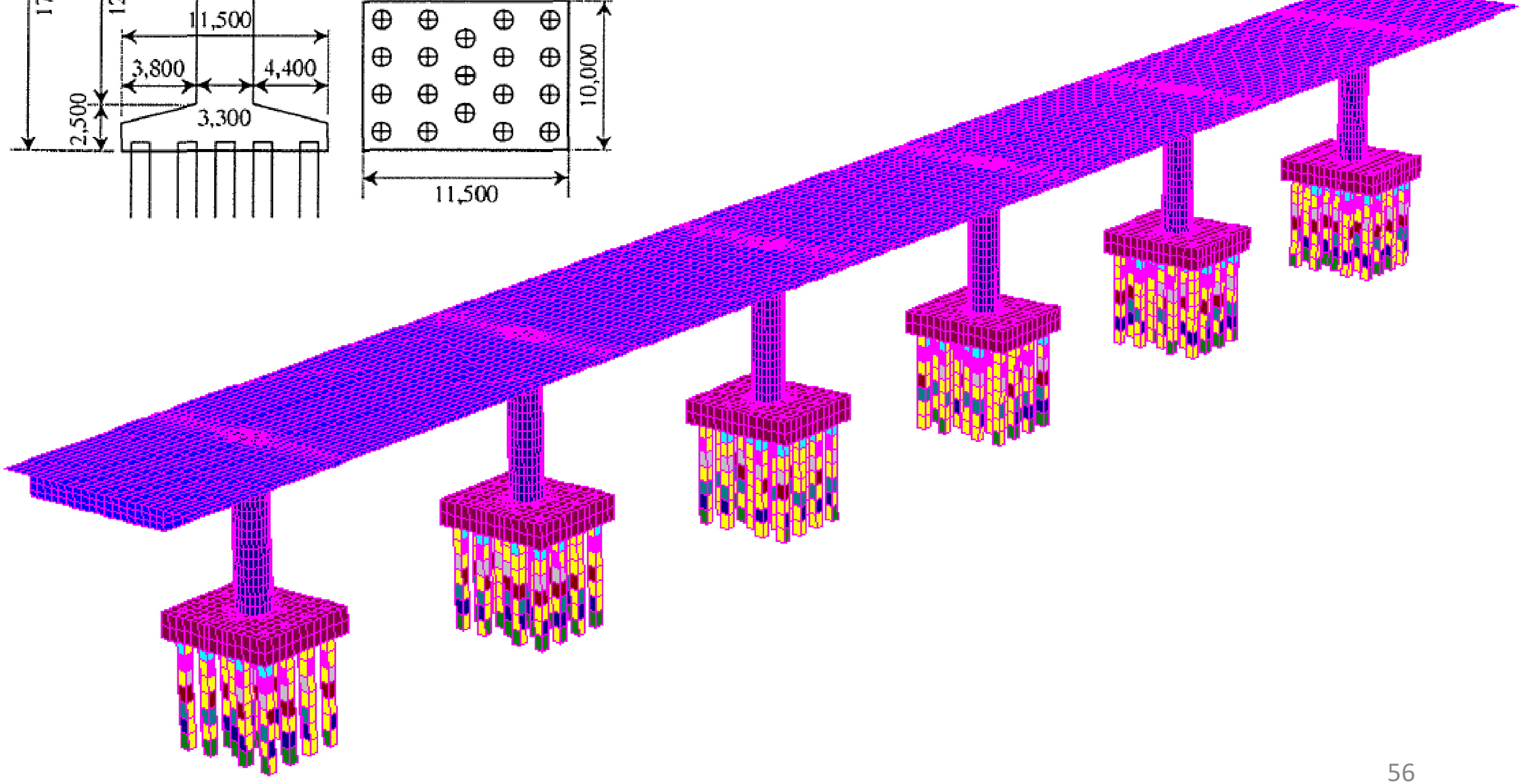

1 Pier SSI Model of Fukae Bridge

深江橋　単一橋脚SSIモデル

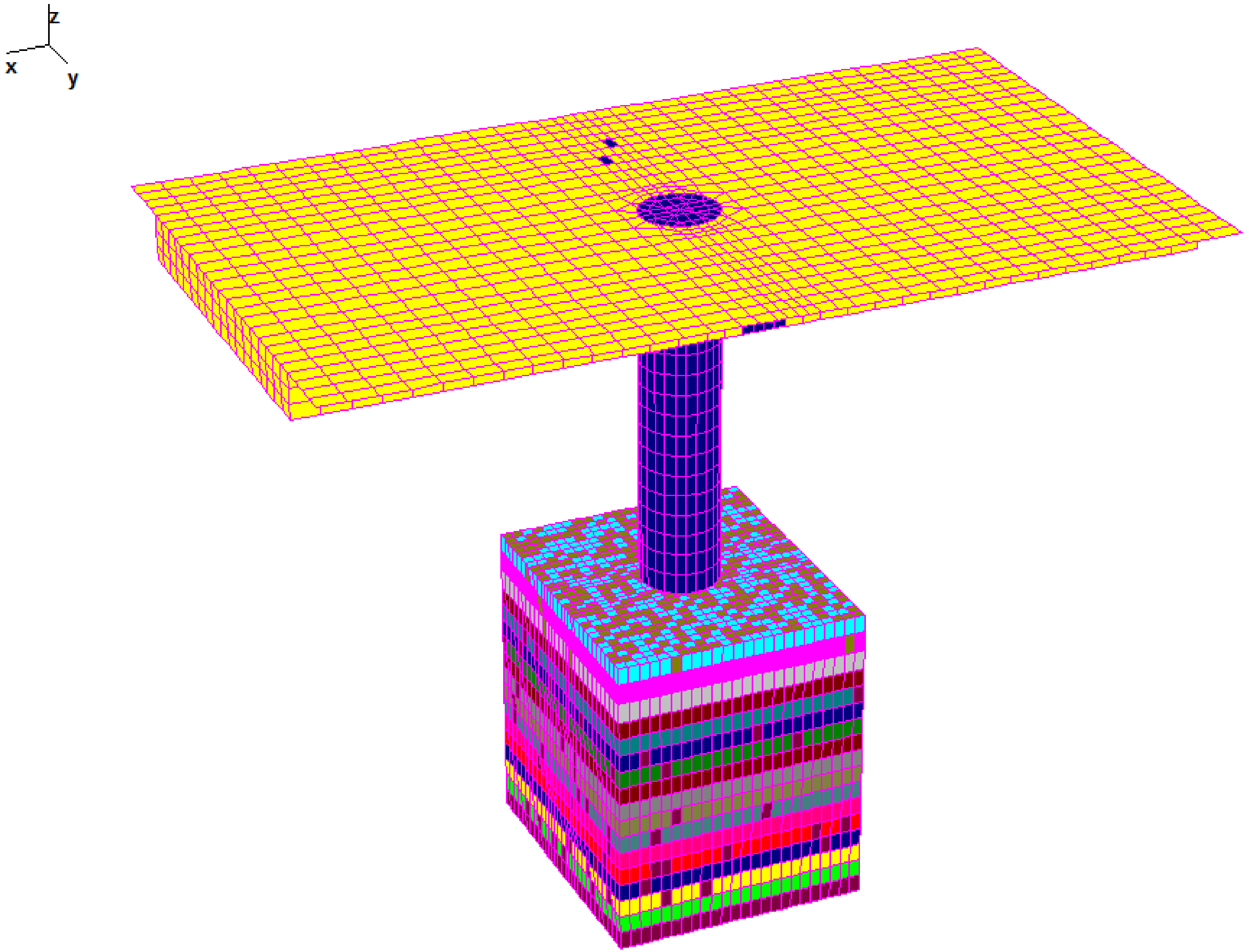

1 Pier SSI Model of Fukae Bridge

深江橋　単一橋脚SSIモデル

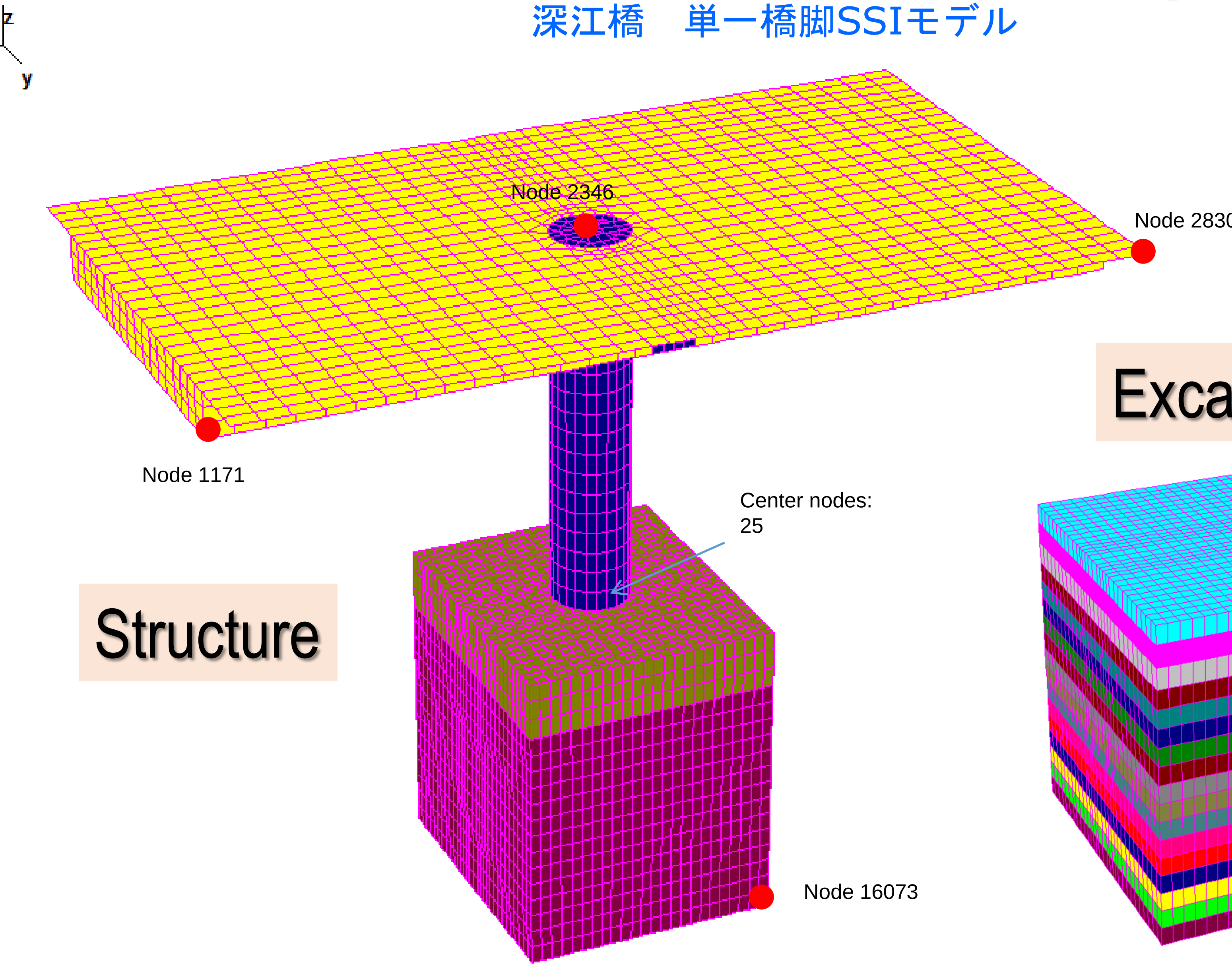

Structure

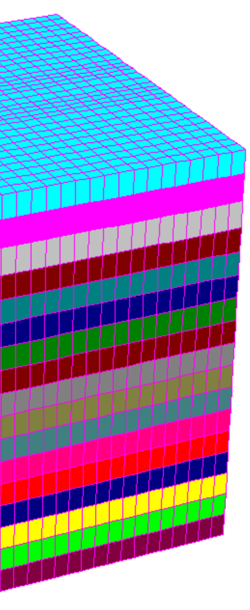

Excavation

1 Pier SSI Model of Fukae Bridge

深江橋　単一橋脚SSIモデル

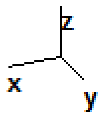

Cap and Piles

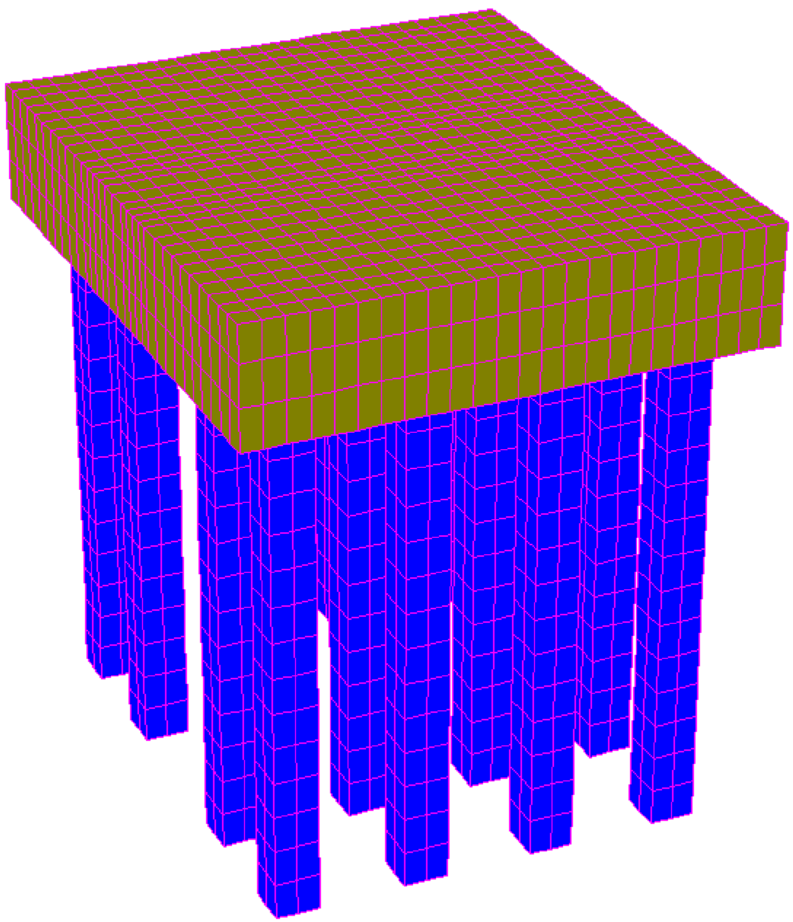

Adjacent Soil

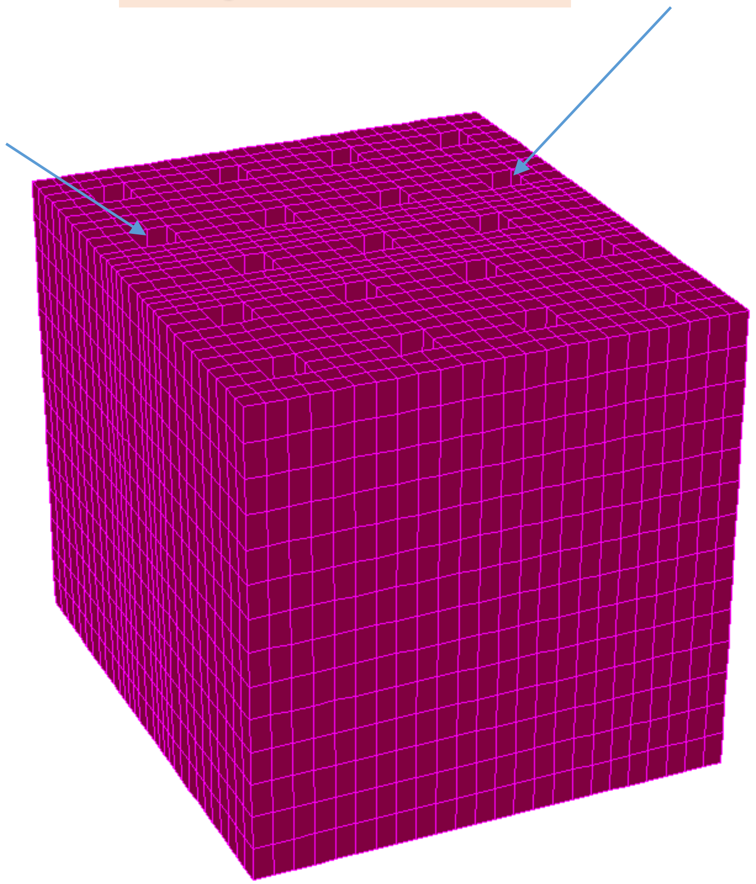

Pier and Pile Relative Displacements Under Coherent Input wrt Free-Field Motion in Y-Direction

橋脚と杭の相対変位 Y方向の地震波によるコヒレント入力

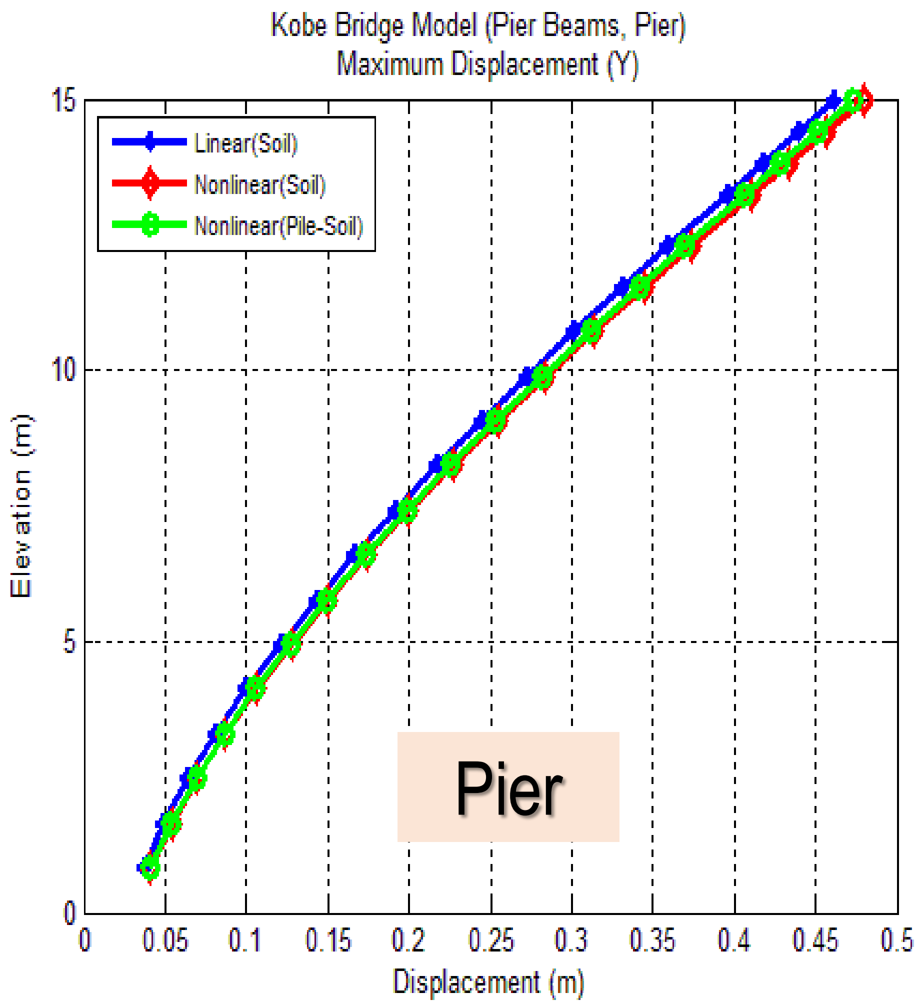

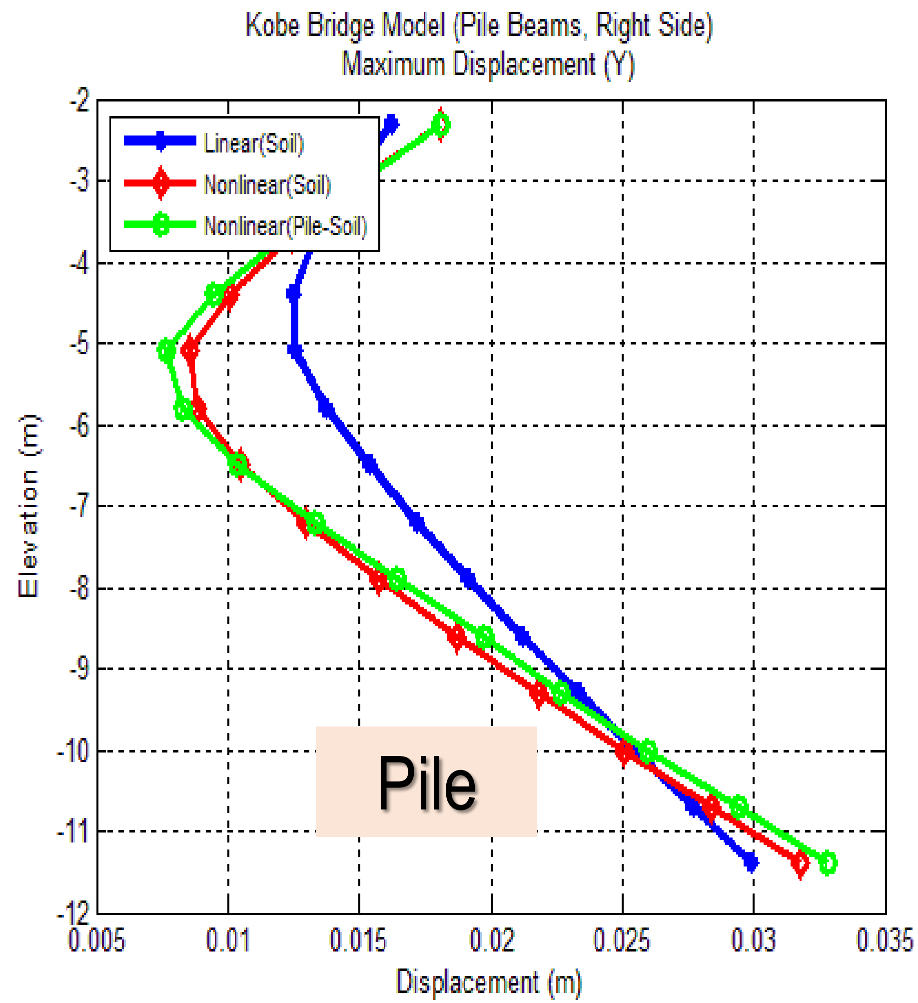

Acceleration RS Under Y-Input (Transverse)

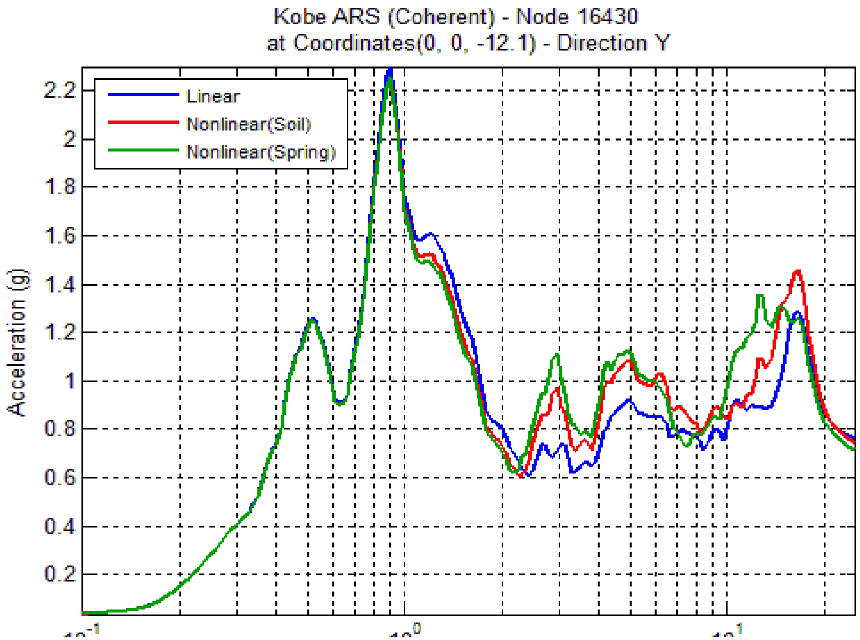

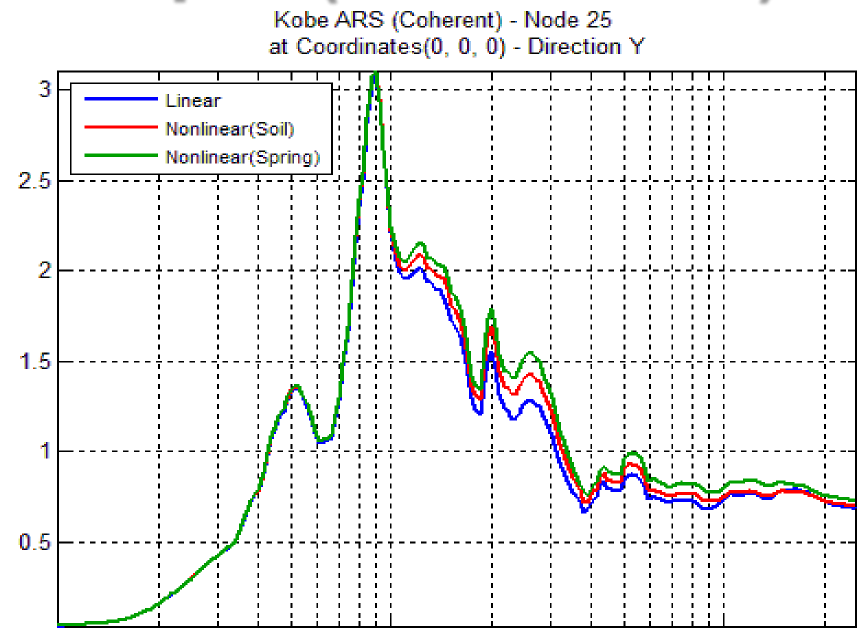

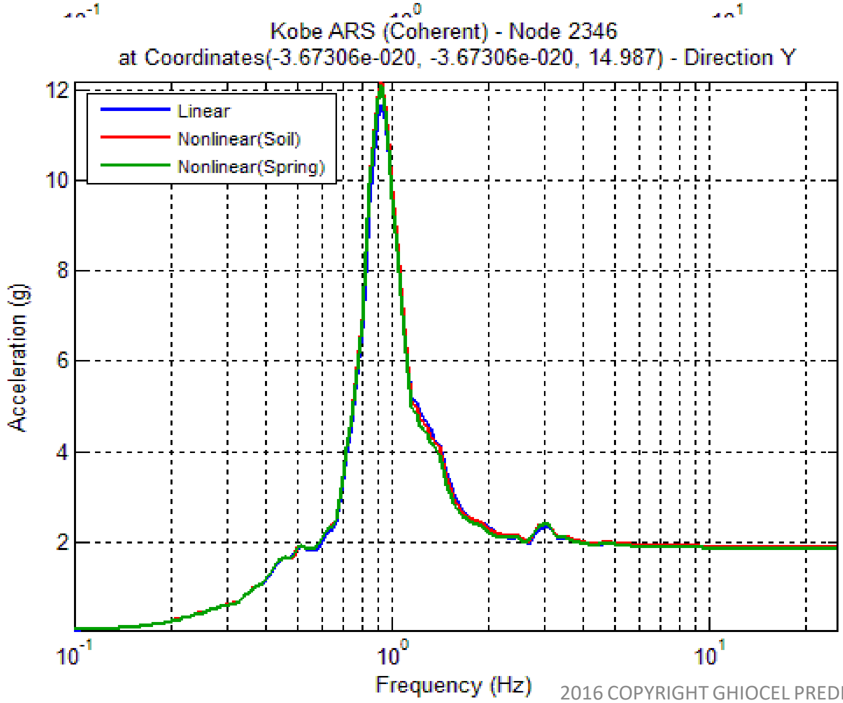

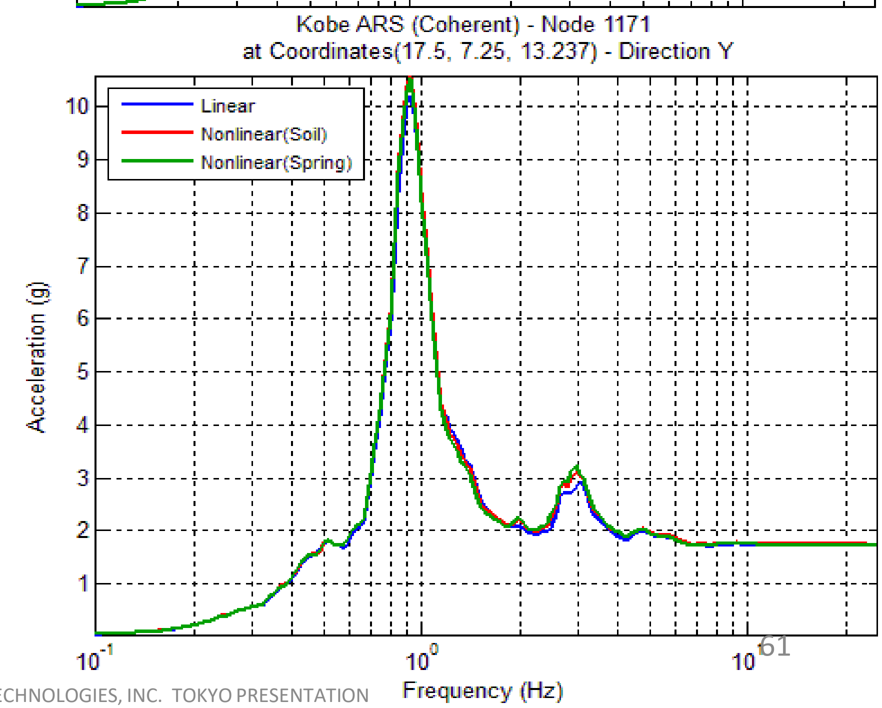

Pier Shear Force and Moment Under Coherent Y-Input (Transverse) 橋脚せん断力とモーメント、Y方向のコヒレント入力

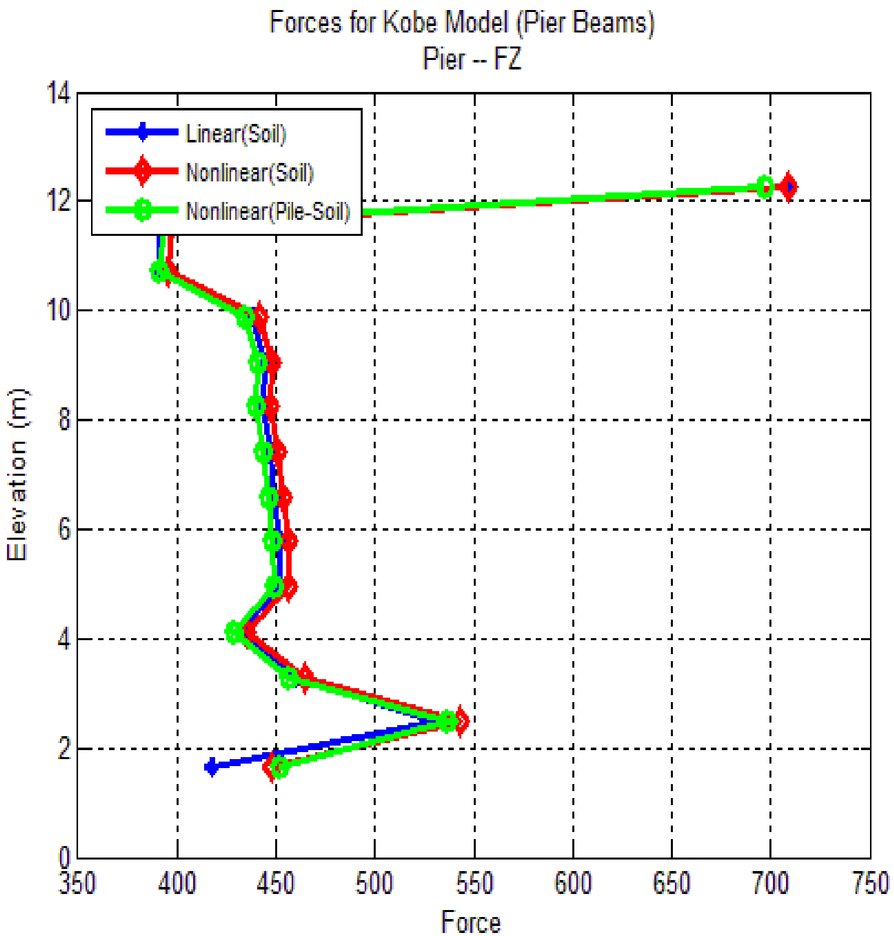

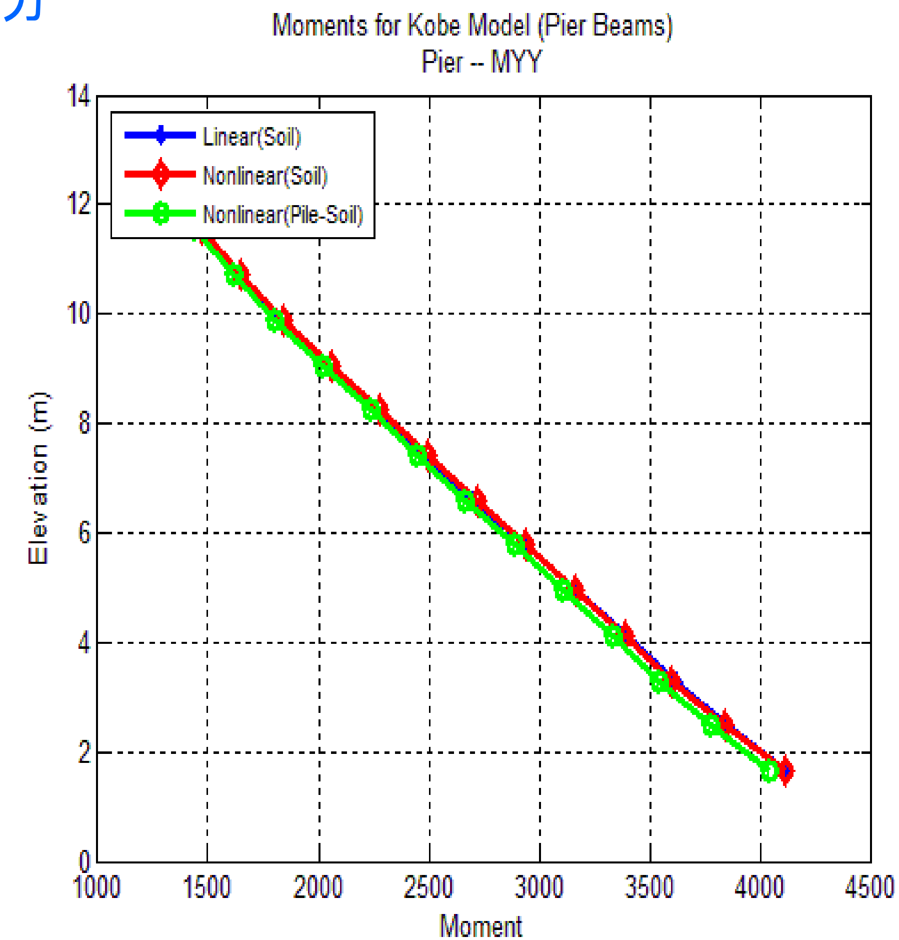

Edge Pile Axial and Shear Forces Under Coherent Y-Input 端部の杭の軸方向力とせん断力、Y方向のコヒレント入力

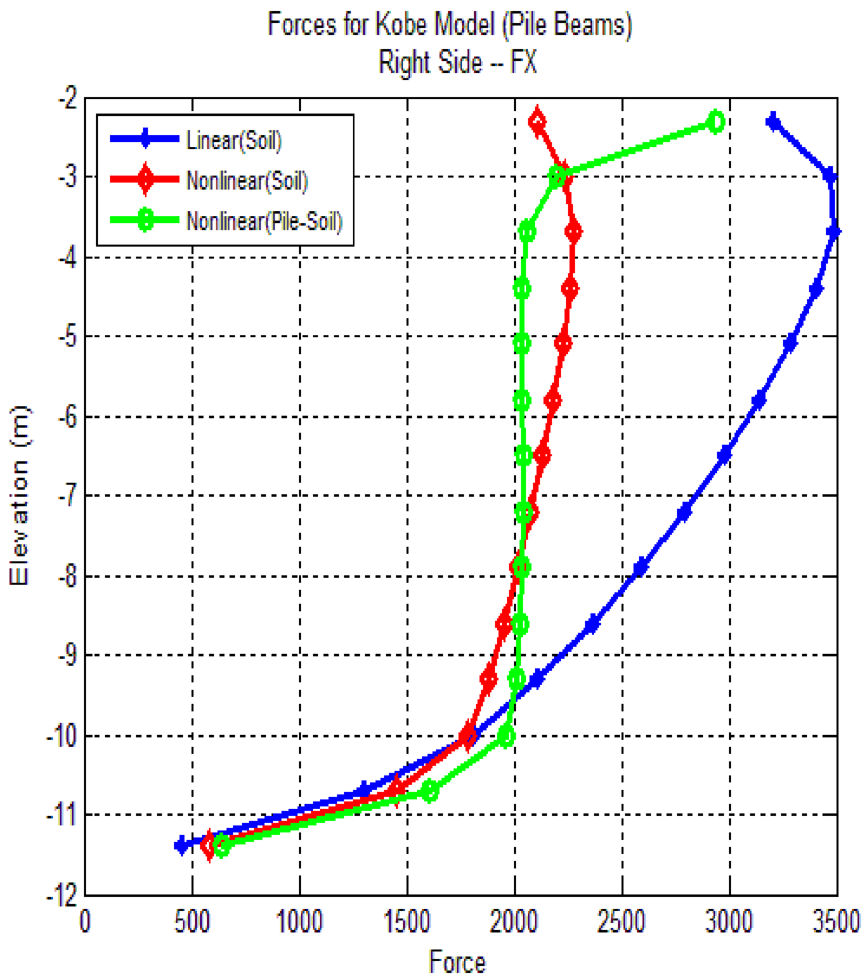

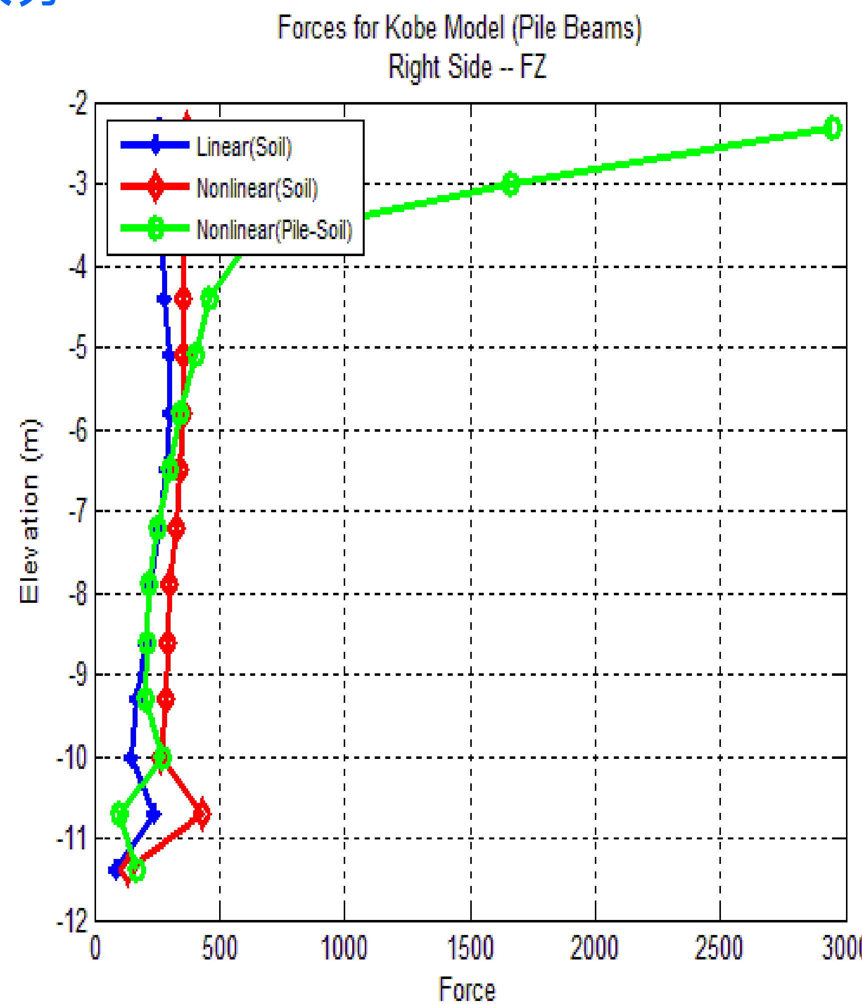

Mid and Edge Pile Shear Forces Under Coherent Y-Input 中央と端部の杭のせん断力、 Y方向のコヒレント入力

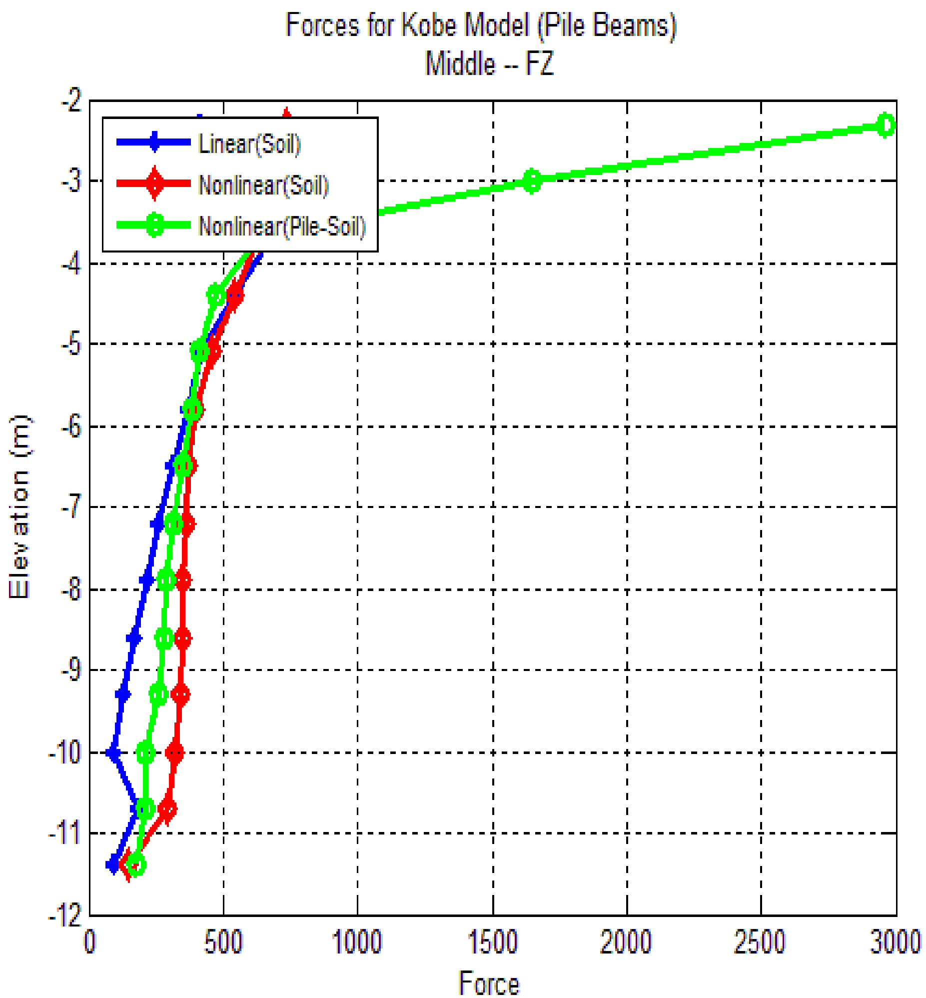

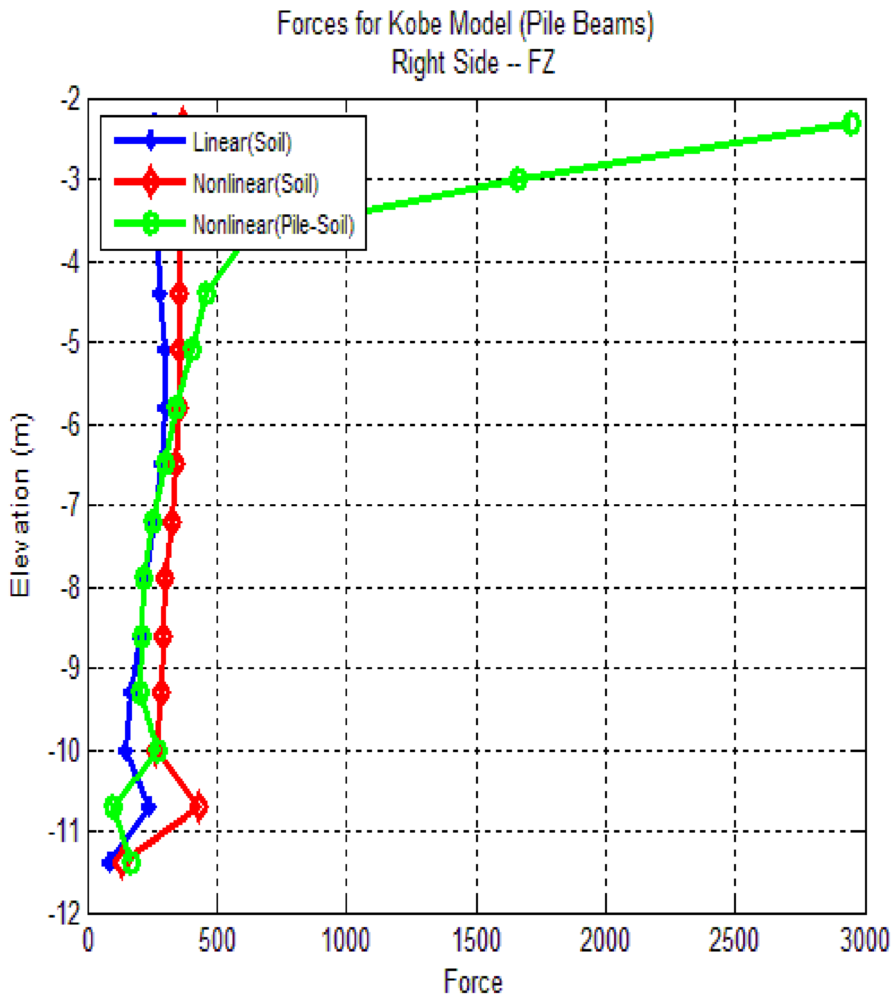

Mid and Edge Pile Moments Under Coherent Y-Input

中央と端部の杭のモーメント、Y方向のコヒレント入力

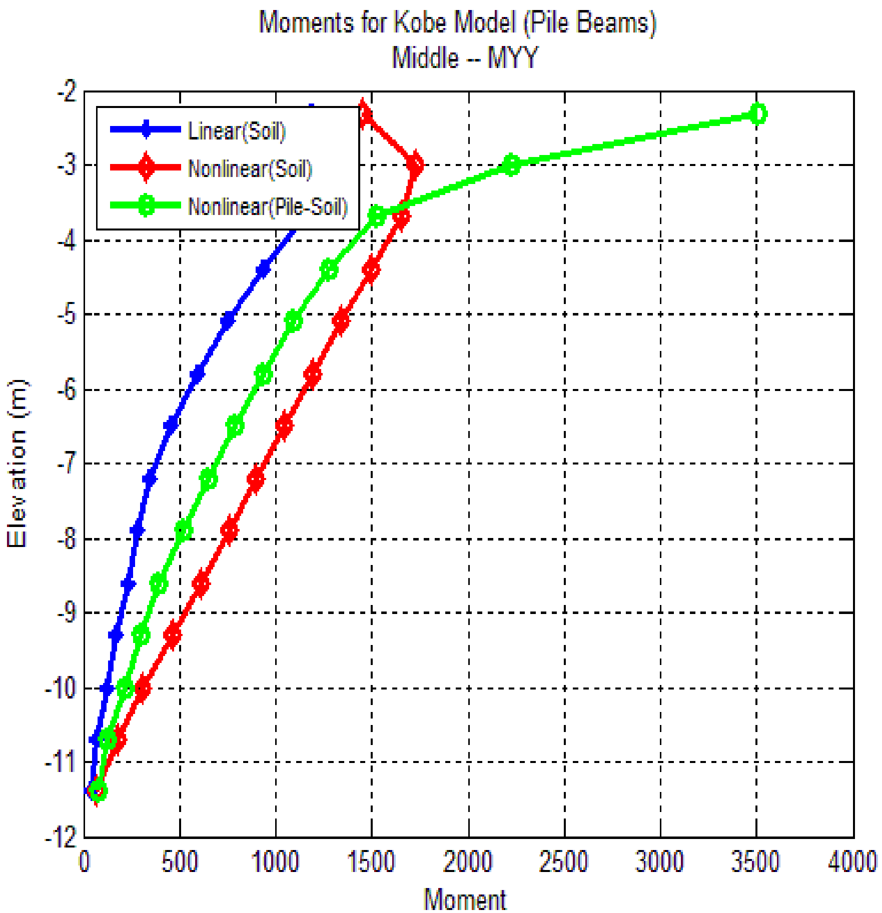

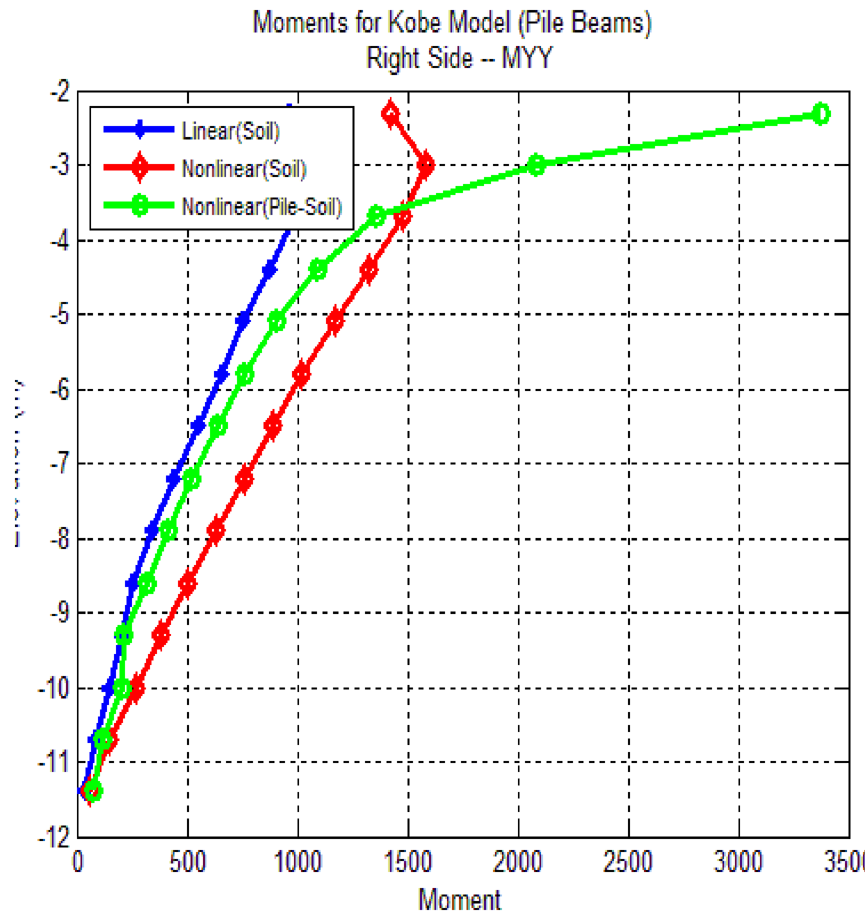

Acceleration RS at Top and Ground Levels Under *Coherent* and *Incoherent* Y-Inputs

頂部と地表面の加速RS、Y方向のコヒレントとインコヒレント入力

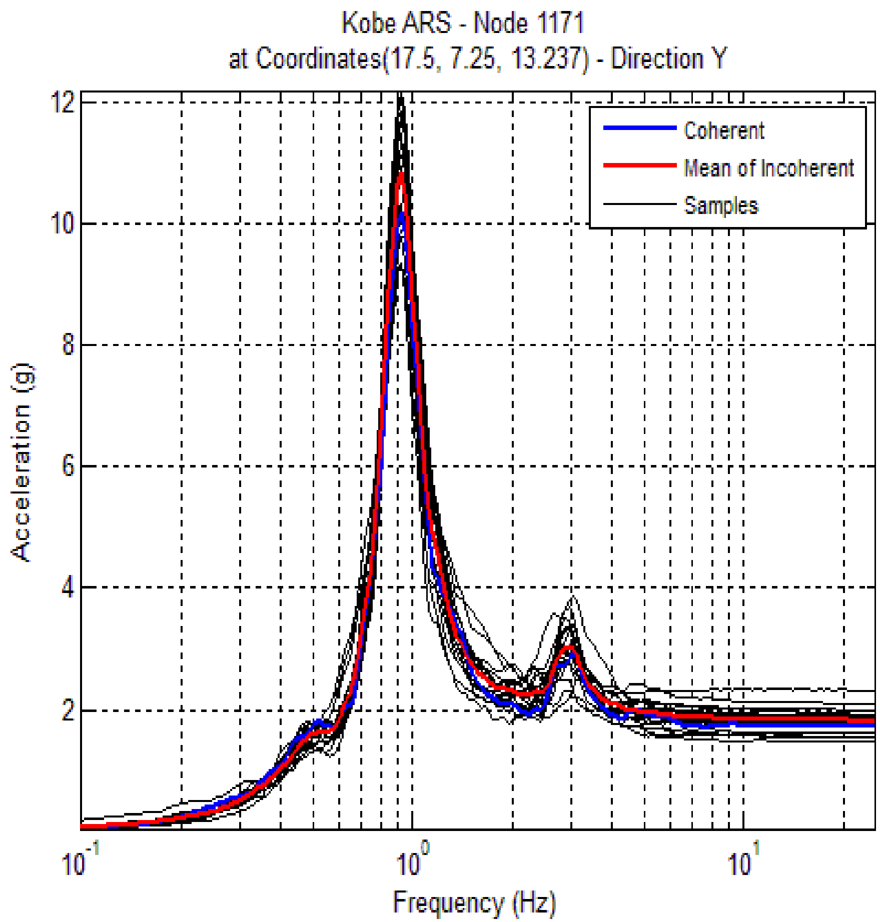

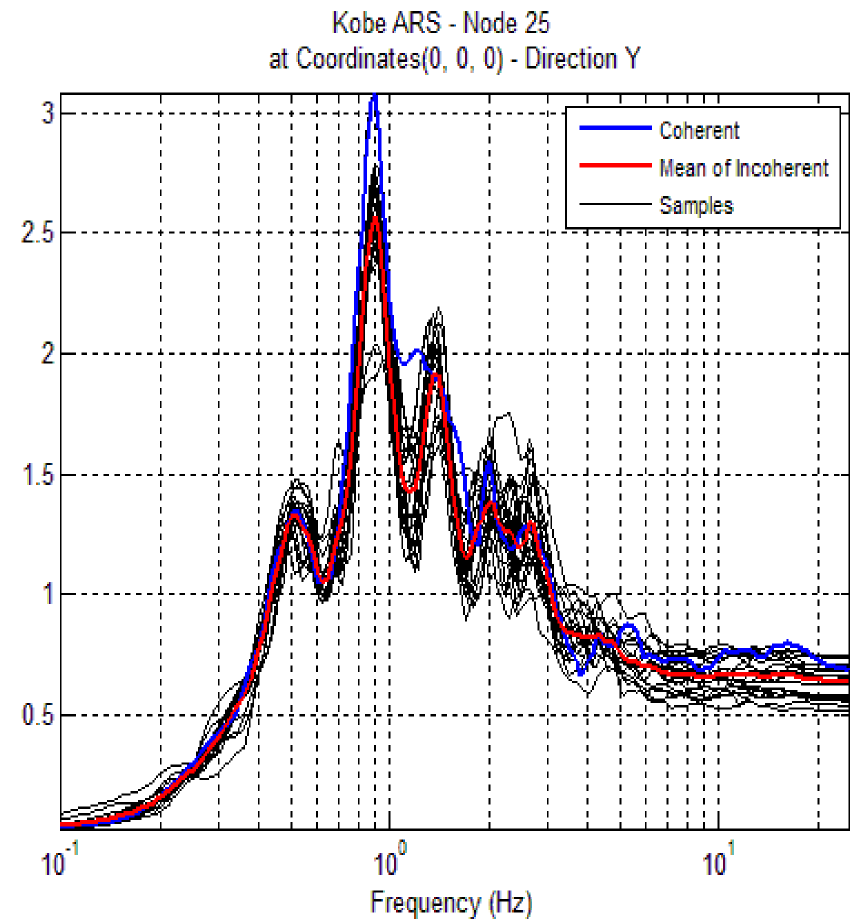

Acceleration RS at Top and Ground Levels Under Coherent and Incoherent Inputs

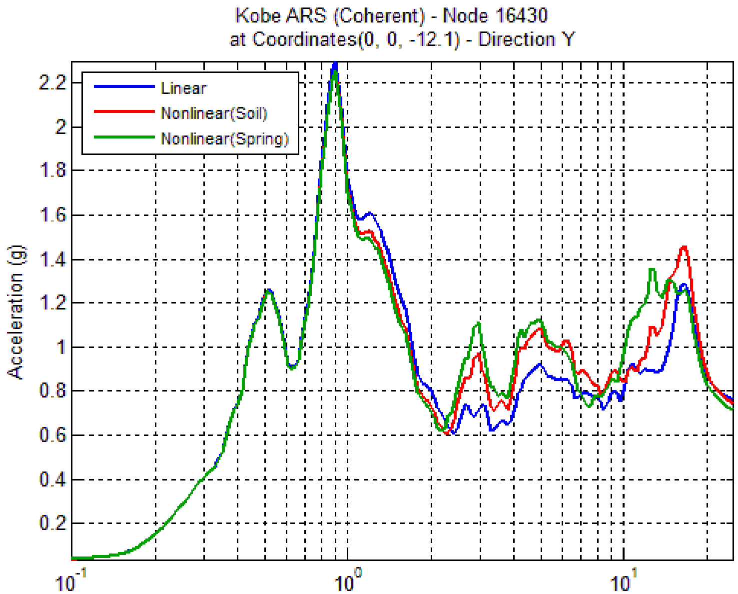

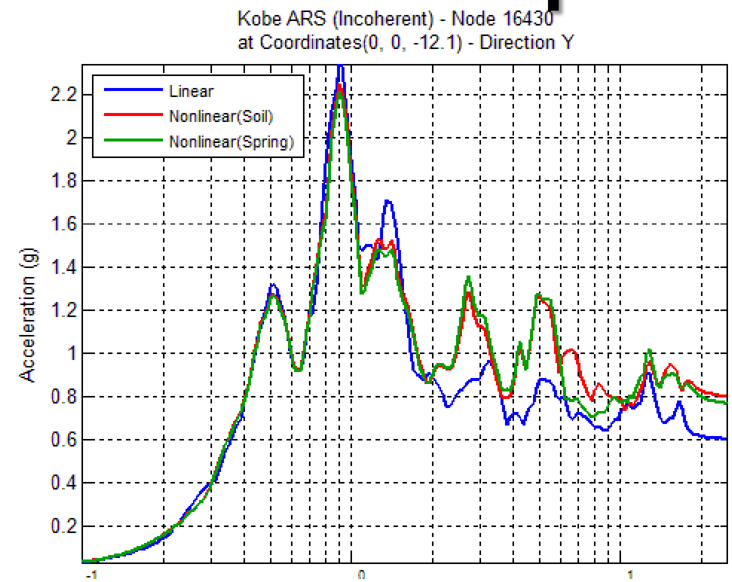

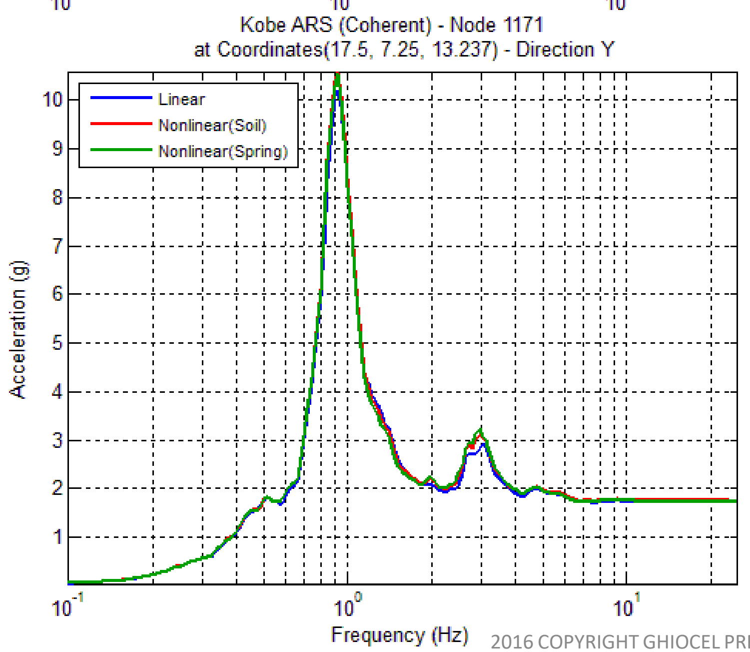

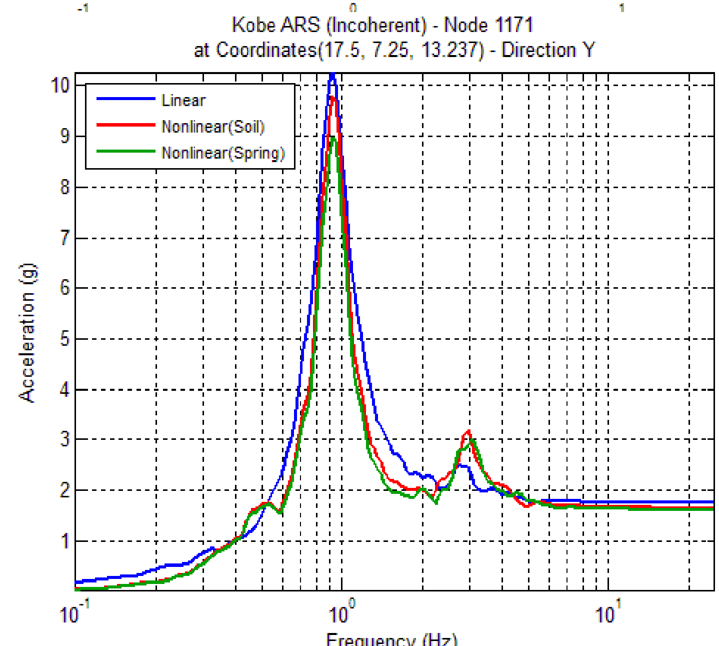

Relative Displacements wrt Free-Field Motion Under Coherent and Incoherent Y-Inputs

相対変位 自由フィールドモーションによる Y方向のコヒレントとインコヒレント入力

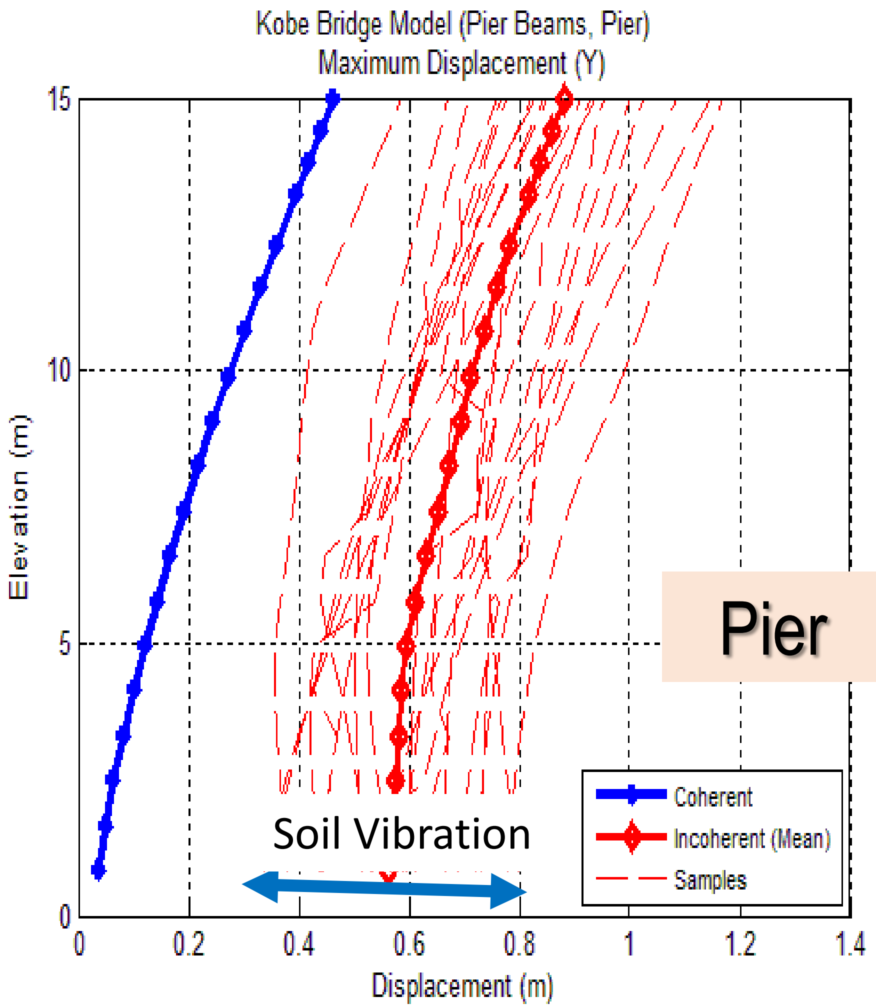

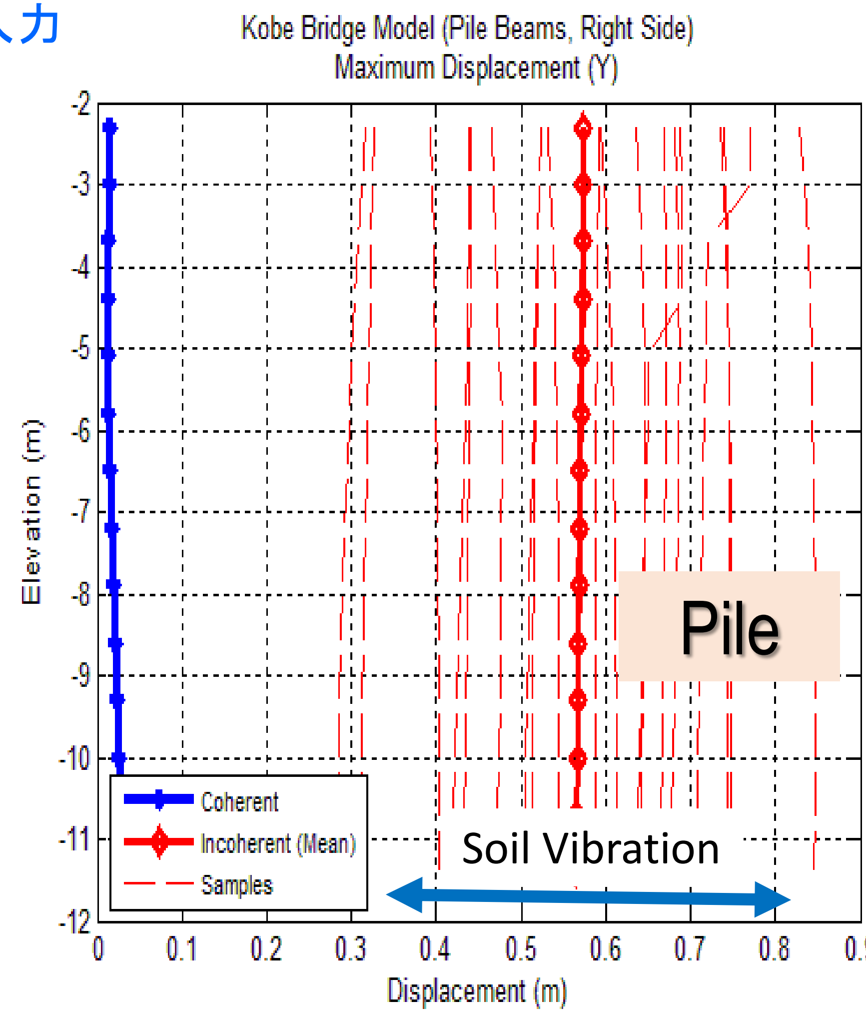

Relative Displacements wrt Free-Field Motion Under Coherent and Incoherent Y-Inputs

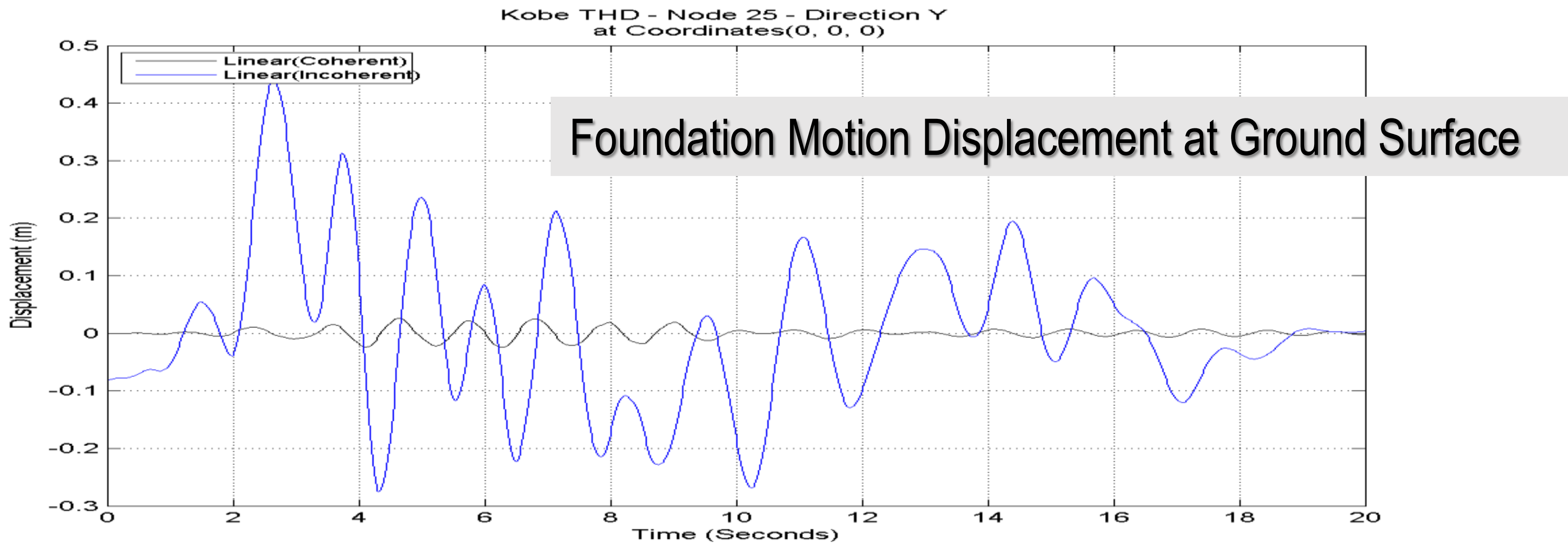

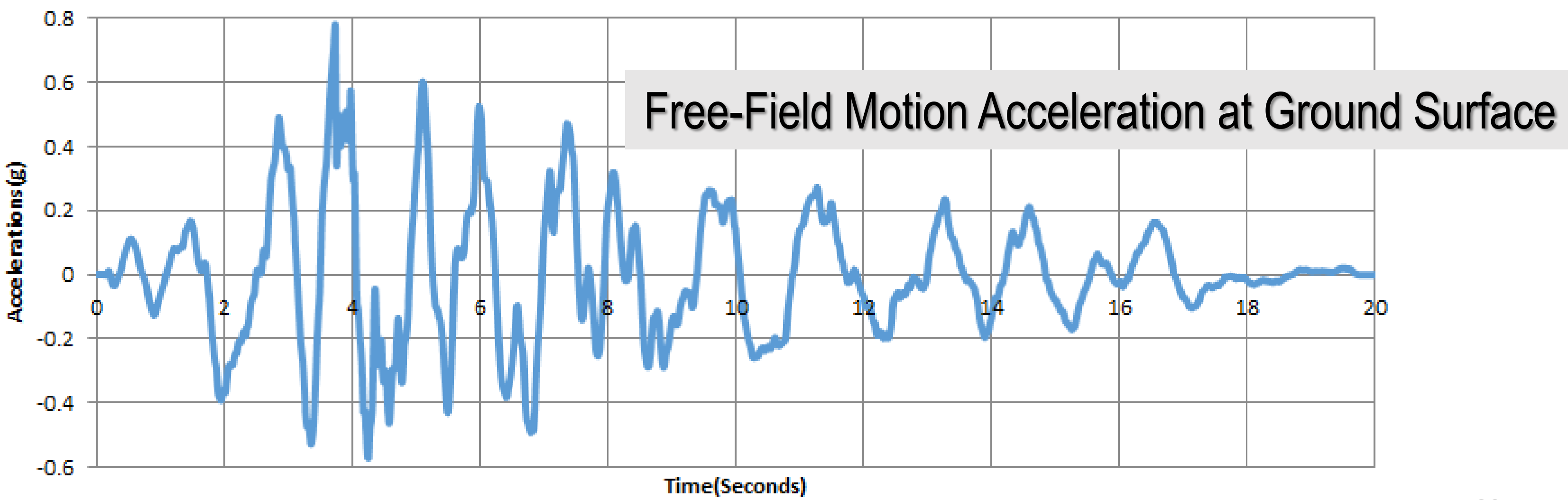

Pier Shear Force Under Coherent and Incoherent Y-Input

橋脚せん断力の比較（コヒレントとインコヒレント入力）

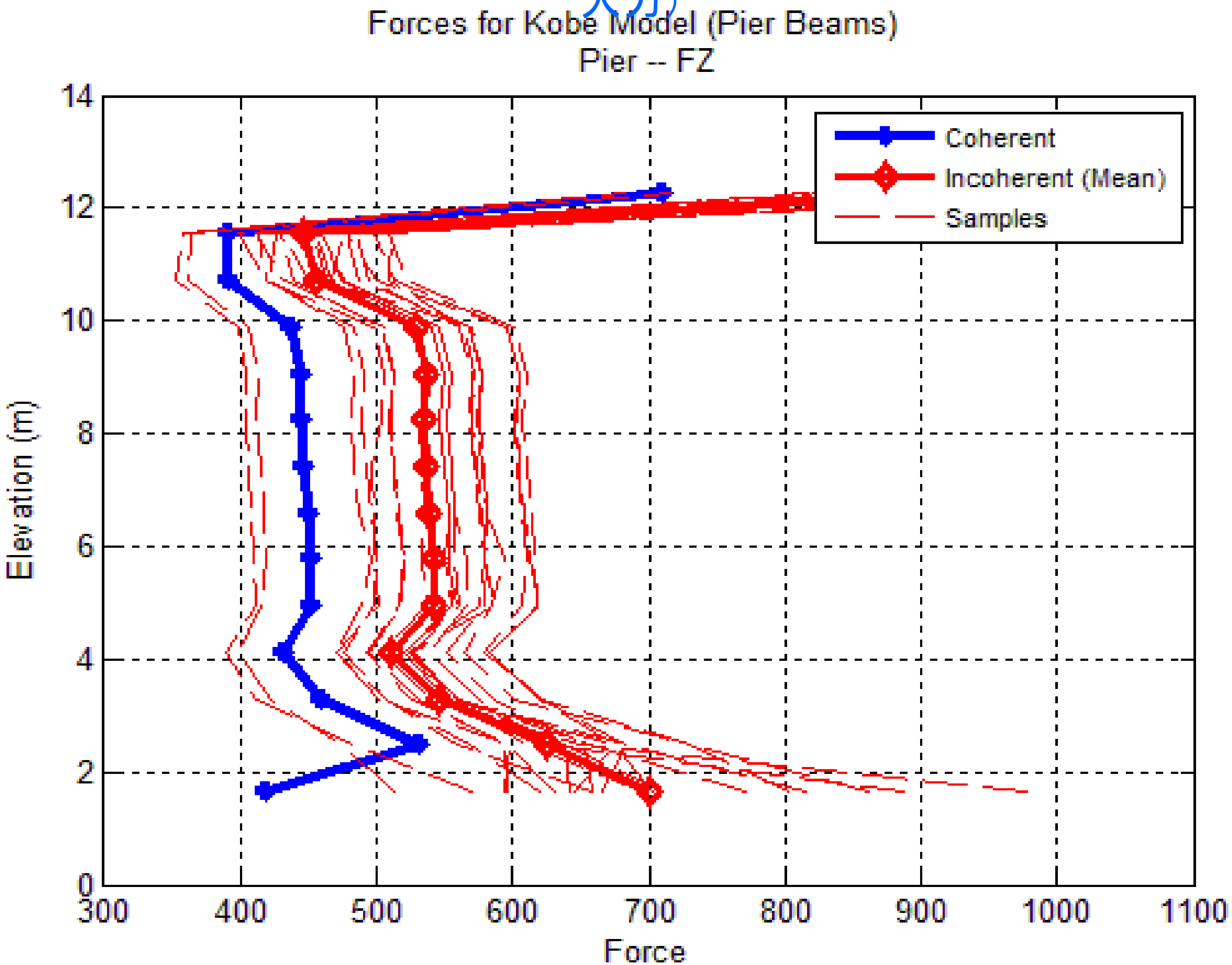

Pier Shear Force Under Y-Input 橋脚せん断力の比較

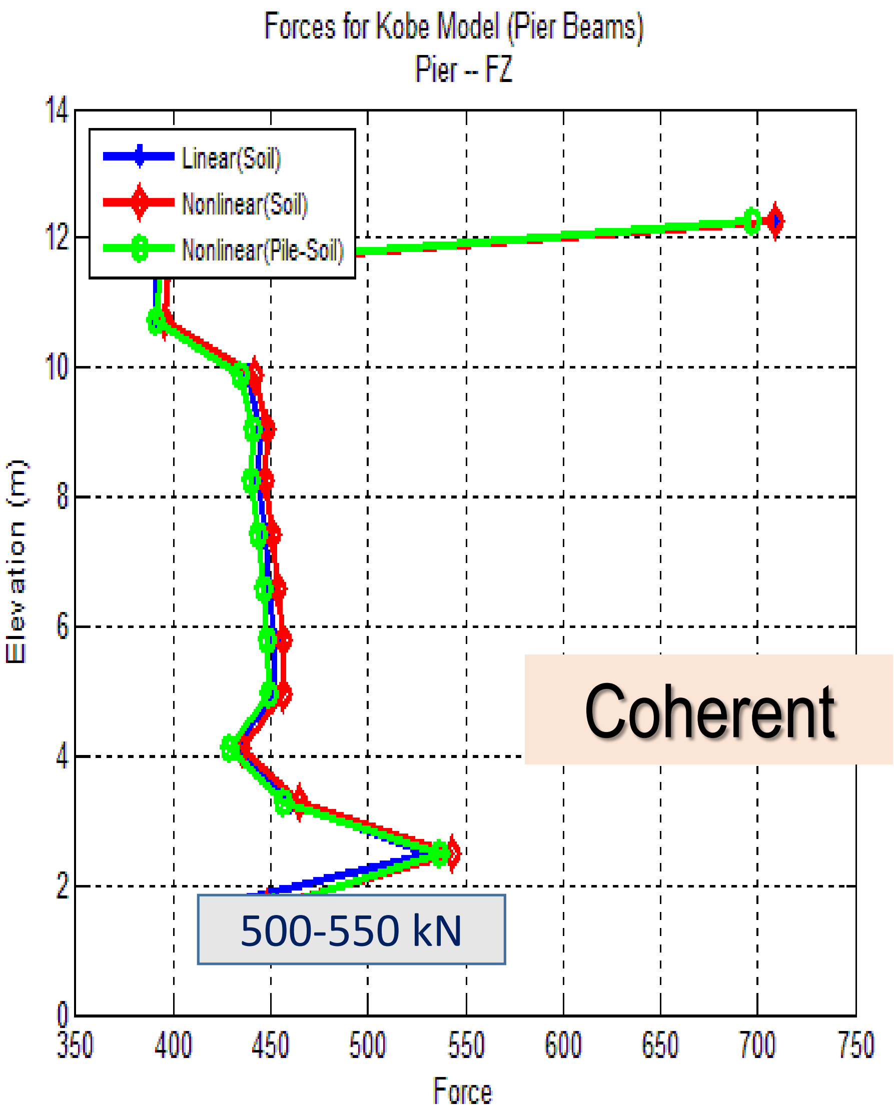

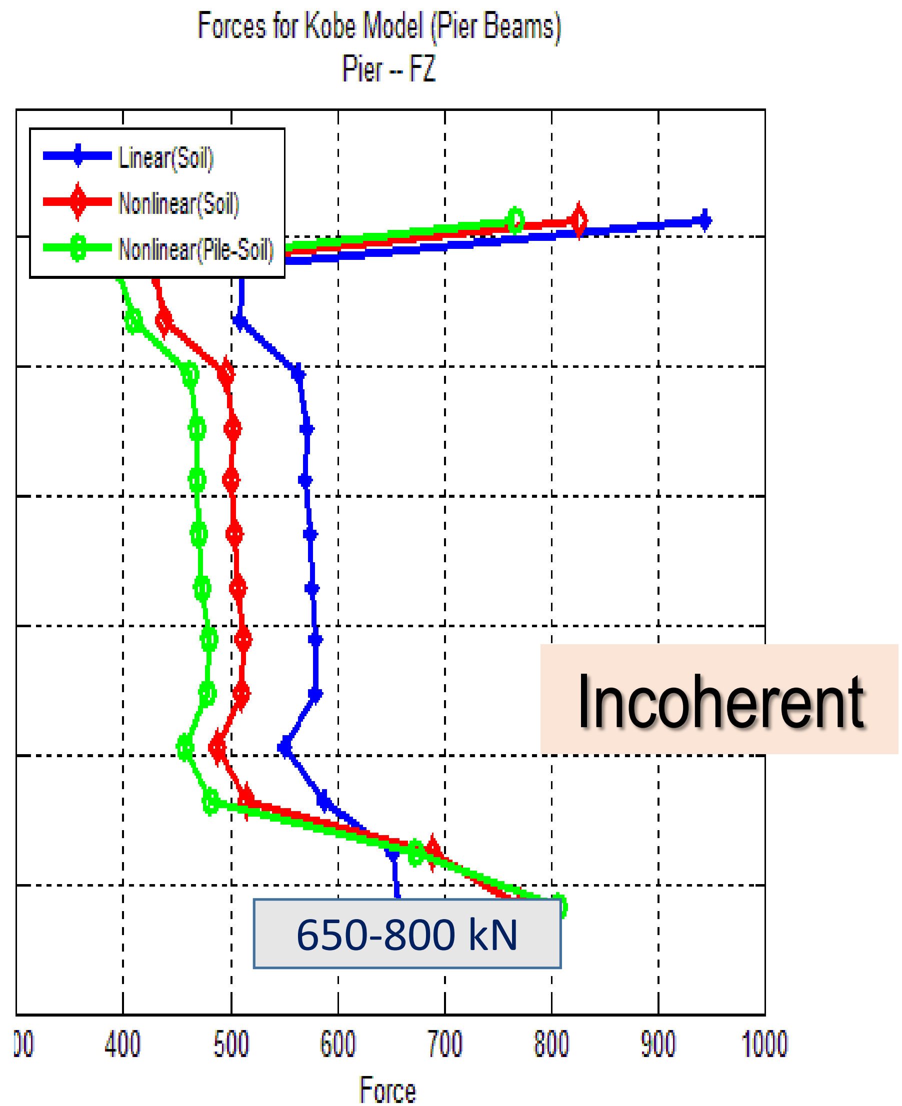

Pier Moment Under Coherent and Incoherent Y-Input 橋脚モーメントの比較

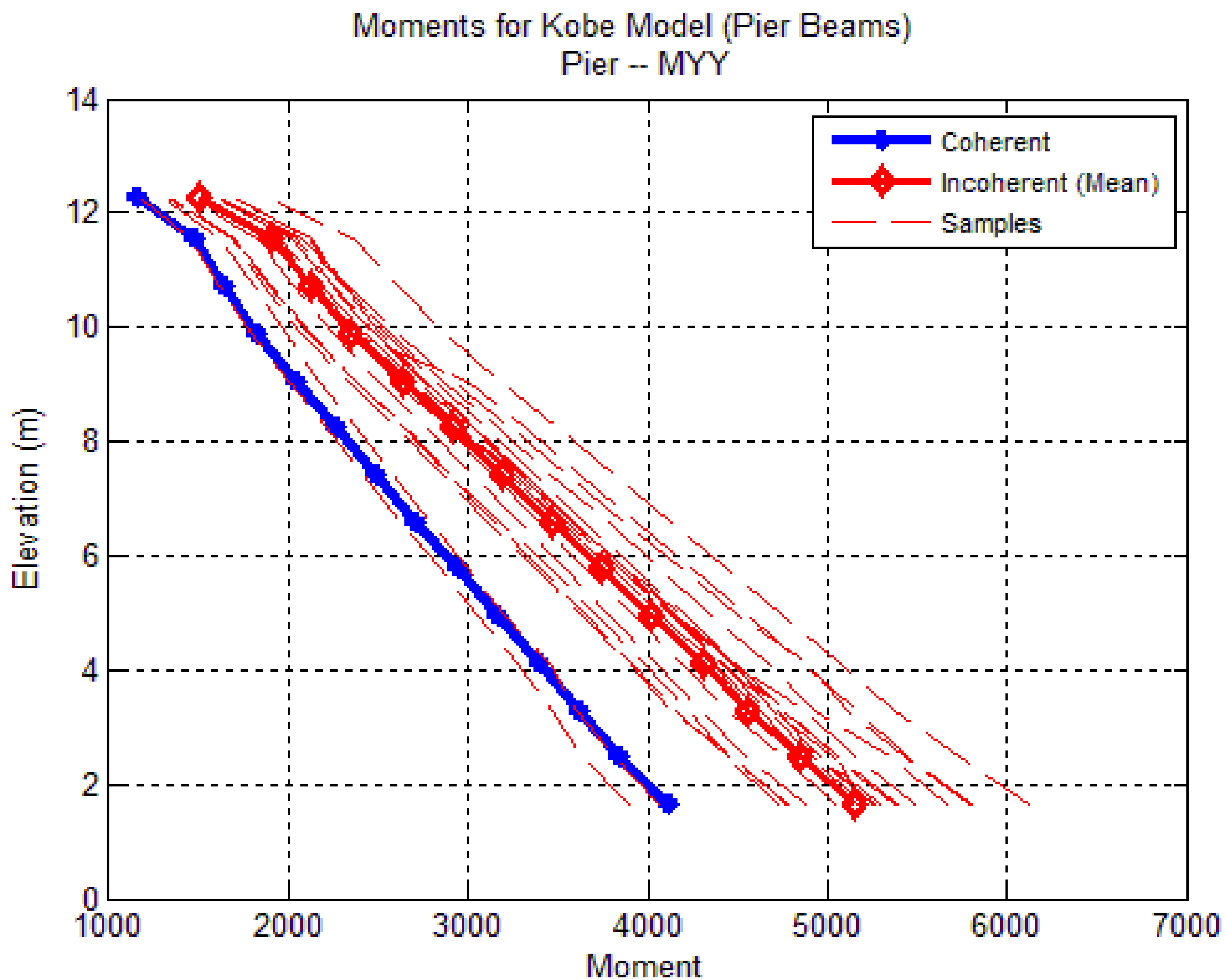

Pier Bending Moment Under Y-Input

橋脚曲げモーメントの比較

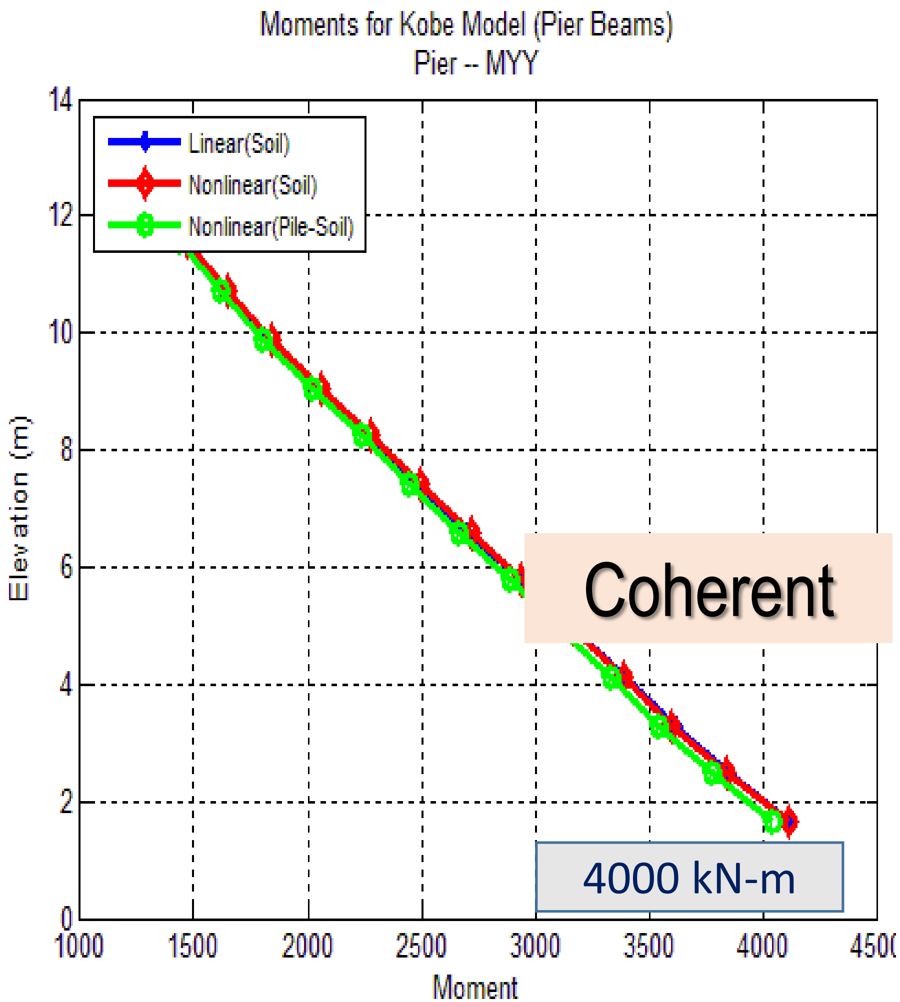

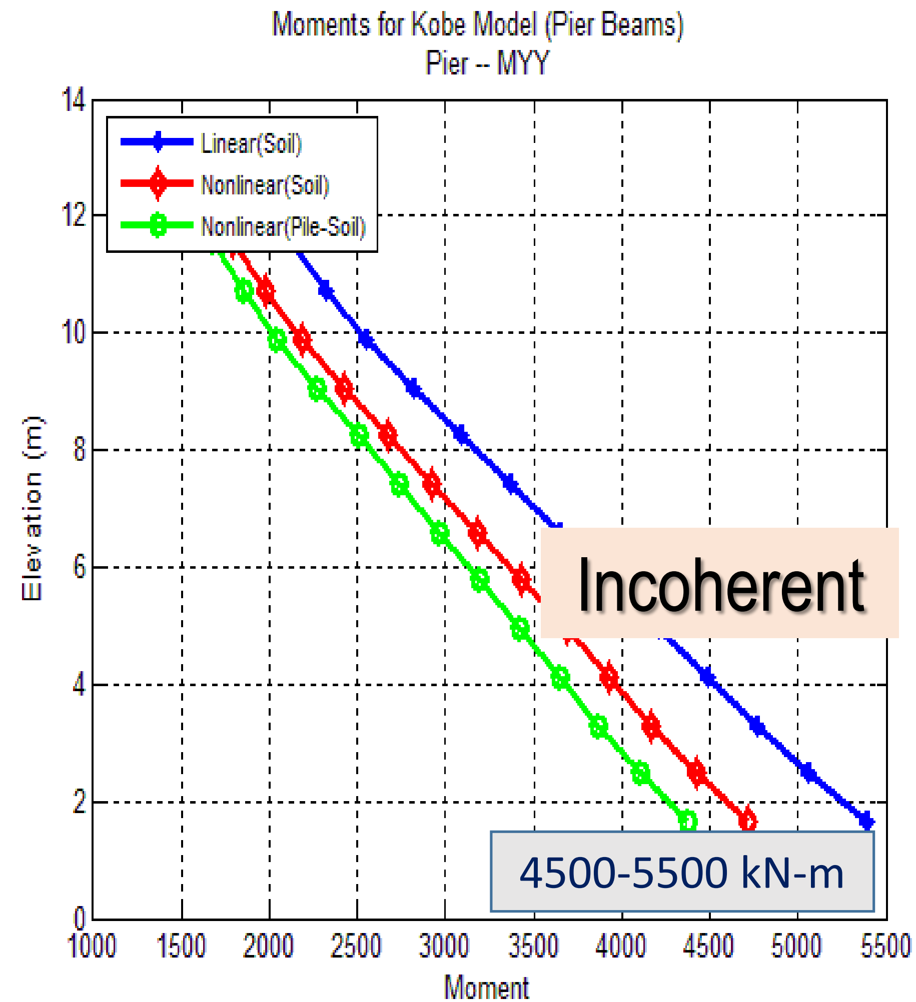

Edge Pile Axial Force Under Coherent and Incoherent Y-Input 端部杭の軸方向力の比較

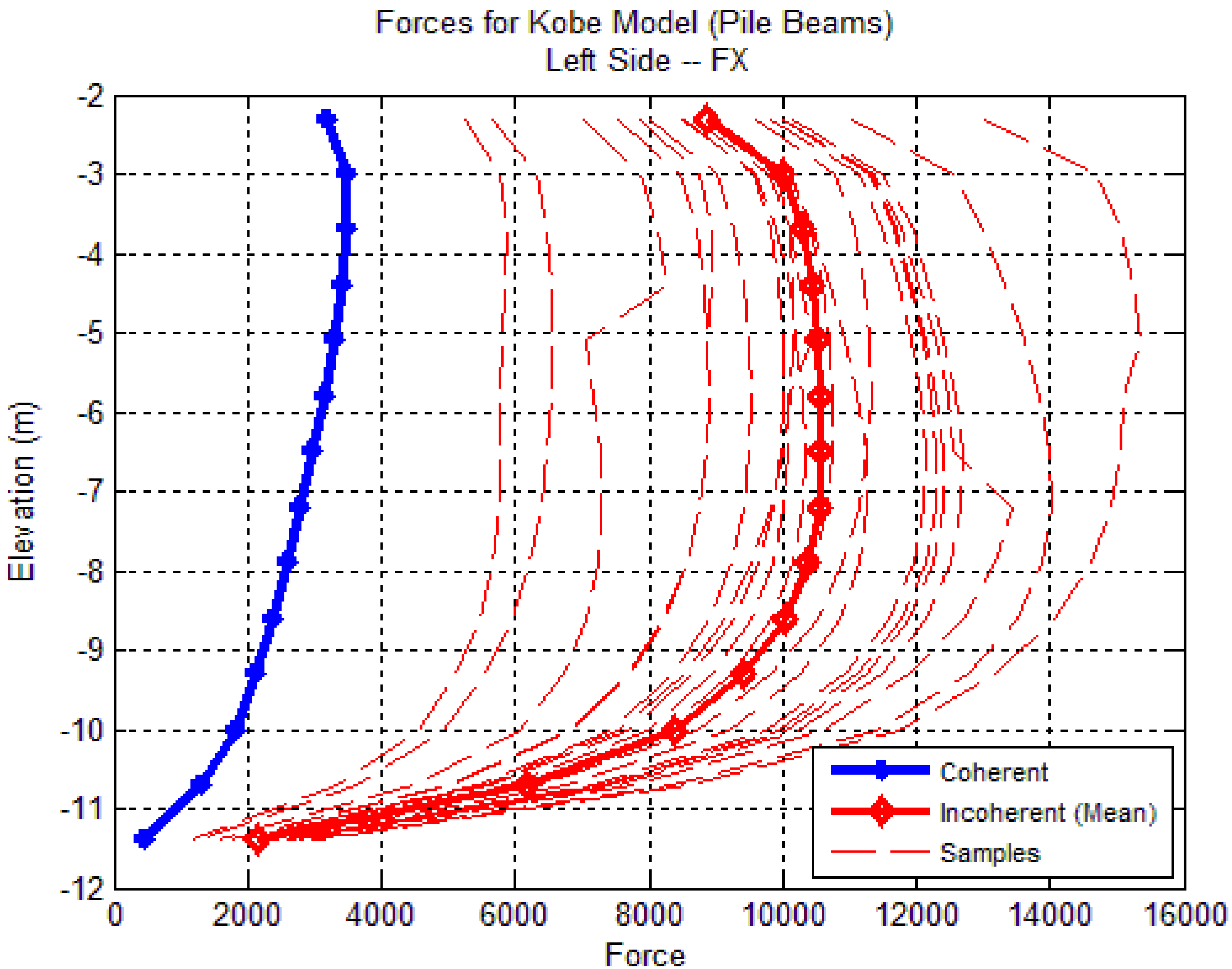

Edge Pile Axial Force Under Y-Input

端部杭の軸方向力の比較

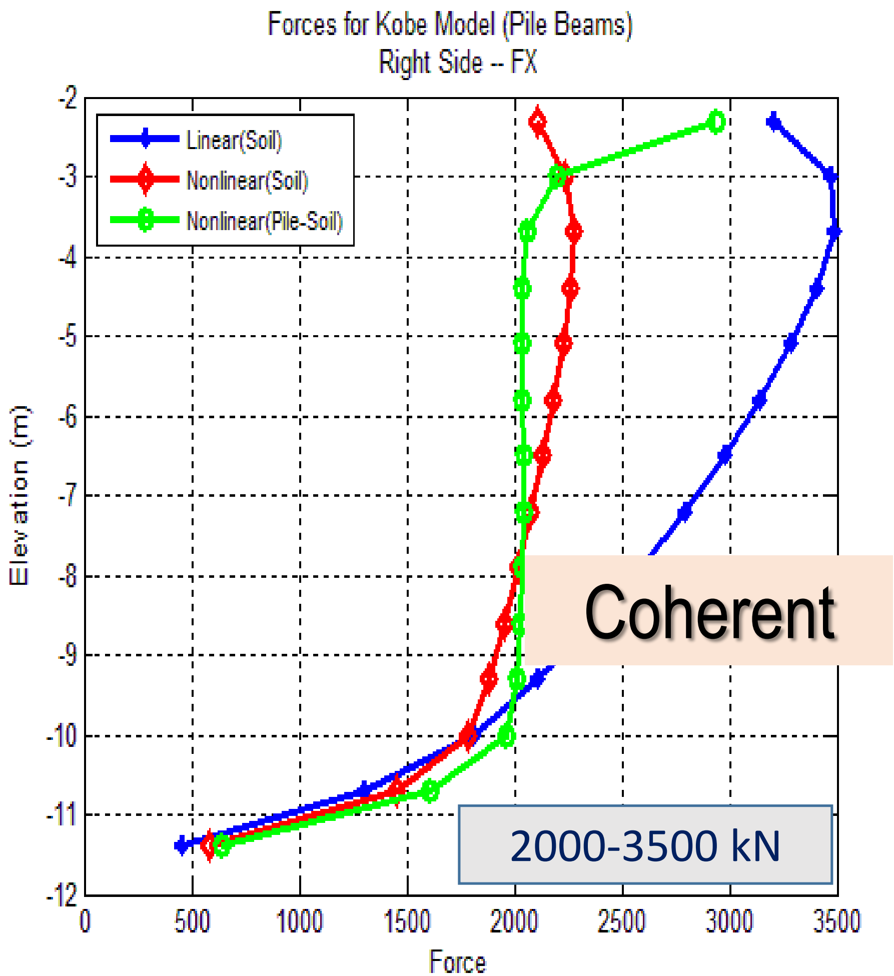

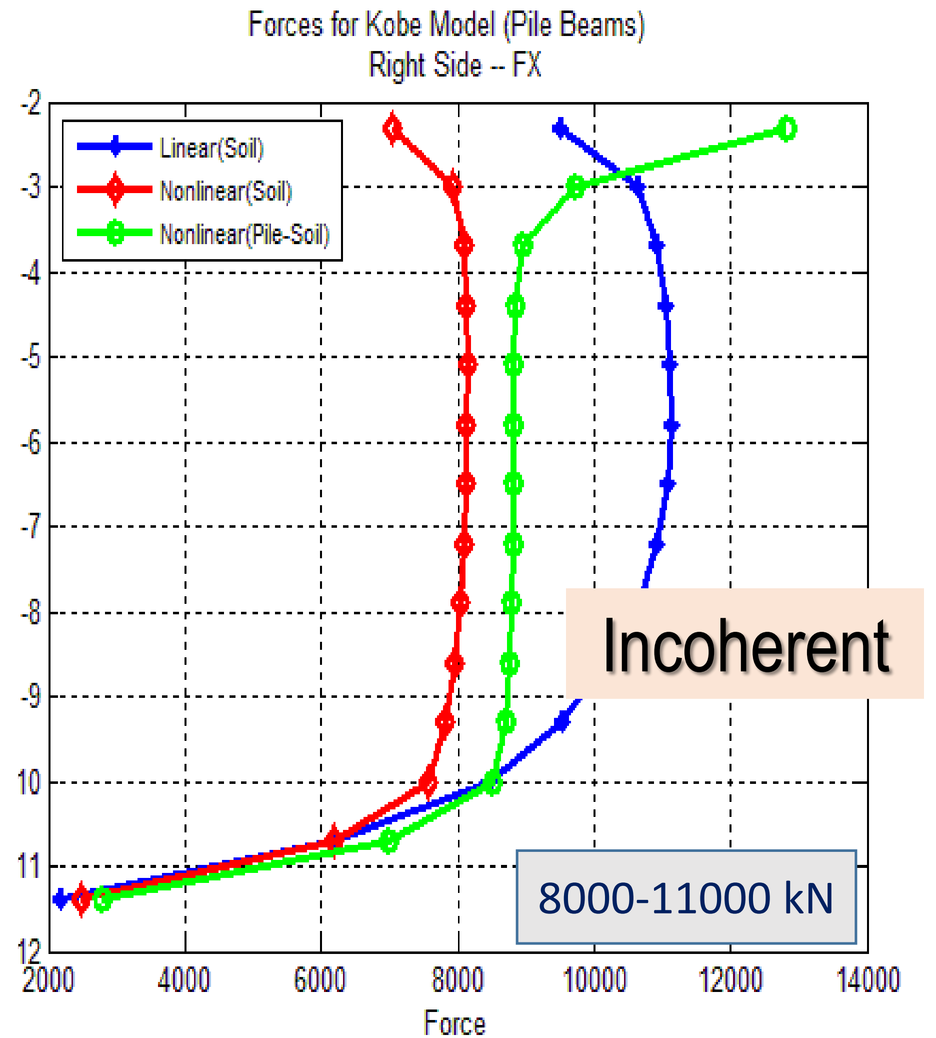

Edge Pile Axial Force Under Coherent and Incoherent Y-Input 端部杭の軸方向力の比較

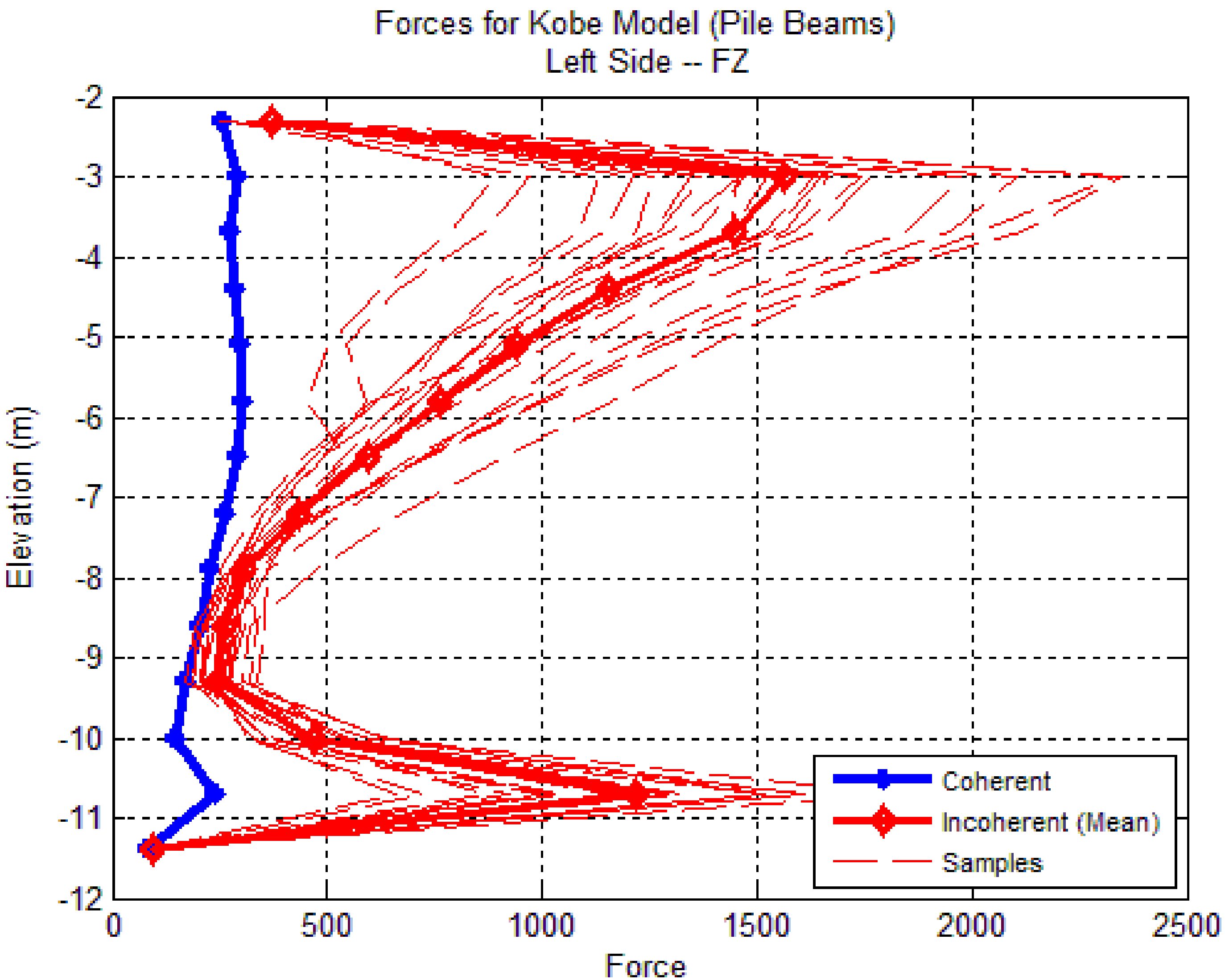

Edge Pile Shear Force Under Y-Input

端部杭のせん断力の比較

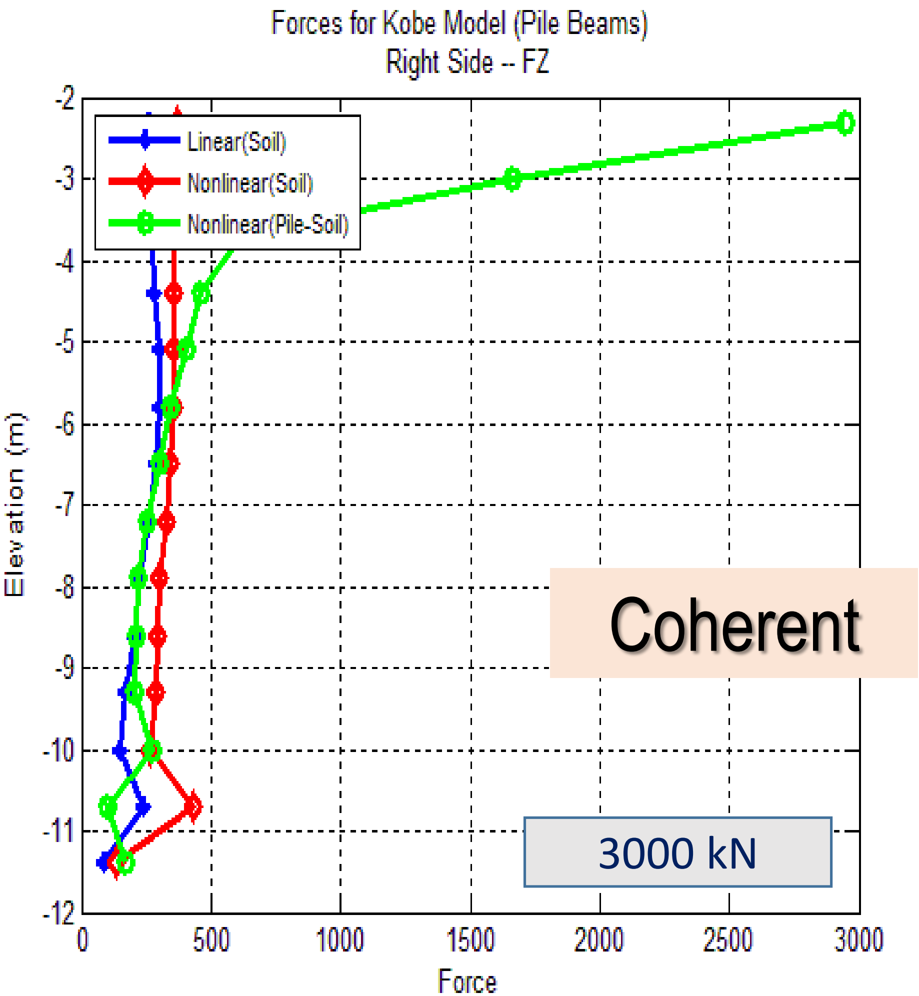

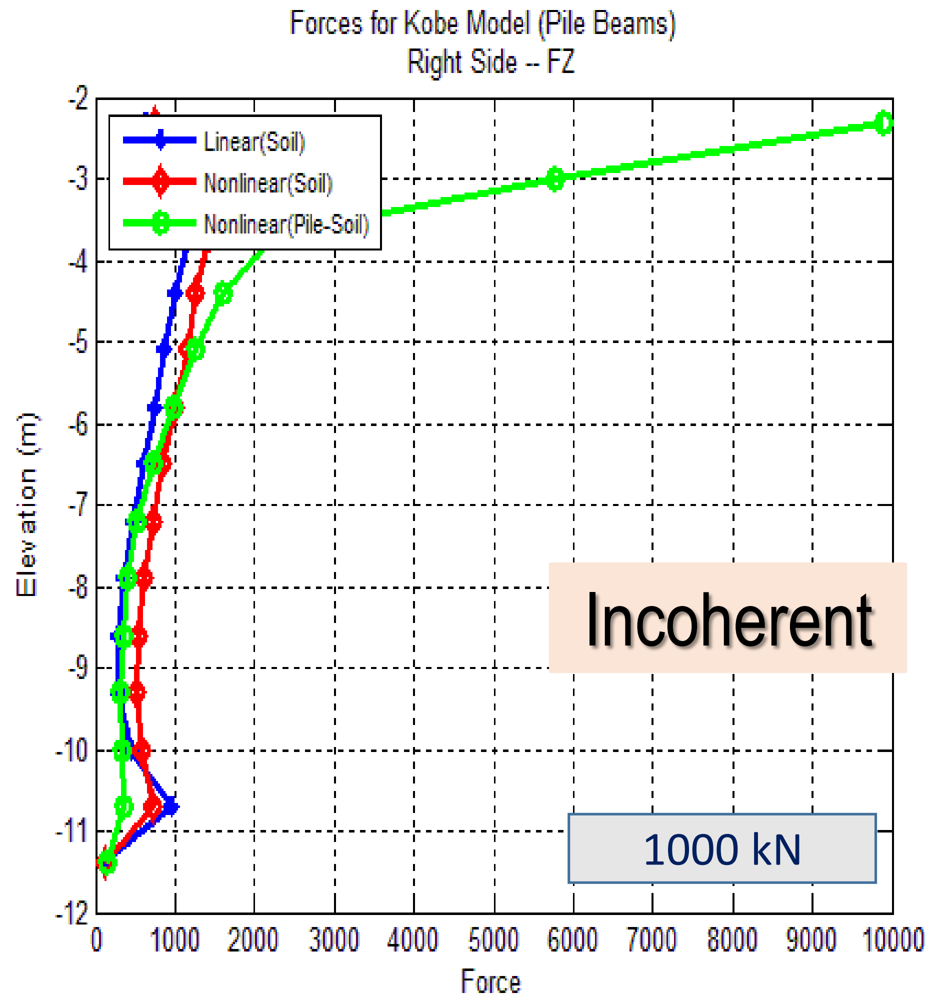

Edge Pile Moment Under Coherent and Incoherent Y-Input 端部杭のモーメントの比較

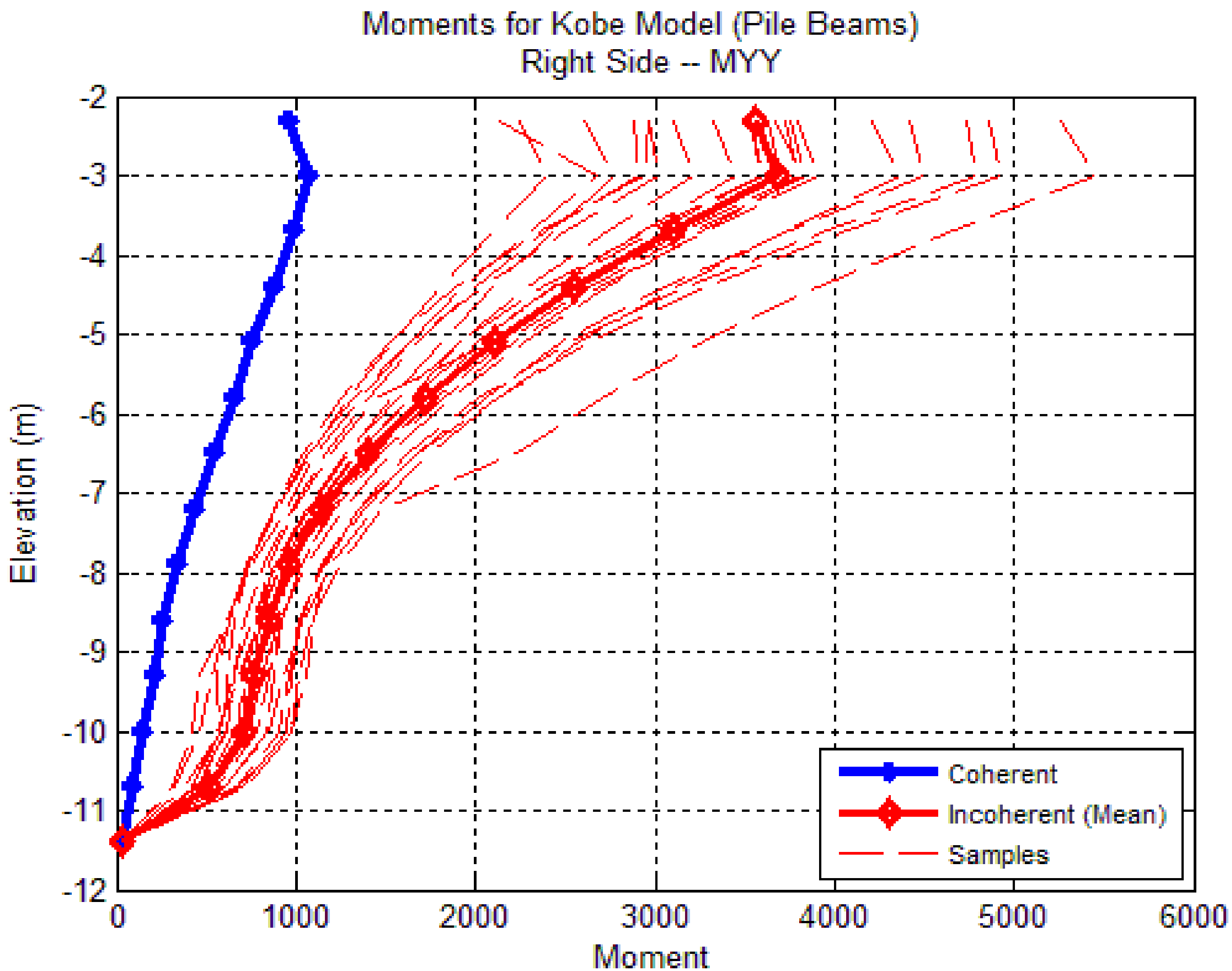

Edge Pile Moment Under Y-Input

端部杭のモーメントの比較

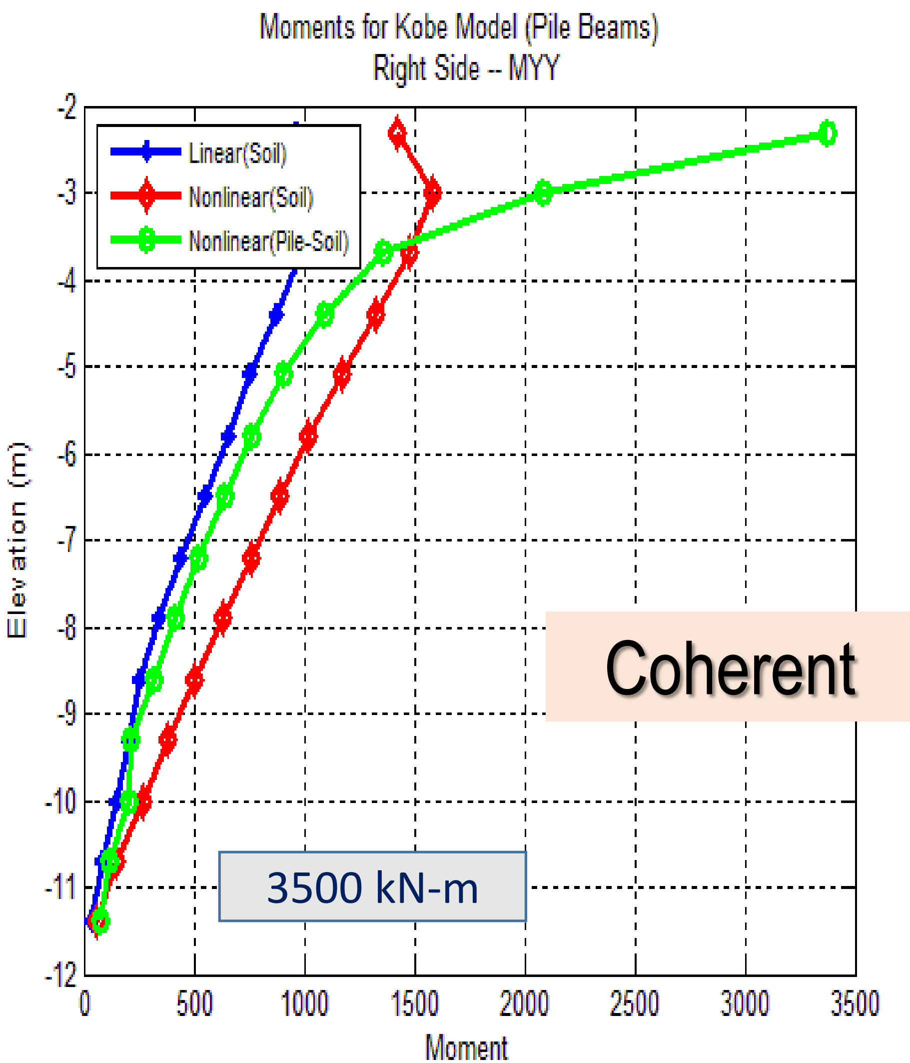

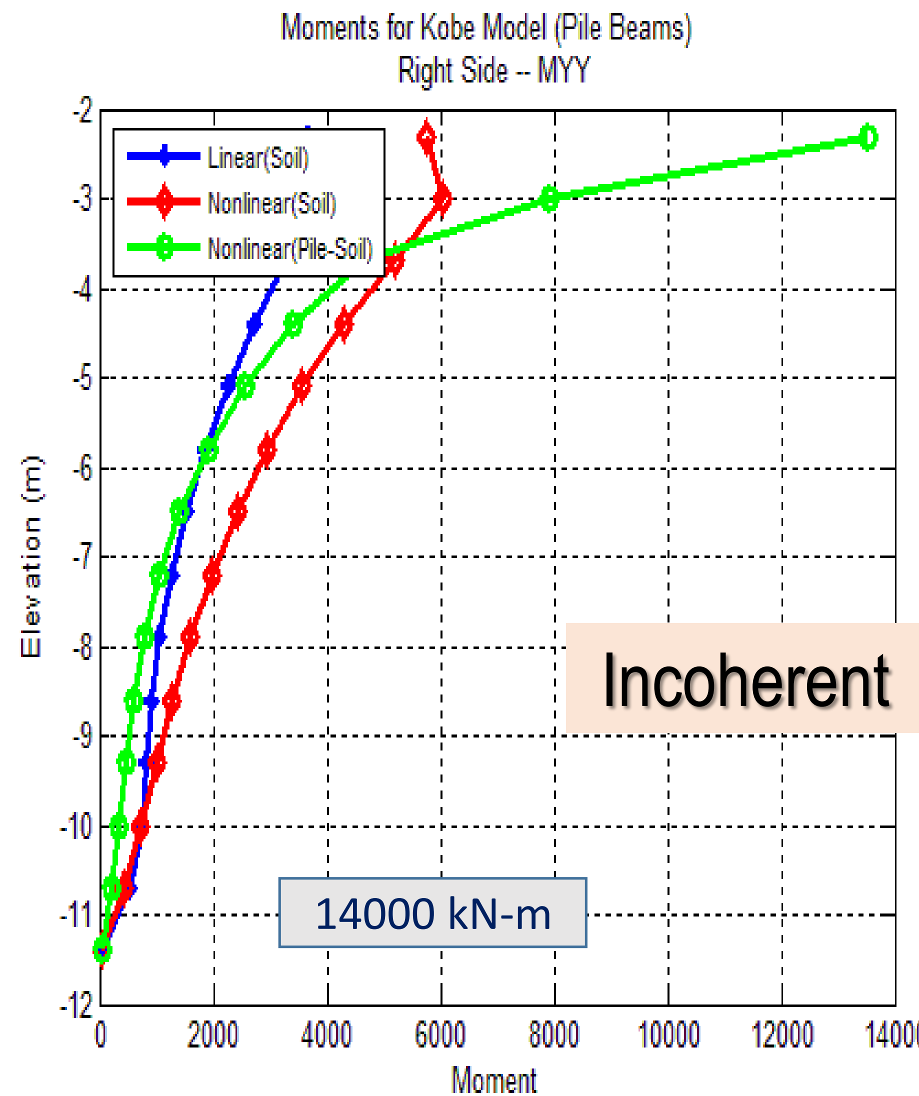

Acceleration of Fukae Bridge Under Coherent and Incoherent Y-Inputs

深江橋加速度の比較

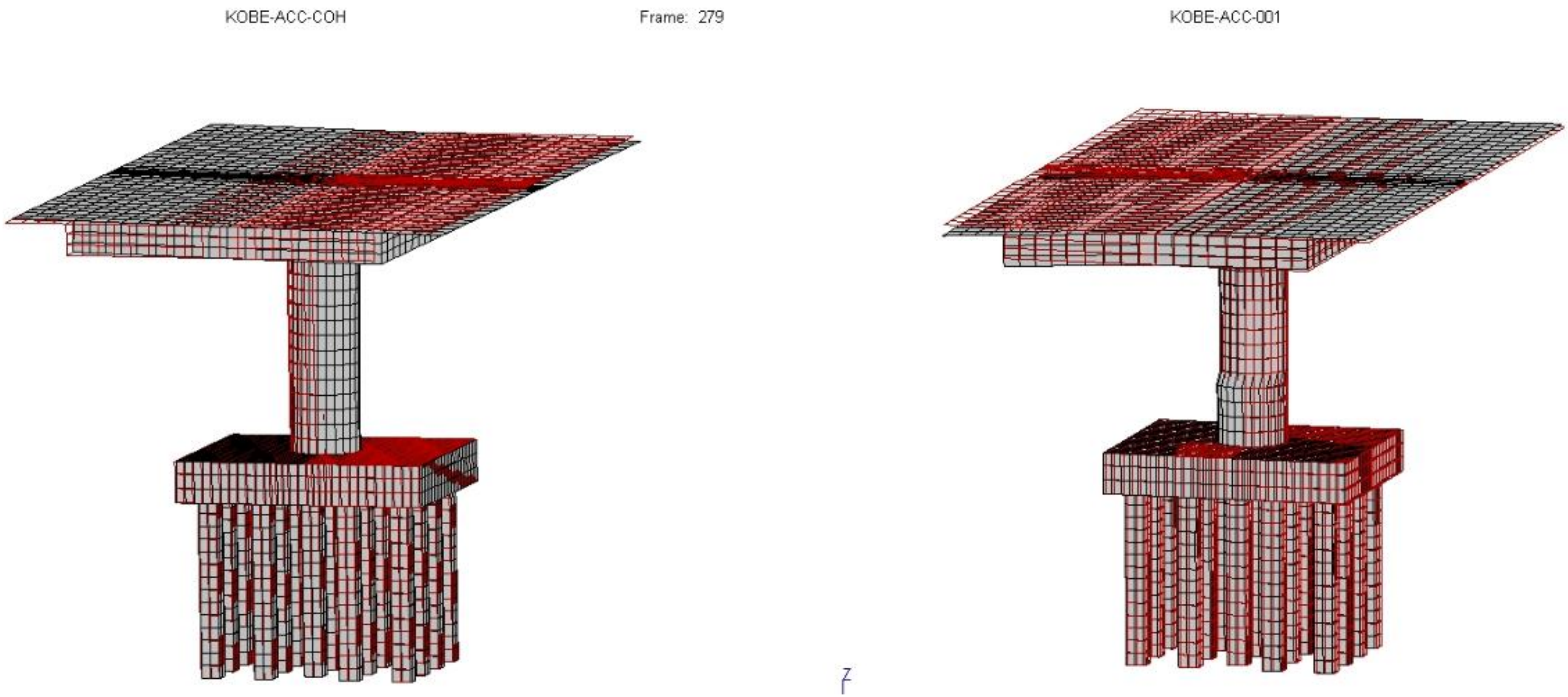

Coherent

Incoherent

ANIMATION 2

Relative Displacements of Fukae Bridge Under Coherent and Incoherent Y-Inputs

深江橋相対変位の比較

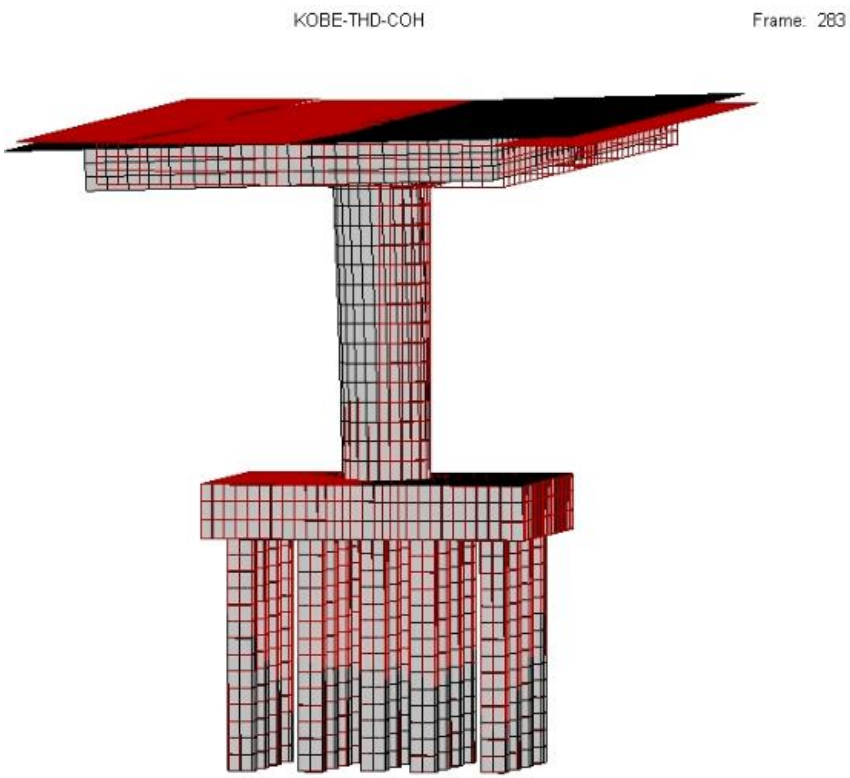

Coherent

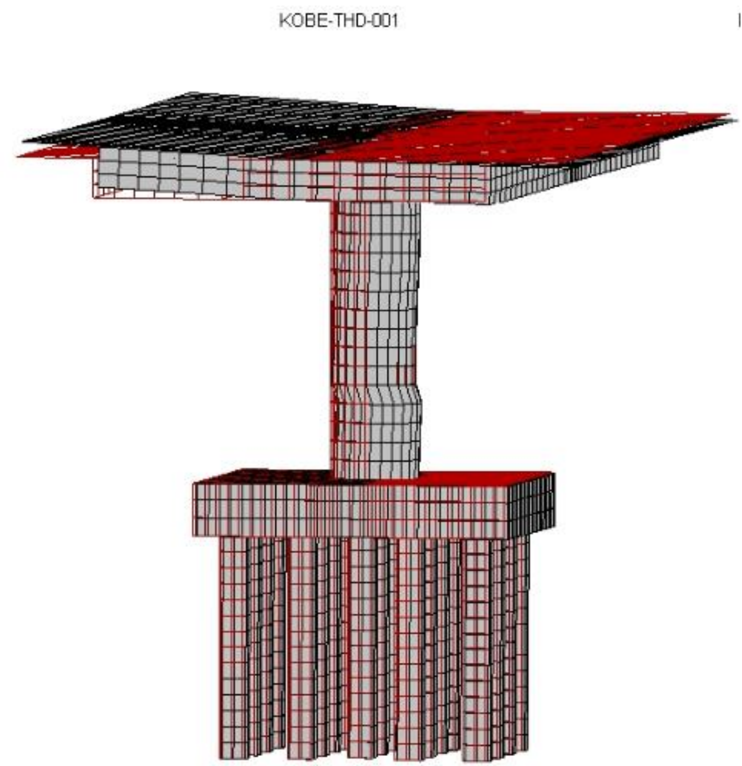

Incoherent

ANIMATION 3

Conclusions of Fukae Bridge Failure

深江橋倒壊スタディ 結論

- The SSI effects combined with the significant motion spatial variations due to non-vertically propagating waves produced much larger seismic loads than originally expected by bridge designers. SSI効果は、非鉛直方向の変動する地震波伝播と連動したために、橋梁設計者の当初の想定よりも相当大きな地震荷重を生じた.

- The bridge pier shear failure was "helped" by the local shear deformation introduced slightly above the pier base by the different phasing of the base motion and the structure vibratory motion due to the motion spatial variation (incoherency and wave passage). 橋脚のせん断破壊は、橋脚基礎の少し上に生じた局所せん断変形によって発生した.地震波の伝播の変動(インコヒレンシー効果と地震波通過効果)によって基礎部の振動と構造部の震動の間の位相が異なり、この局所せん断変形が生じた.

Fukae Bridge After Failure

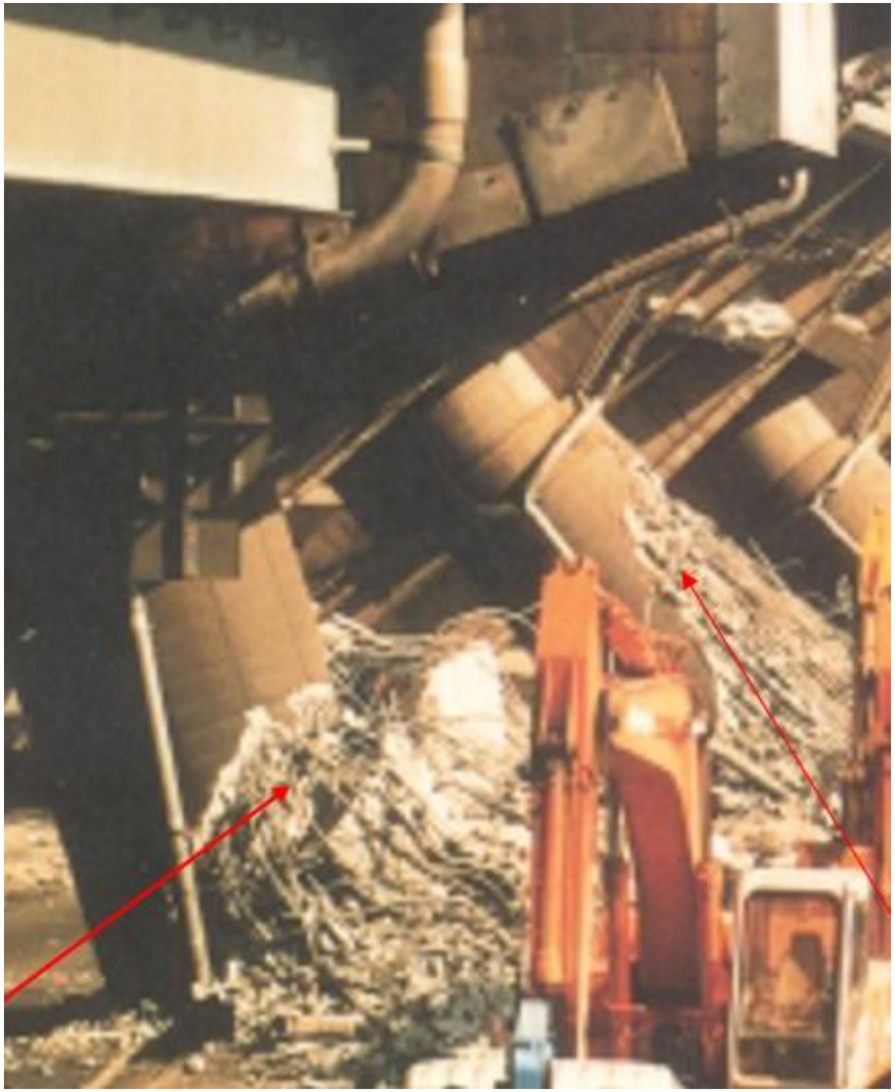

ACS SASSI SSI Analysis Explains Pier Shear Failure

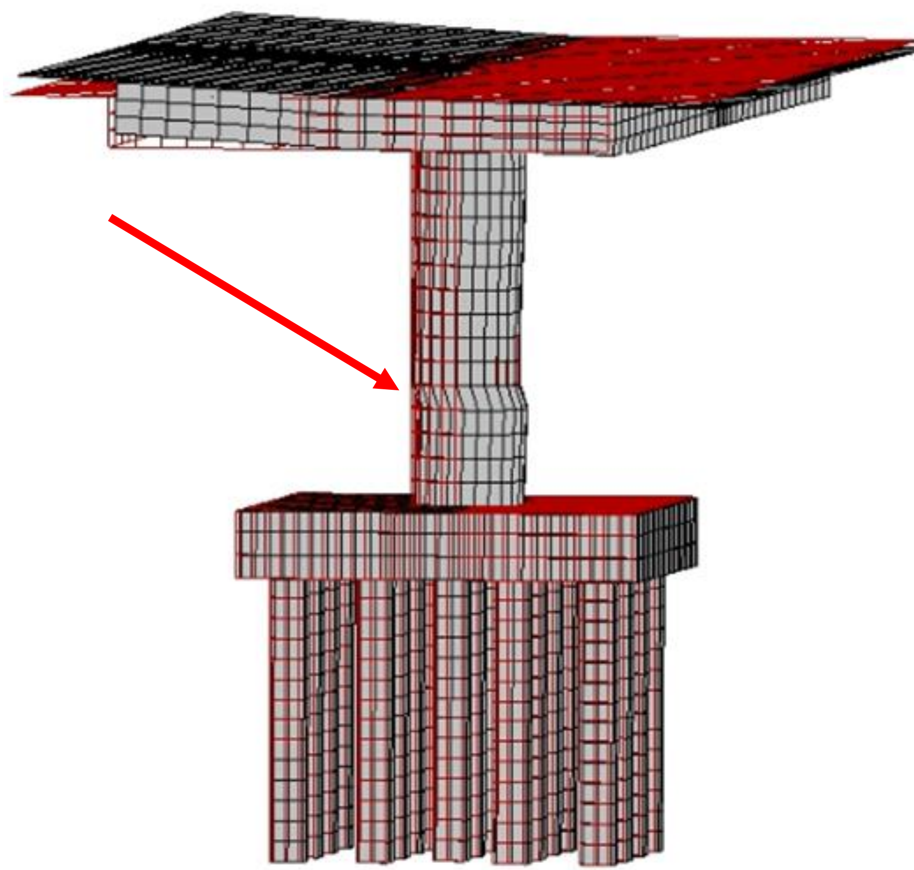

Thank You !